NMR: Examples

Vesna Mitrović, Brown University

Boulder Summer School, 2008

To Remember

Static NMR Spectrum Measurements $\Rightarrow$
Local Magnetic Field Probability Distribution

$$\omega_n = \gamma_n H_{loc} = \gamma_n \left(H_0 + \langle H_{hf} \rangle \right)$$

$$\langle H_{hf} \rangle = \sum_n -A_{n,k} \langle S_k \rangle$$

Width of an NMR spectrum $\Rightarrow$ **Distribution of** $\langle \vec{S}_z(r) \rangle$

$$K(T) \propto \chi'(q = 0, \omega \rightarrow 0)$$

Shift of an NMR spectrum $\Rightarrow$ **Magnetic susceptibility**

In metals:

$$K(T) \propto N(E_F)$$

$$T_1^{-1} \propto \chi''(q, \omega \rightarrow 0)$$

$$T_2^{-1} \propto \chi'(q, \omega \rightarrow 0)$$

2D Electron Gas - T_1 Contrast Imaging

MBE heterostructures

M242 and **M280**

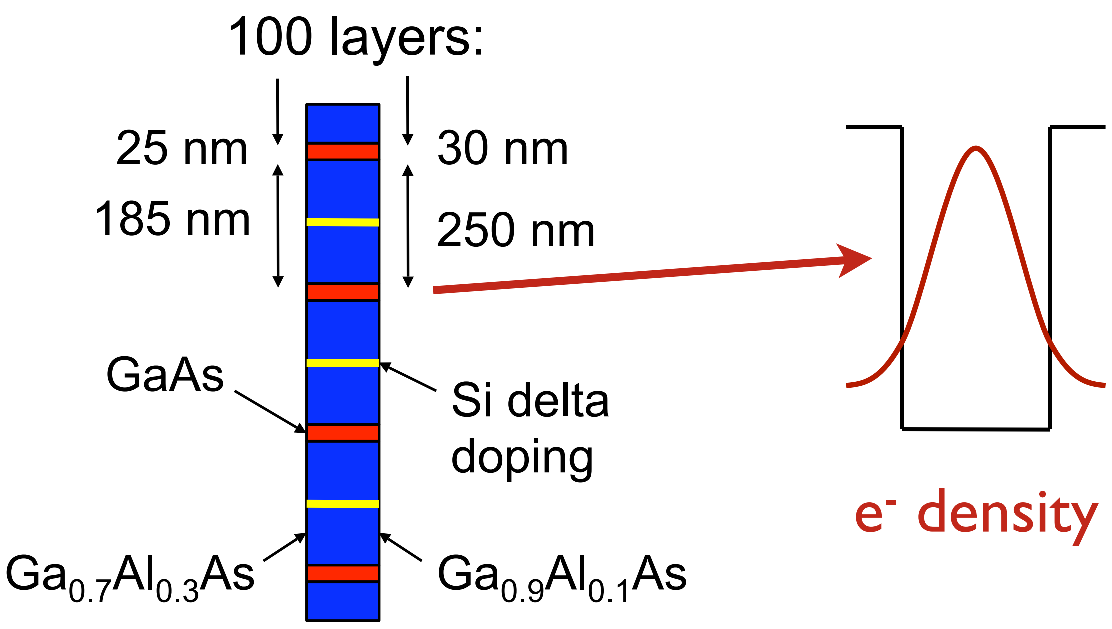

(S.E. Barrett and collaborators, Yale University)

(M. Horvatic & C. Bertier and collaborators, GHMFL,Grenoble)

2D Electron Gas - T_1 Contrast Imaging

MBE heterostructures

M242 and **M280**

100 layers:

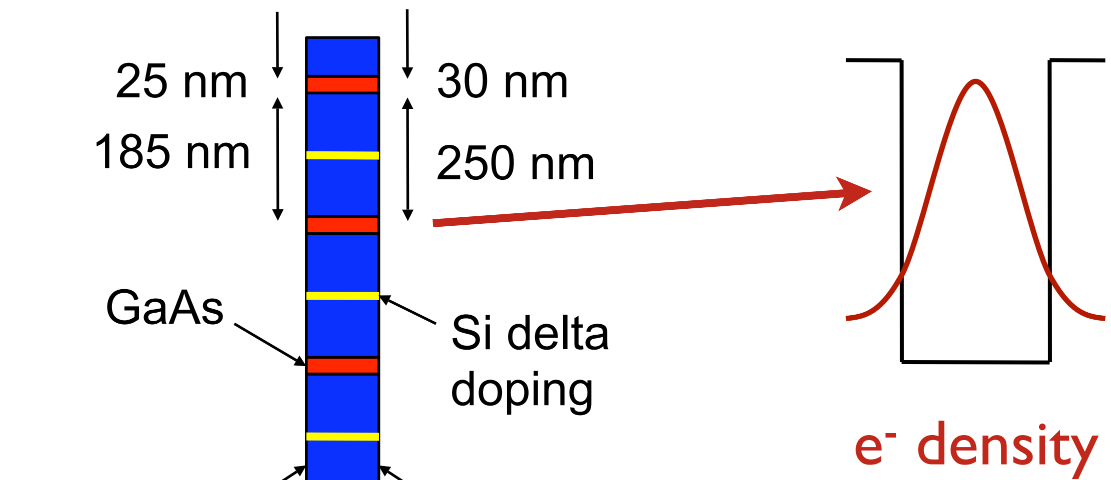

2D Electron Gas in $H_0 \parallel z$:

$B = 0 \rightarrow B >> 0$

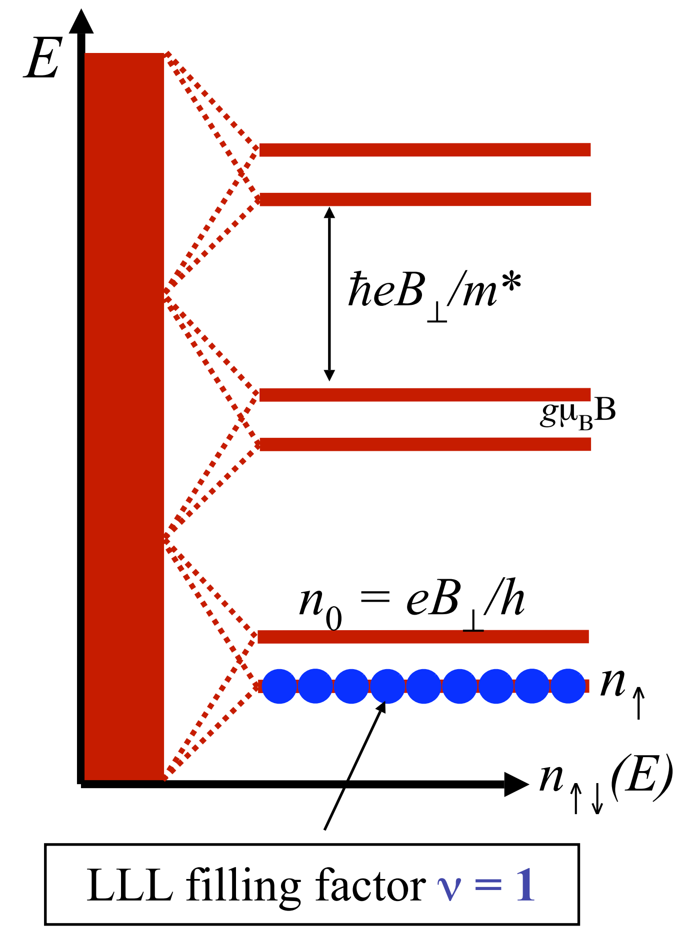

(S.E. Barrett and collaborators, Yale University)

(M. Horvatic & C. Bertier and collaborators, GHMFL,Grenoble)

2D Electron Gas - T_1 Contrast Imaging

MBE heterostructures

M242 and **M280**

100 layers:

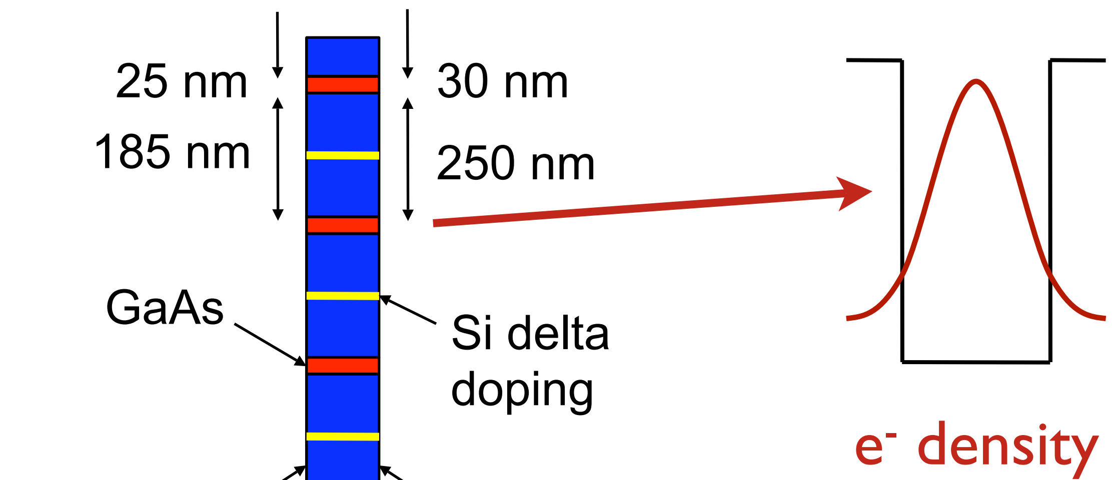

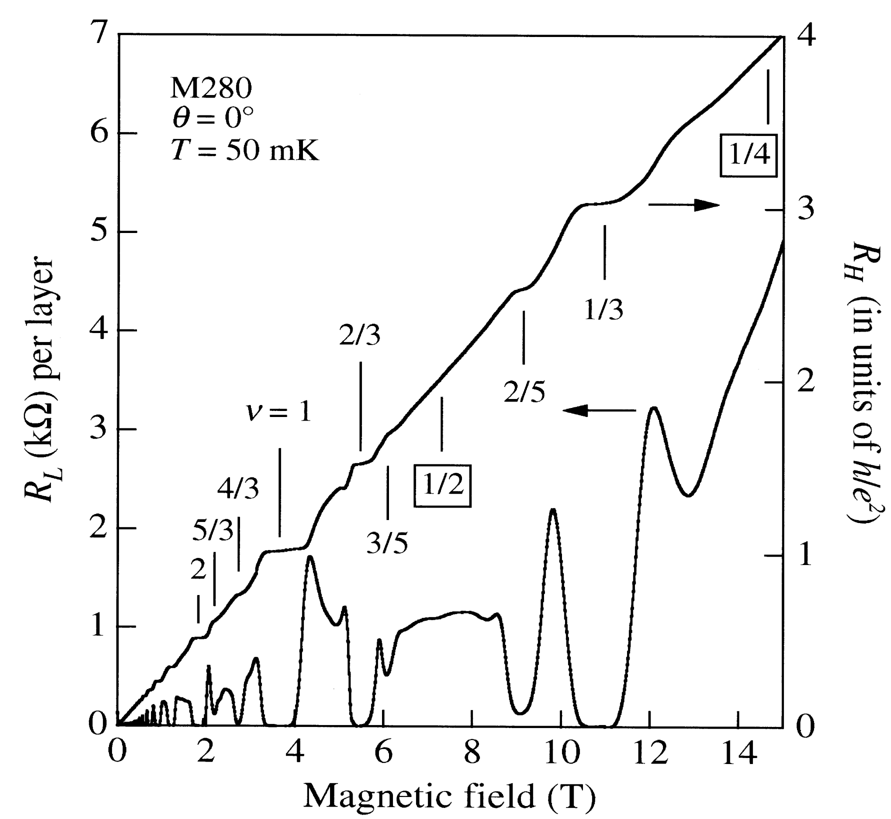

[Fig: S. Melinte, PhD thesis (2001)]

2D Electron Gas in $H_0 \parallel z$:

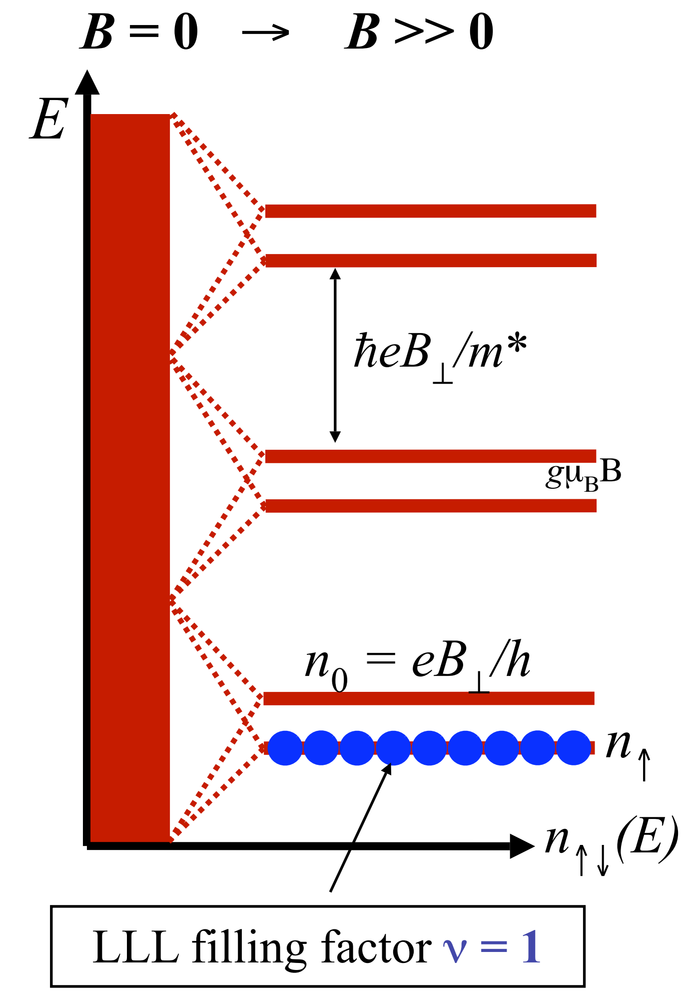

(S.E. Barrett and collaborators, Yale University)

(M. Horvatic & C. Bertier and collaborators, GHMFL,Grenoble)

Static Shift Measurements :

NMR line-shift (^{69,71}Ga)

$$K_S \propto P = \frac{N_\uparrow - N_\downarrow}{N_\uparrow + N_\downarrow} = \frac{2}{n}\sum_k S_k^z$$

average spin polarisation

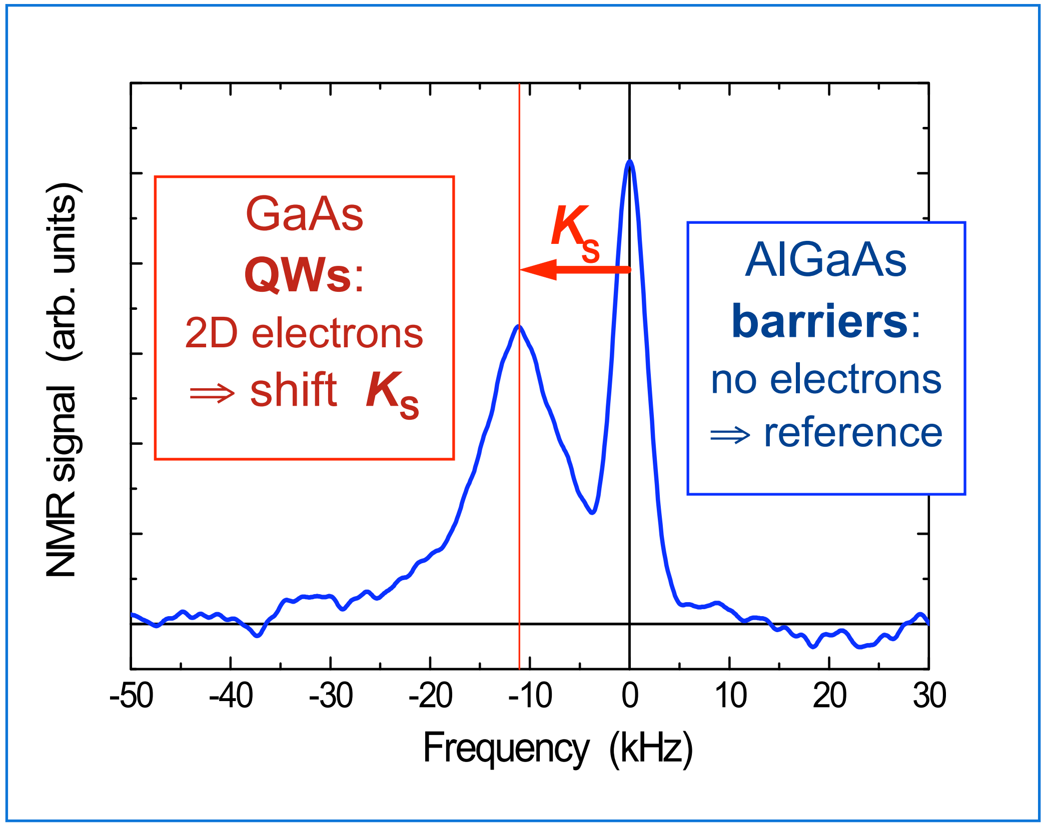

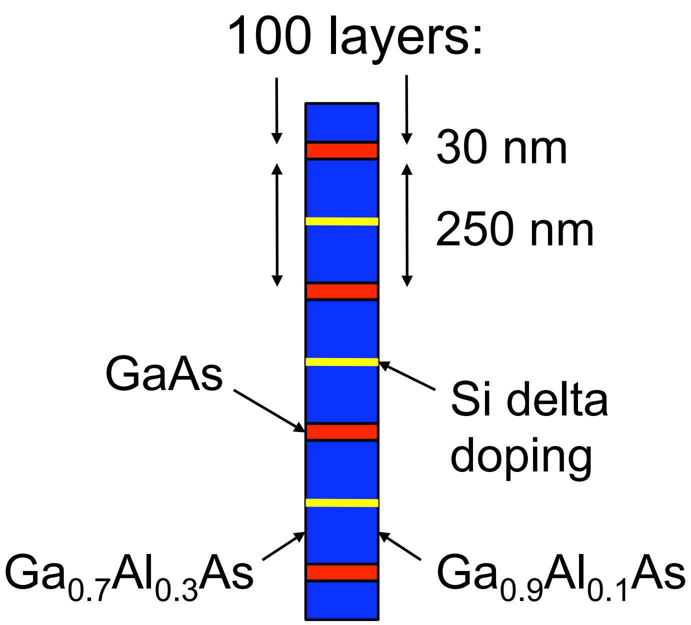

(GHMFL,Grenoble)

Static Shift Measurements :

NMR line-shift (^{69,71}Ga)

$$\mathbf{K_S} \propto \mathbf{P} = \frac{N_\uparrow - N_\downarrow}{N_\uparrow + N_\downarrow} = \frac{2}{n}\sum_k S_k^z$$

average spin polarisation

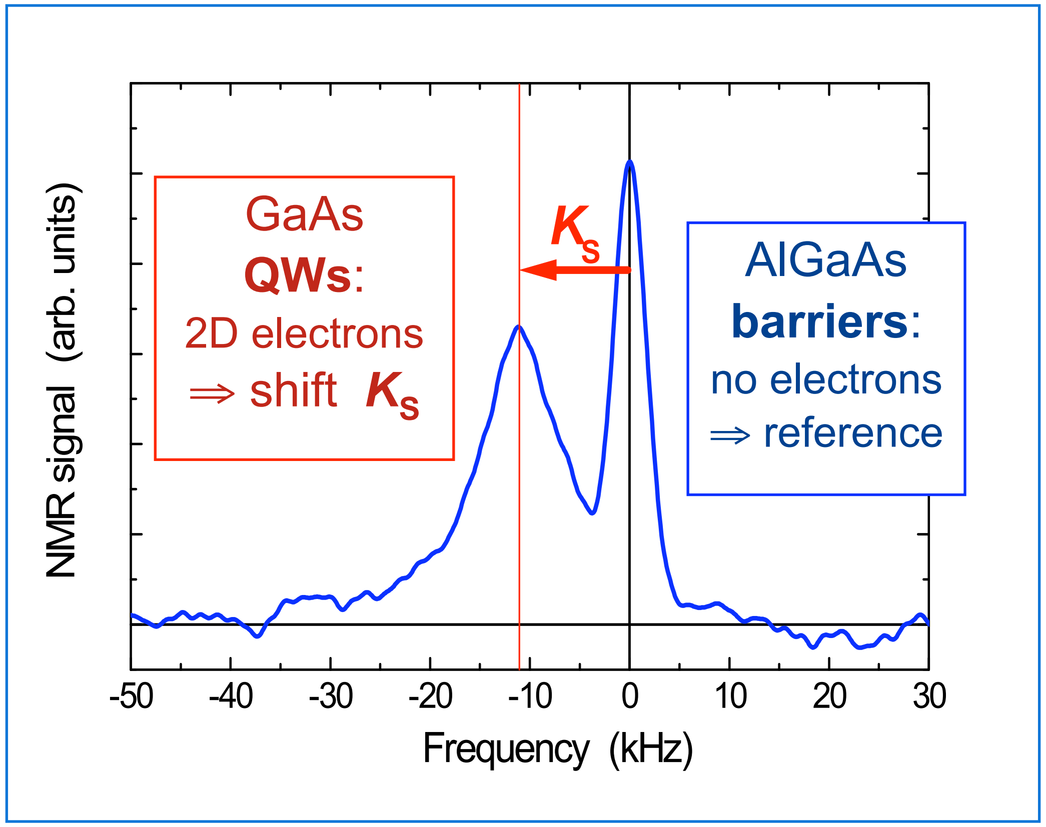

(GHMFL,Grenoble)

Static Shift Measurements :

NMR line-shift (^{69,71}Ga)

$$K_S \propto P = \frac{N_\uparrow - N_\downarrow}{N_\uparrow + N_\downarrow} = \frac{2}{n}\sum_k S_k^z$$

average spin polarisation

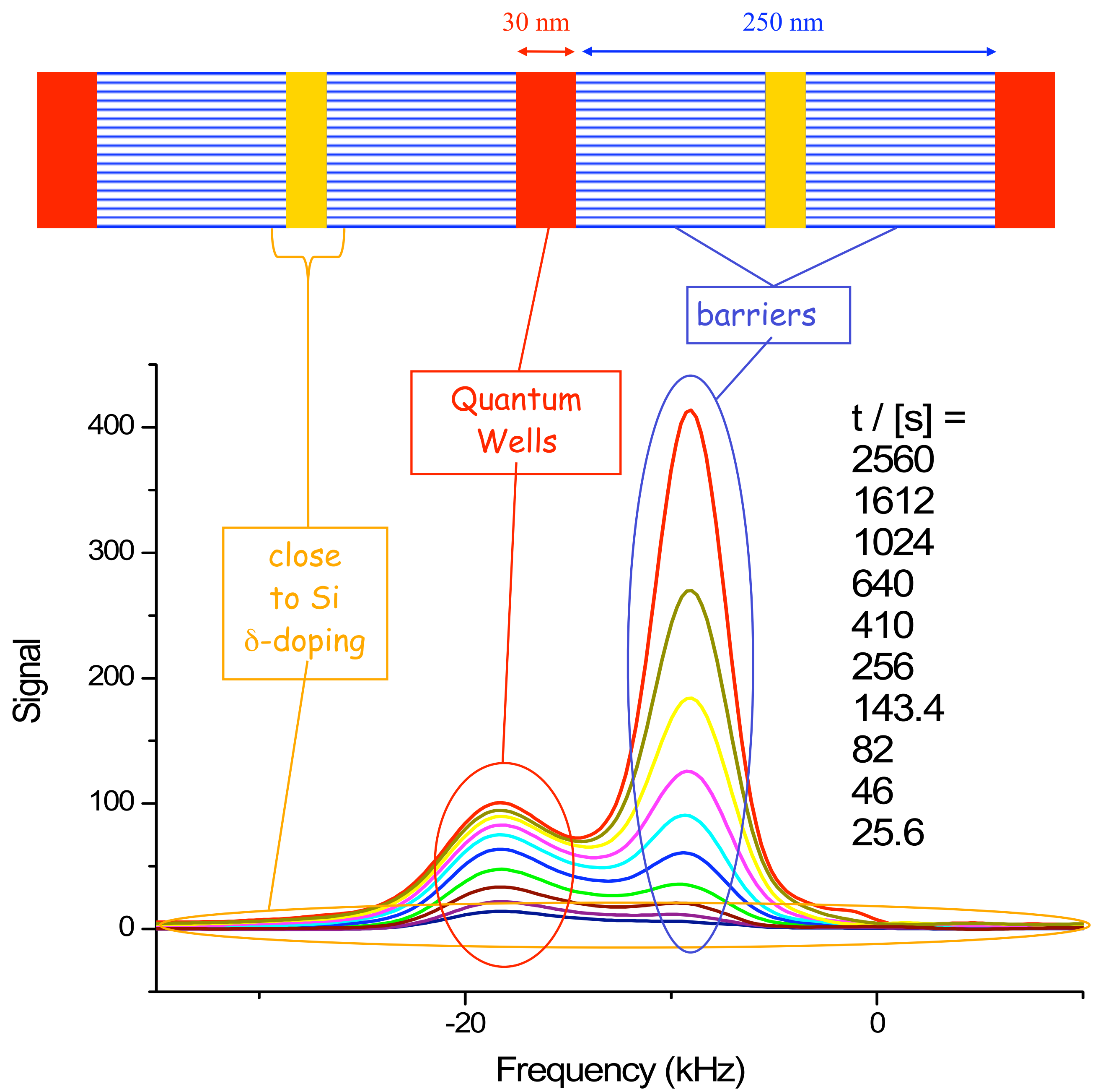

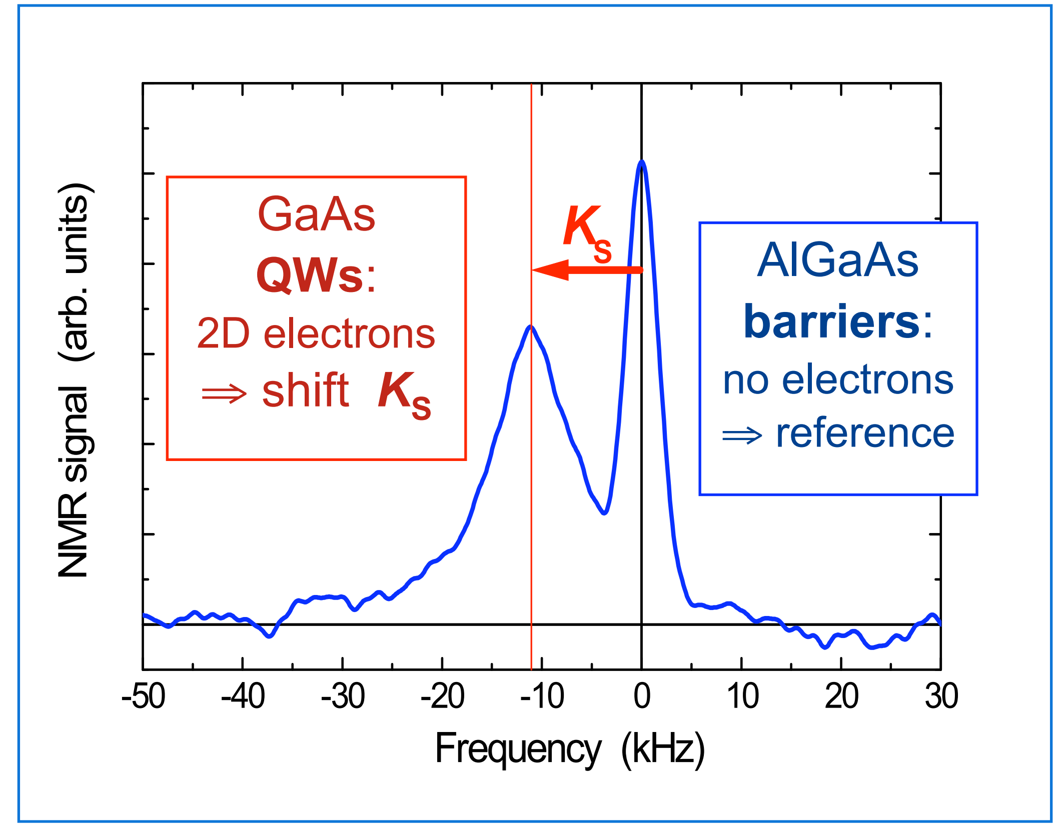

(GHMFL,Grenoble)

Static Shift Measurements :

NMR line-shift (^{69,71}Ga)

$\downarrow$

$$\mathbf{K_S} \propto \mathbf{P} = \frac{N_\uparrow - N_\downarrow}{N_\uparrow + N_\downarrow} = \frac{2}{n}\sum_k S_k^z$$

$\uparrow$

average spin polarisation

$$|\mathcal{P}(g\mu_B H/k_B T)| \to 0$$

What if g -> 0?

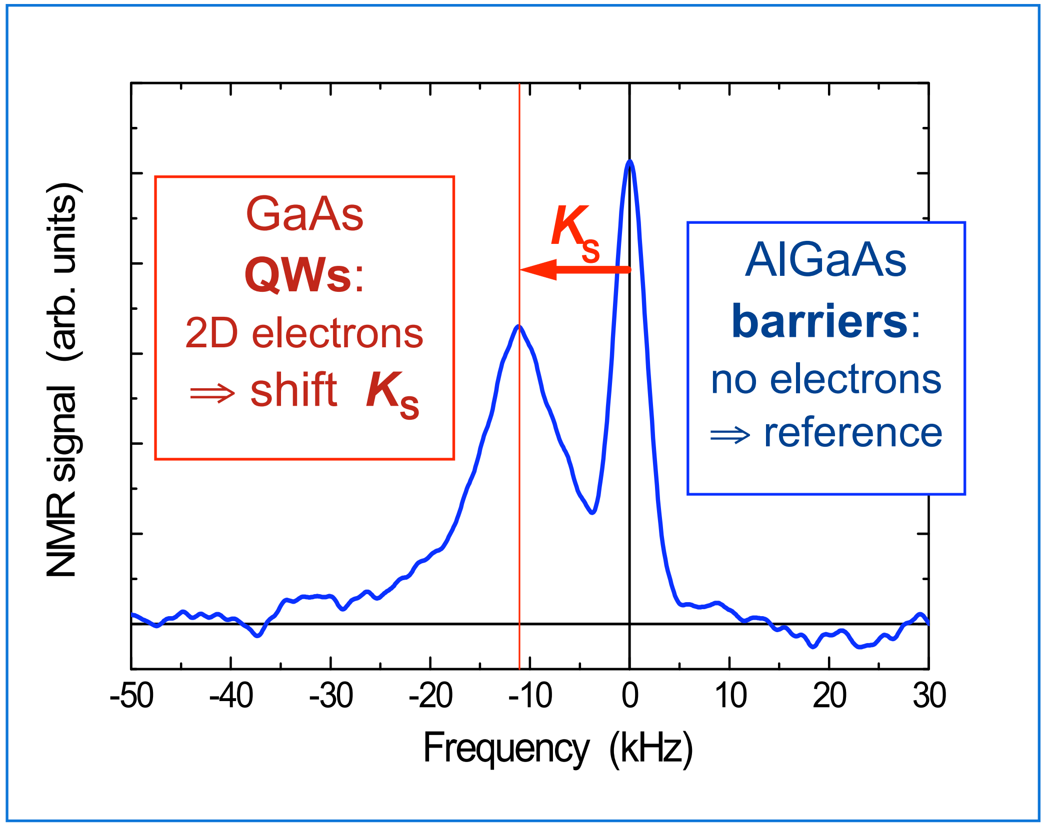

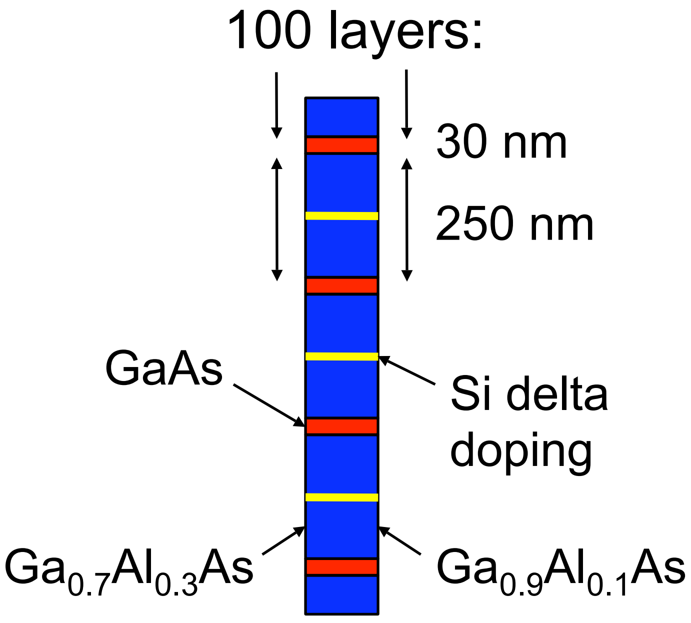

(GHMFL,Grenoble)

Static Shift Measurements :

NMR line-shift (^{69,71}Ga)

↓

$$K_S \propto P = \frac{N_\uparrow - N_\downarrow}{N_\uparrow + N_\downarrow} = \frac{2}{n}\sum_k S_k^z$$

↑

average spin polarisation

$$|\mathcal{P}(g\mu_B H/k_B T)| \to 0$$

What if g -> 0?

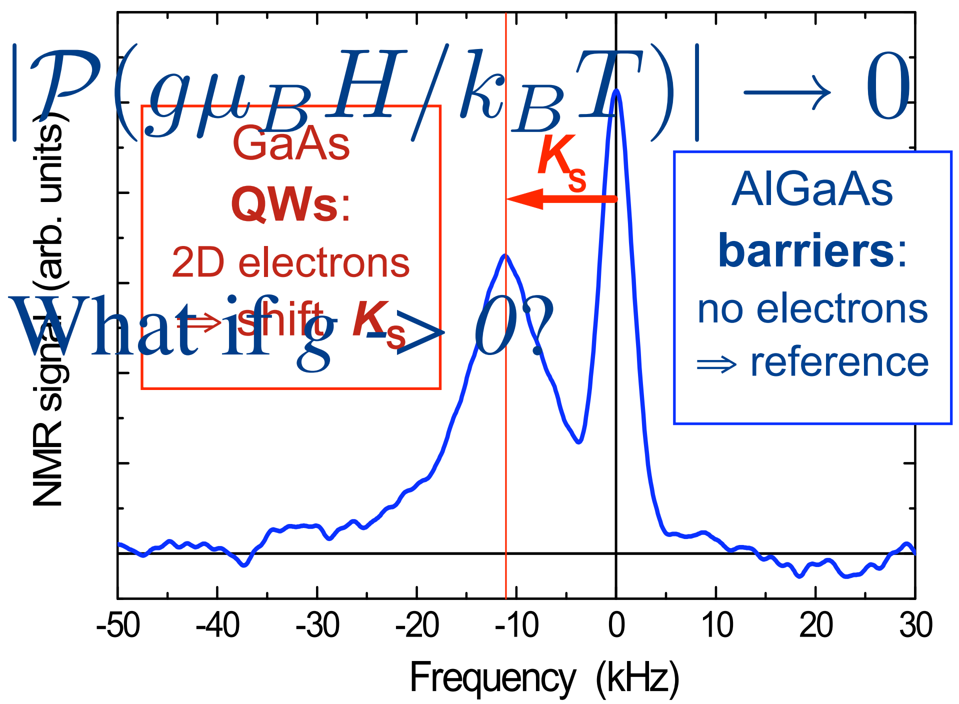

(GHMFL,Grenoble)

$\nu = 1$ state - elementary excitations ?

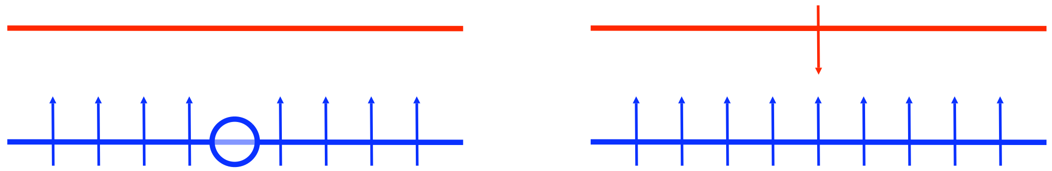

Localized **holes** and **electrons**

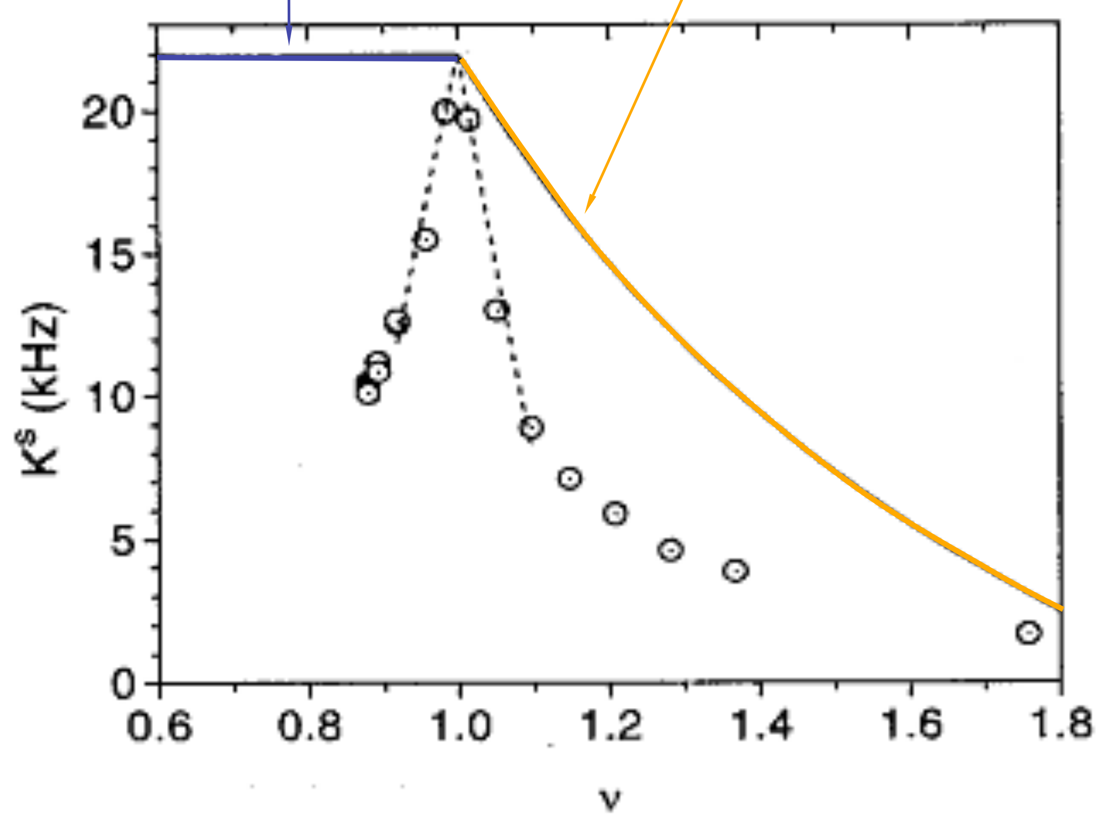

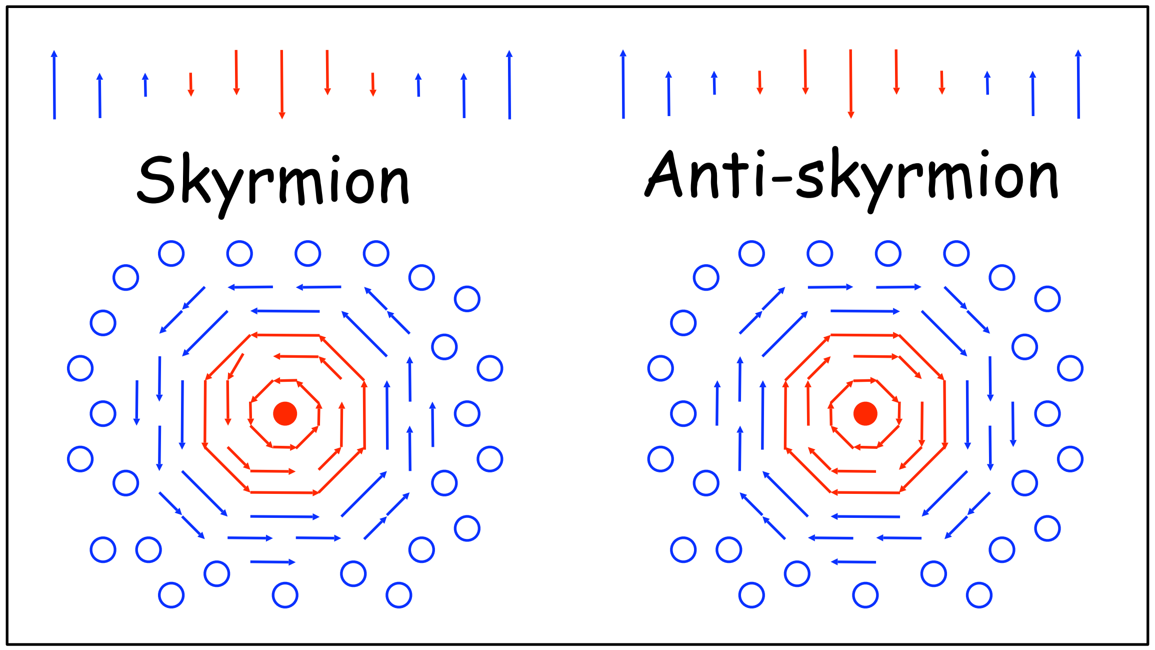

Energy gap & size (s) $\Rightarrow$

$$\boxed{\tilde{g} = \frac{E_z}{E_c}}$$

S.E. Barrett *et al.*, Phys. Rev. Lett. **74**, 5112 (1995)
P. Khandelwal *et al.*, Phys. Rev. Lett. **86**, 5353 (2001)

Skyrmion Size (s)

Energy gap & size
(s = Nº of reversed spins within an excitation) $\Rightarrow$

$$\boxed{\tilde{g} = \frac{E_z}{E_c}}$$

Limits # of spin-flips

$$E_z = |g|\mu_B B$$

Favors FM ordering

$$E_c = e^2/\varepsilon l_B$$

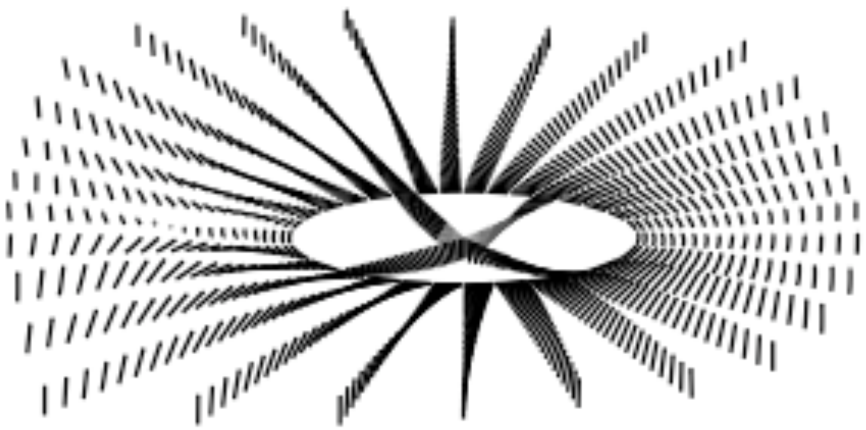

$$\boxed{\tilde{g} \to 0 \Rightarrow s \to \infty}$$

To vary skyrmion size $\to$ tune $\boldsymbol{g}$:

$g \to 0$

- hydrostatic pressure
- $Al_{0.13}Ga_{0.87}As$ - QW ($\boldsymbol{g_{theory} = -0.04}$; $\boldsymbol{g_{GaAs} = 0.44}$)

Large Skyrmions in $Al_{0.13}Ga_{0.87}As$ ($g \cong 0$) Quantum Wells

Magnetotransport measurements in $Al_{0.13}Ga_{0.87}As$ QW

(S. P. Shukla *et al.*, PRB **61**, 4469 (2000)) $\Rightarrow$ $\boldsymbol{s \approx 50}$

Small ***g*** sample:

30 QWs

$g_{\text{theory}} = -0.04 \leftrightarrow g_{\text{GaAs}} = 0.44$

$n_{2D} = 1.1 \times 10^{11}$ cm^{-2}

$m_0 = 30\,000$ cm^2 / Vs

QW: 24 nm of $Al_{0.13}Ga_{0.87}As$

barriers: 75+57 nm of $Al_{0.35}Ga_{0.65}As$

Problem:
How to separate the signals?

$$|\mathcal{P}(g\mu_B H/k_B T)| \to 0$$

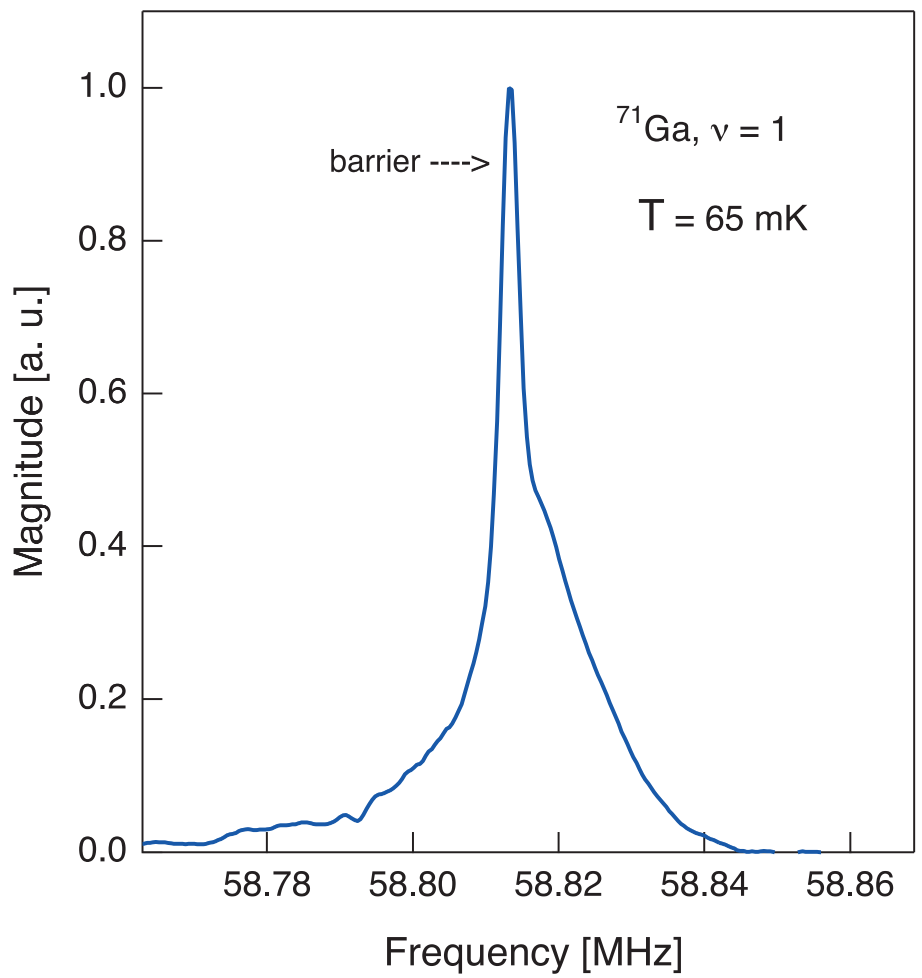

Separate overlapping QW and barriers' signal ?

Small tip angle technique :

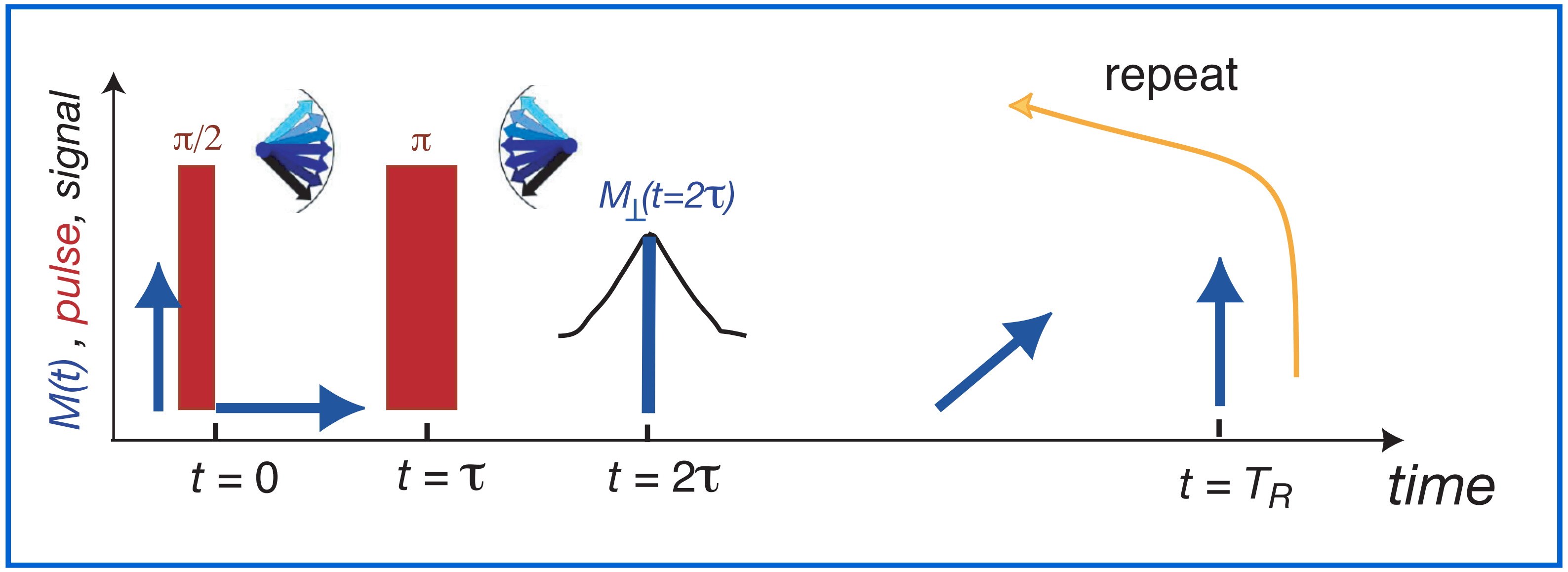

$$\boxed{\frac{S}{N} = f\left(\frac{T_R}{T_1}, \text{Tip Angle}\right)}$$

Separate overlapping QW and barriers' signal ?

Small tip angle technique :

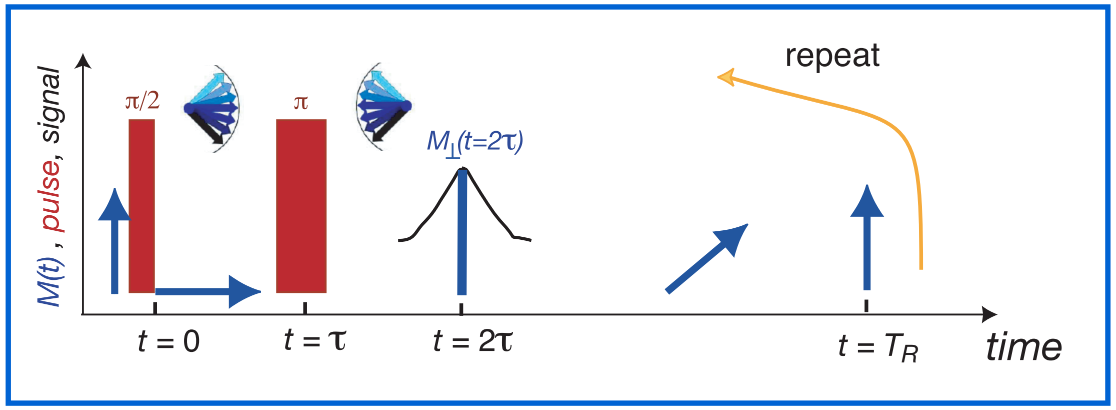

$$\boxed{\frac{S}{N} = f\left(\frac{T_R}{T_1}, \text{Tip Angle}\right)}$$

Separate overlapping QW and barriers' signal ?

Small tip angle technique :

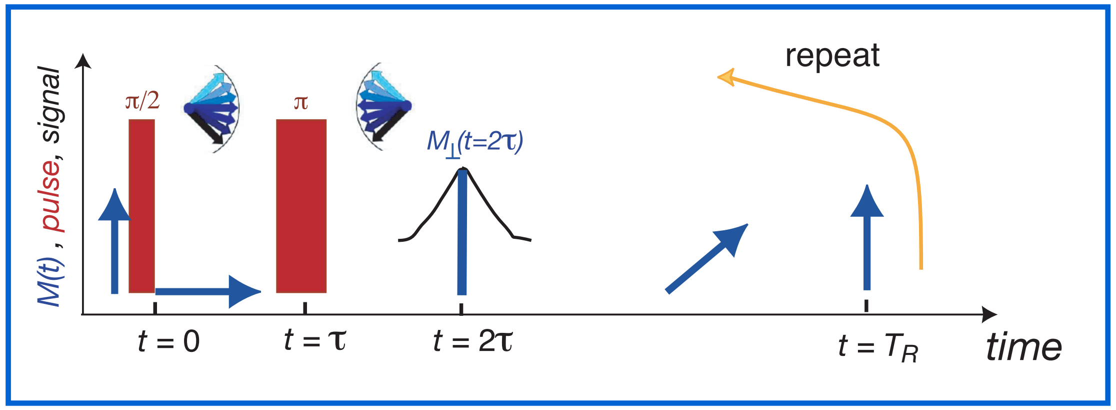

$$\frac{S}{N} = f\left(\frac{T_R}{T_1}, \text{Tip Angle}\right)$$

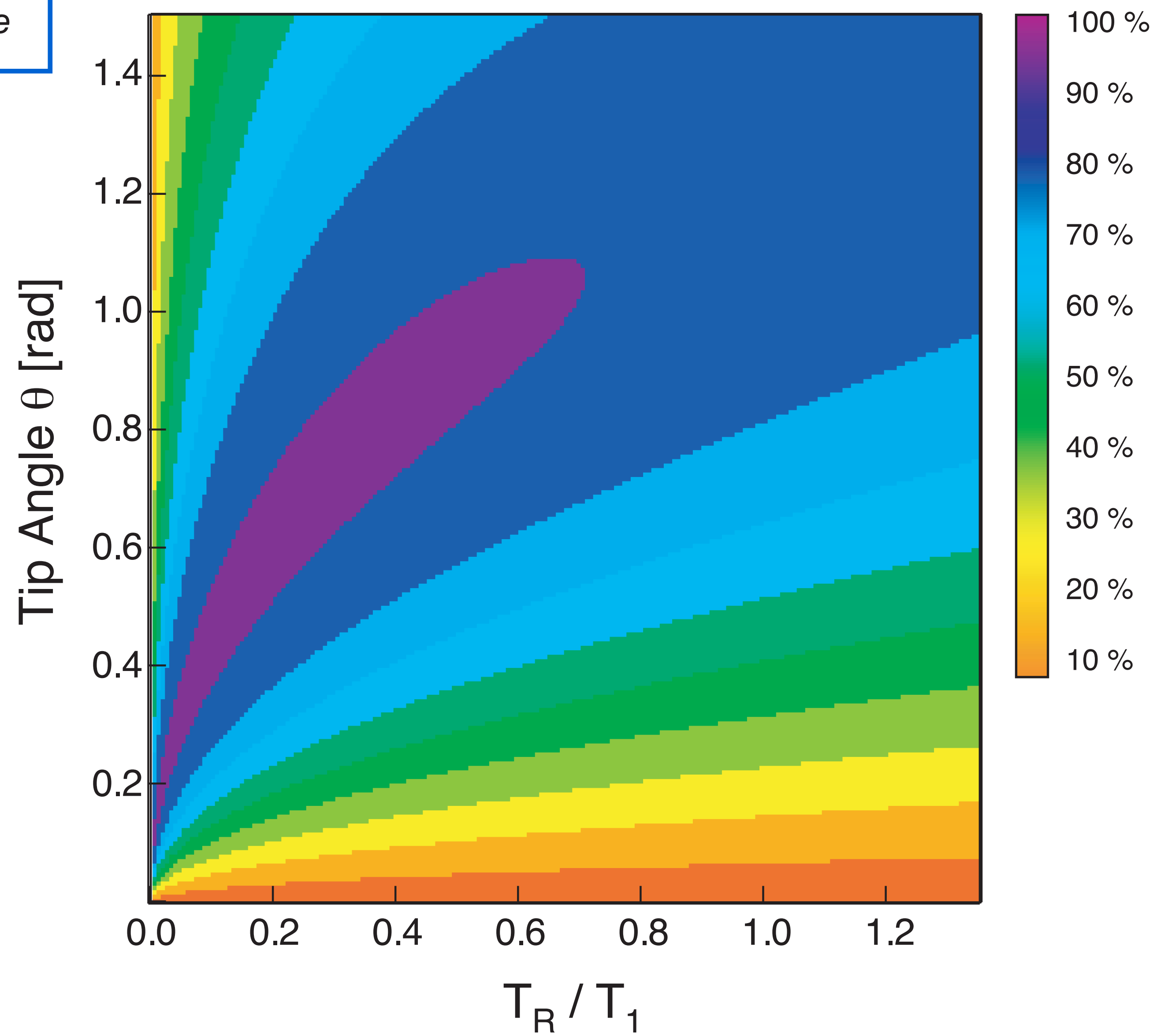

Separate overlapping QW and barriers' signal ?

Small tip angle technique :

$$\boxed{\frac{S}{N} = f\left(\frac{T_R}{T_1},\ \text{Tip Angle}\right)}$$

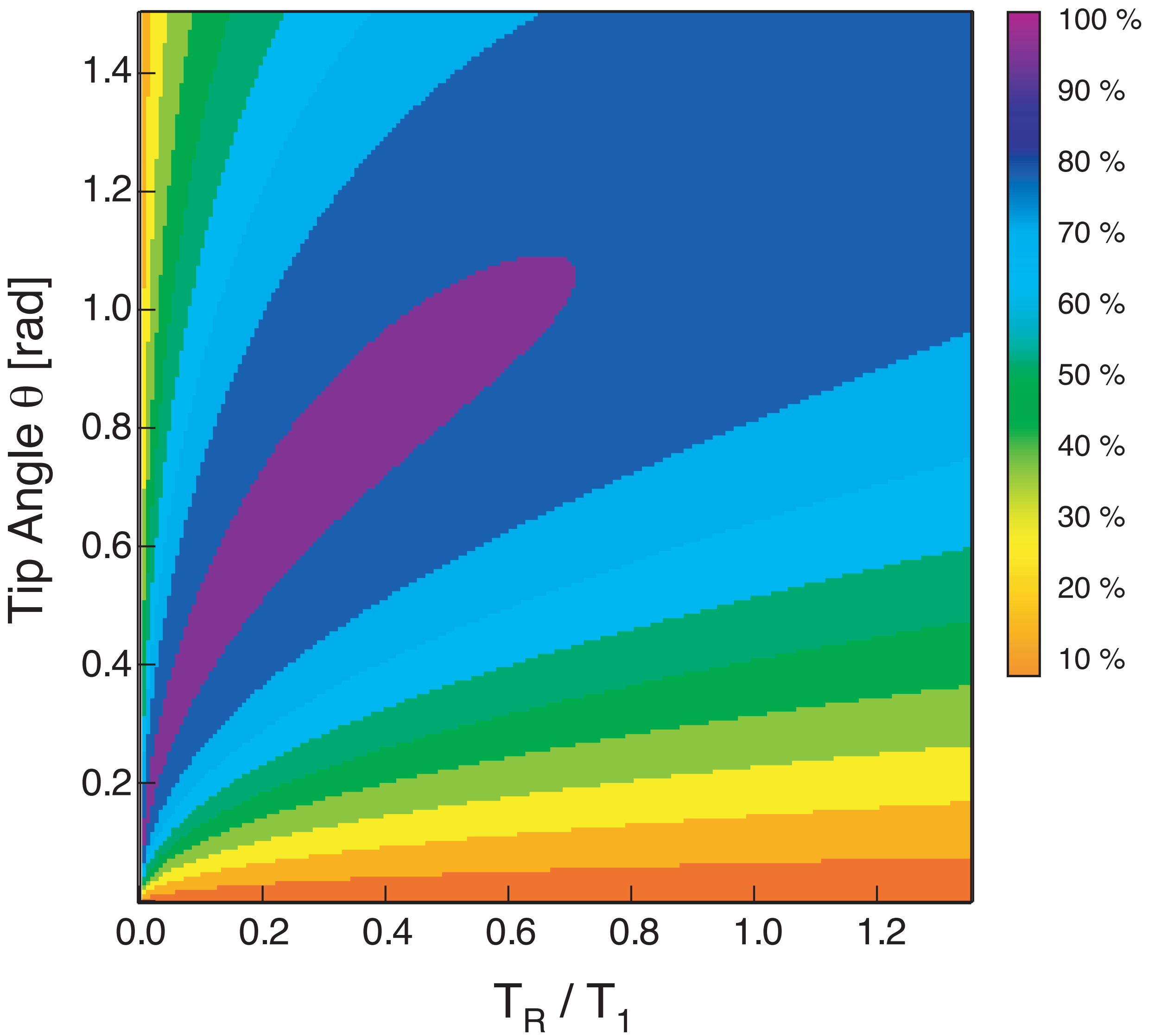

Separate overlapping QW and barriers' signal ?

Small tip angle technique :

$$\frac{S}{N} = f\left(\frac{T_R}{T_1}, \text{Tip Angle}\right)$$

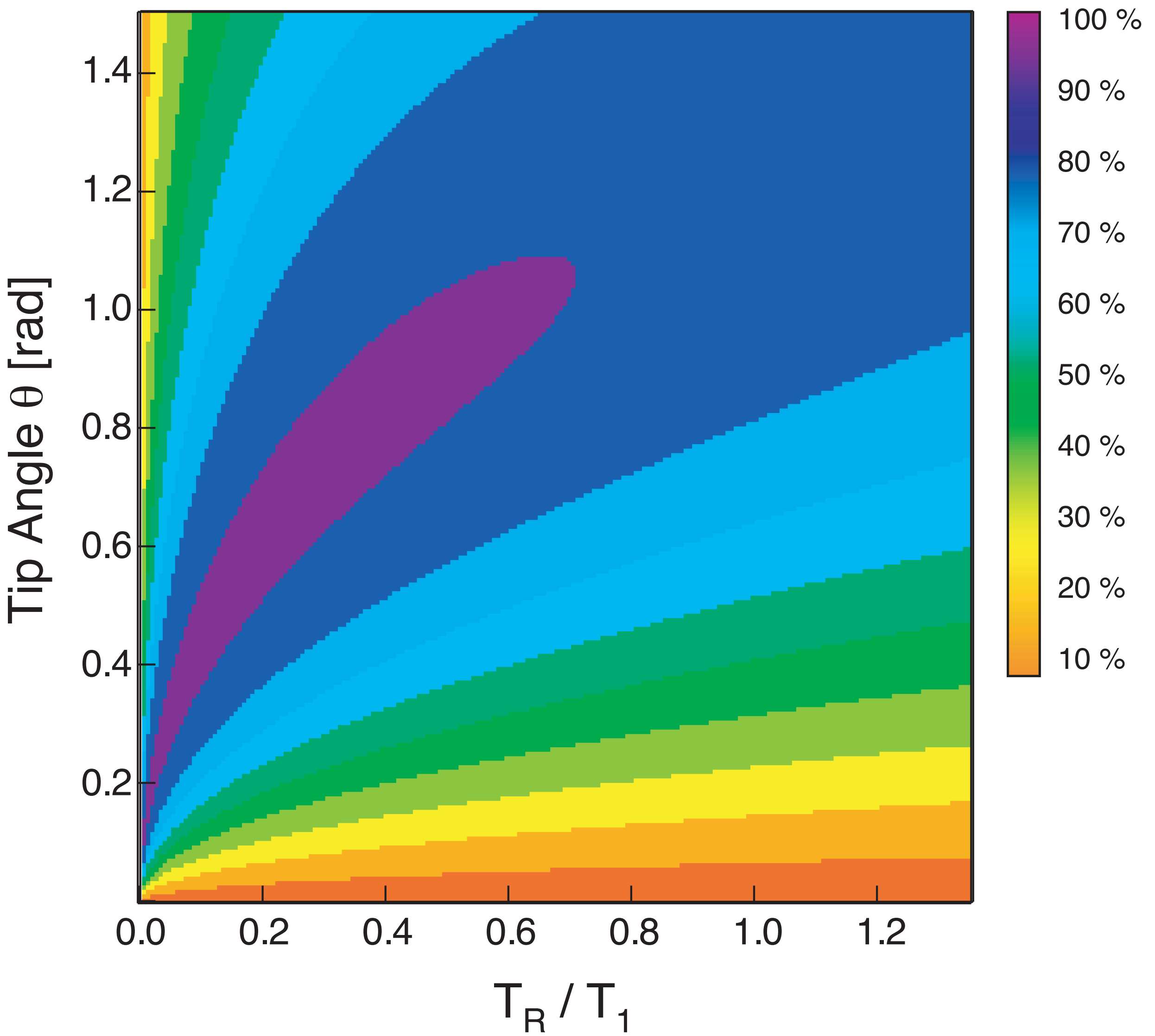

GOOD !!! very different T_1 for QW and barriers'

Pulse power dependence :

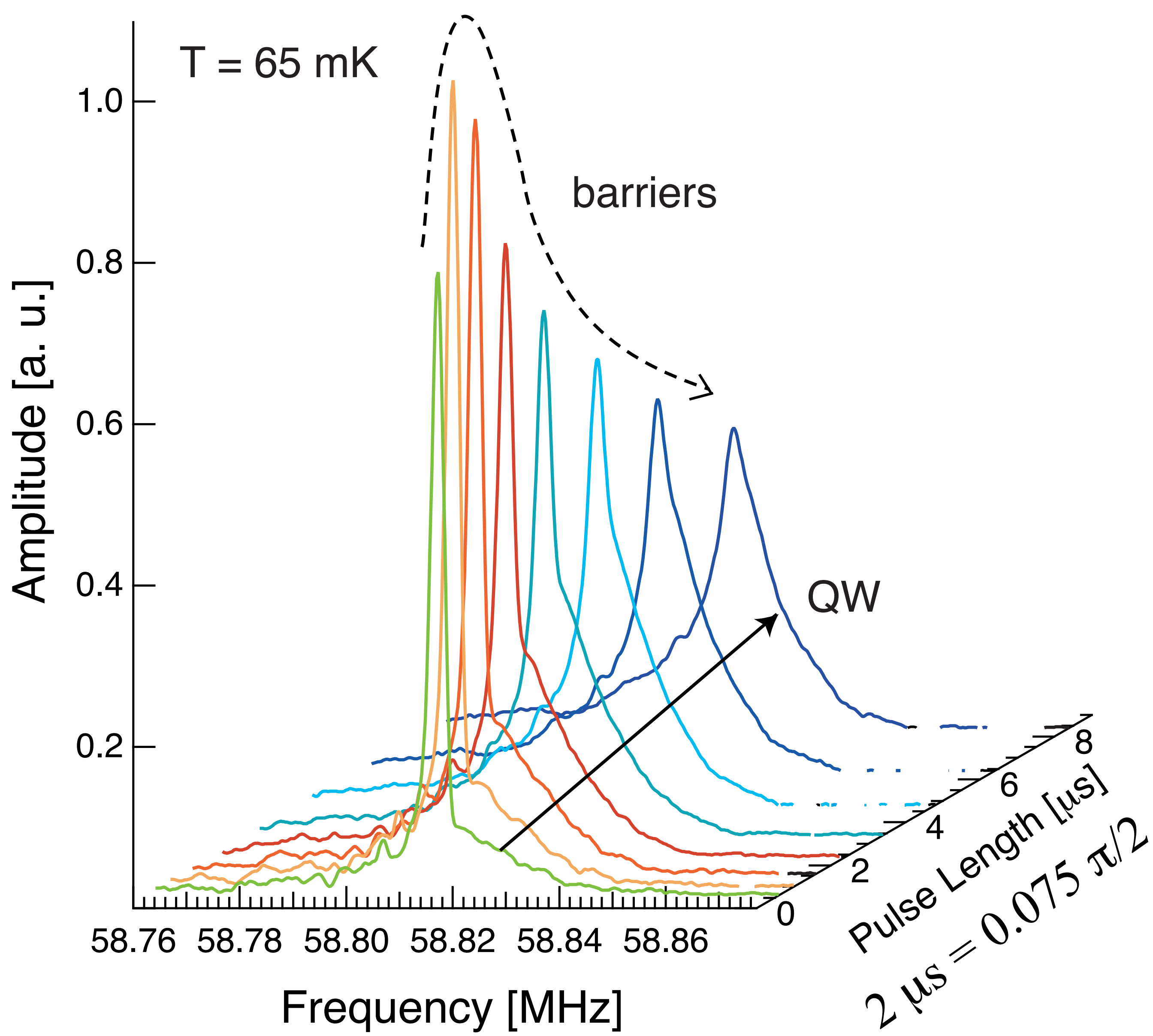

[V. Mitrović *et al.*, 2007]

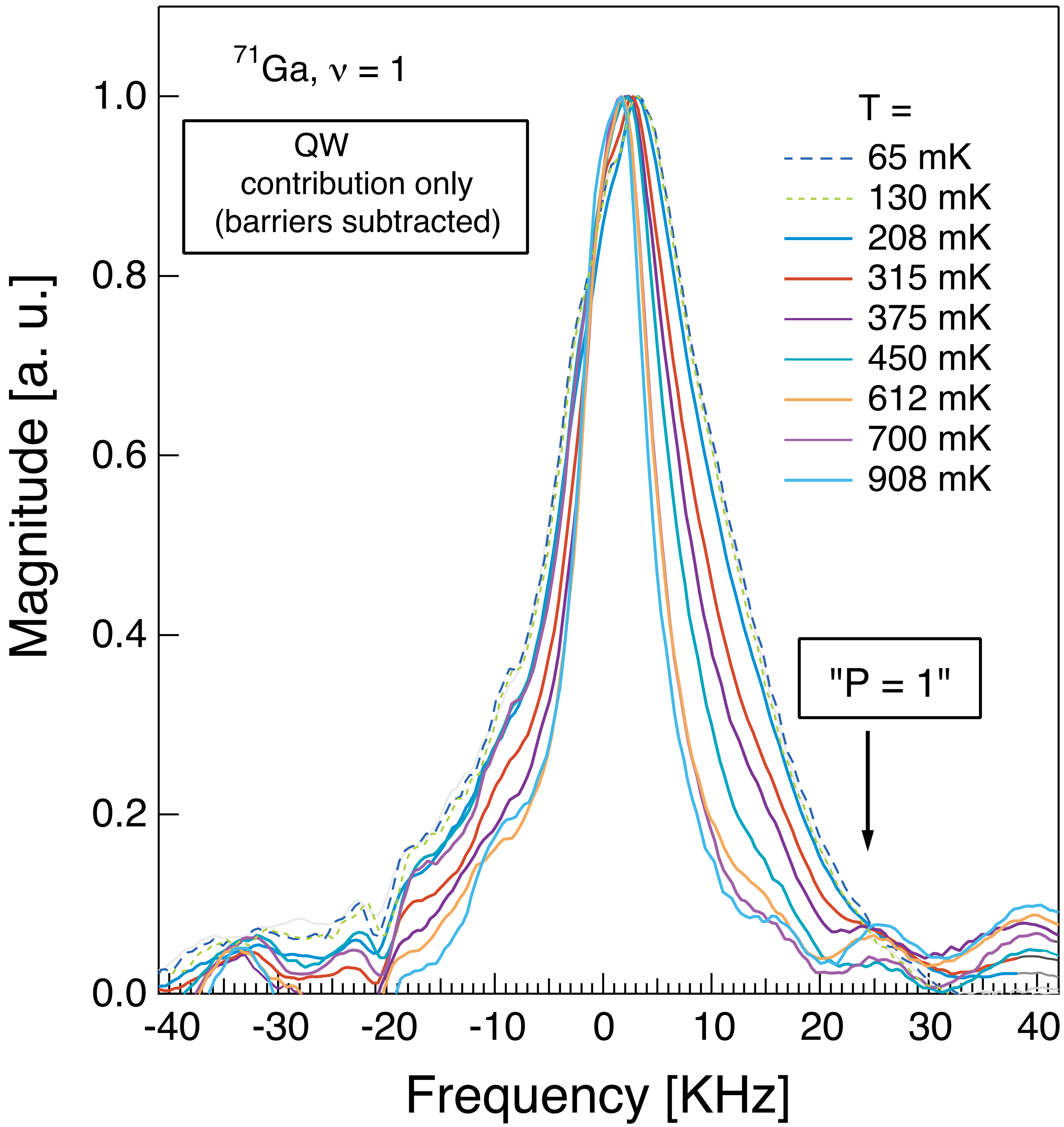

^{71}Ga, ν = 1
QW contribution only (barriers subtracted)
T =
65 mK
130 mK
208 mK
315 mK
375 mK
450 mK
612 mK
700 mK
908 mK
"P = 1"
Magnitude [a. u.]
1.0
0.8
0.6
0.4
0.2
0.0
-40
-30
-20
-10
0
10
20
30
40
Frequency [KHz]

QW signal

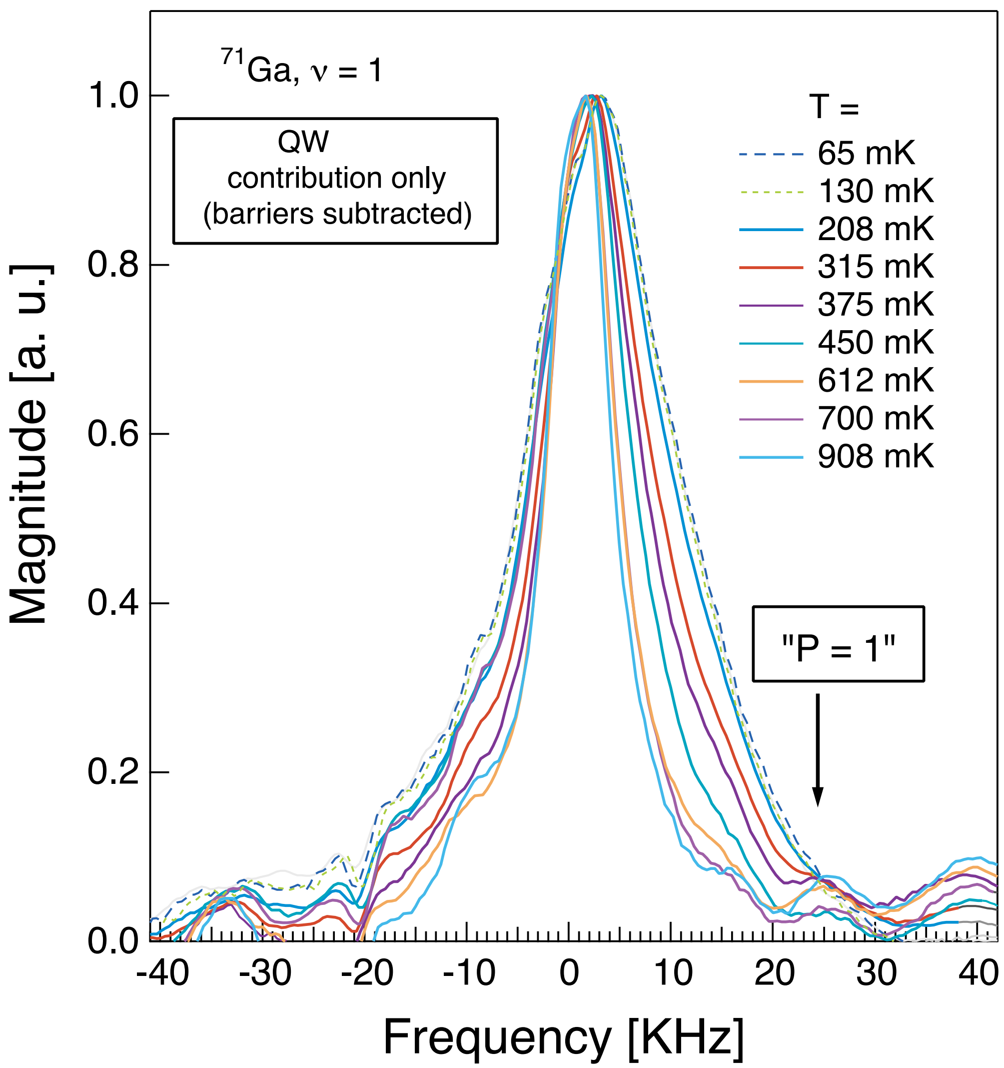

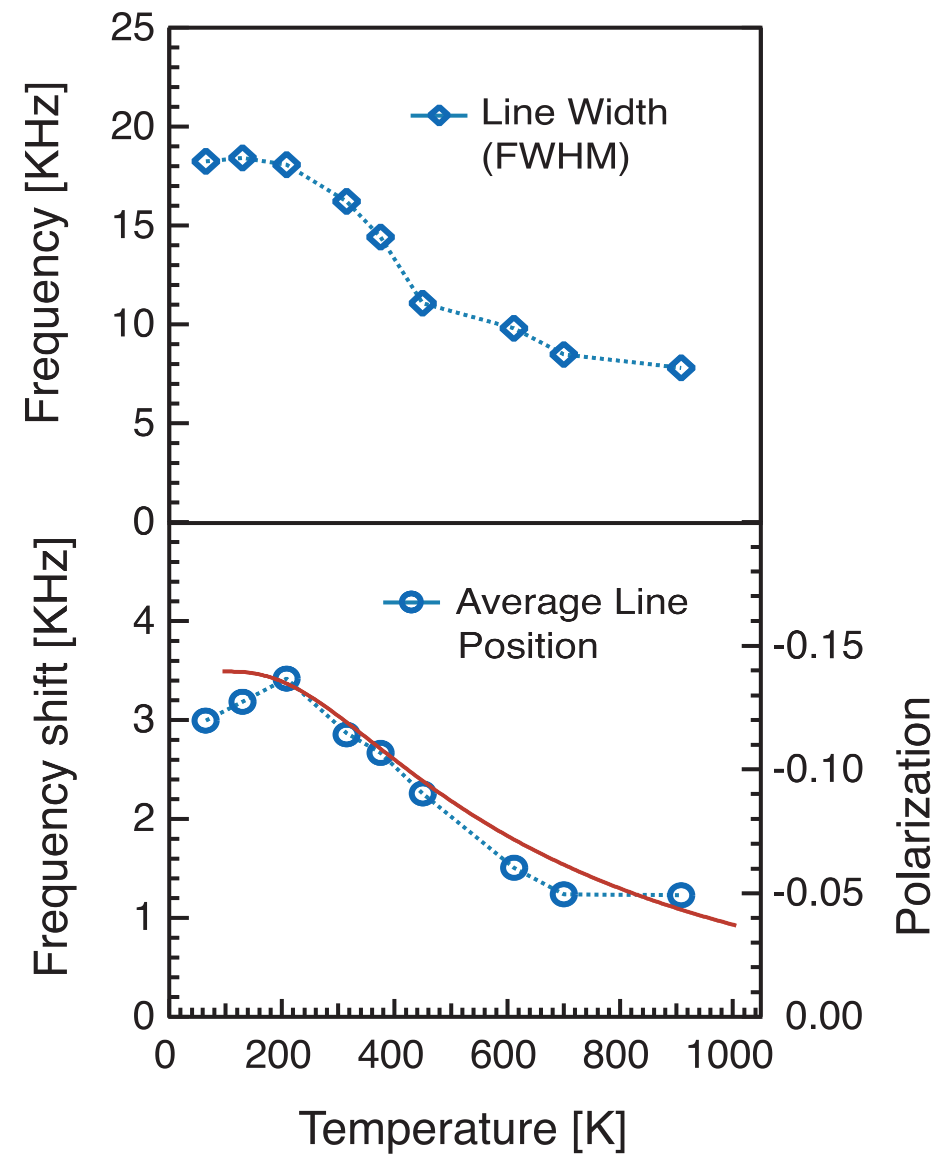

$g \cong -0.1 \times g_{\mathrm{GaAs}}$

at low-T : **"negative"**, small, strongly inhomogeneous polarization

Inhomogeneous Systems

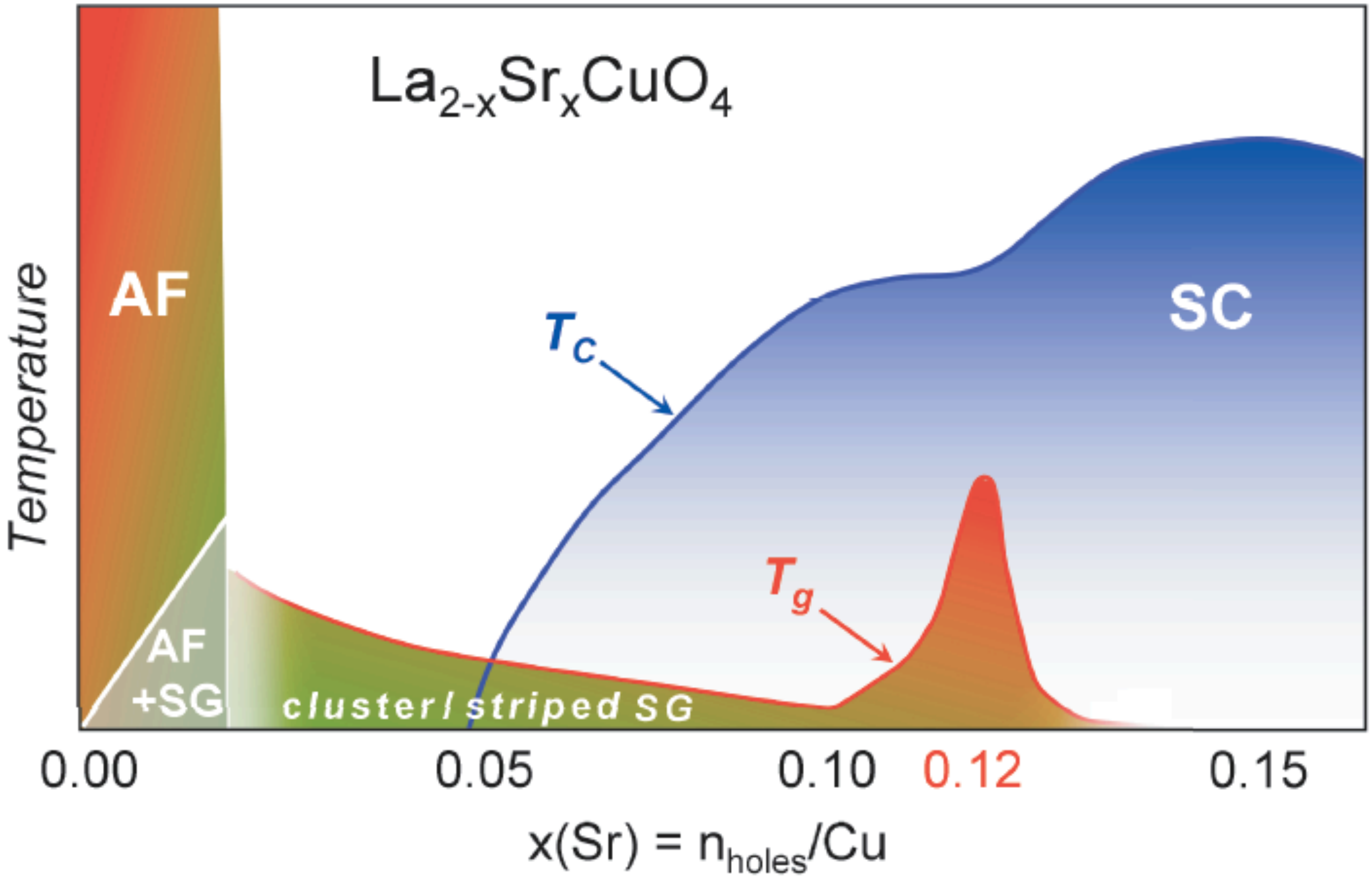

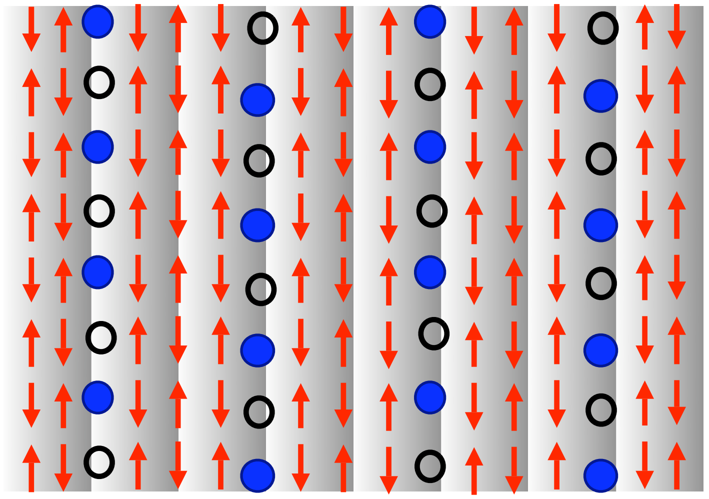

Stripe phase (Tranquada *et al.*, Nature 1995)

(T. Imai and collaborators, MIT & McMaster University)
(M. Julien and collaborators, UJF & GHMFL,Grenoble)
(C.Hamel, N. Curro and collaborators, LANL)

What's going on in LSCO ?

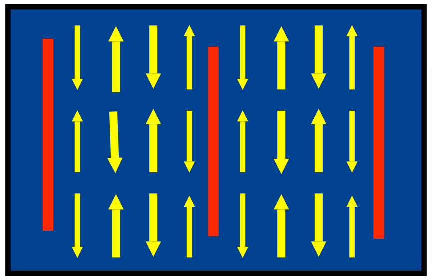

« Inc. » AF LRO
(stripe pattern)

Suzuki et al.
Kimura et al.
Wakimoto et al.

Glassy freezing
Cluster spin-glass

?

Inhomogneeity
&
Phase Separation

Niedermayer et al.,
Julien et al.

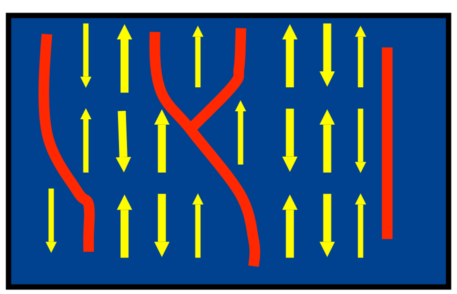

Singer et al.

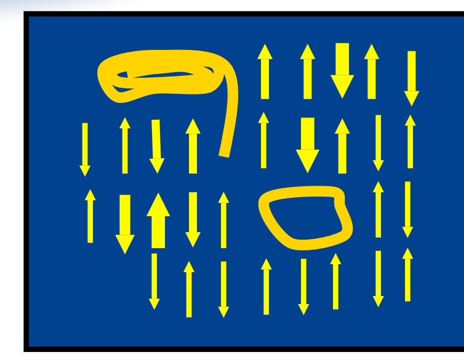

Enhanced AF order
from vortex cores

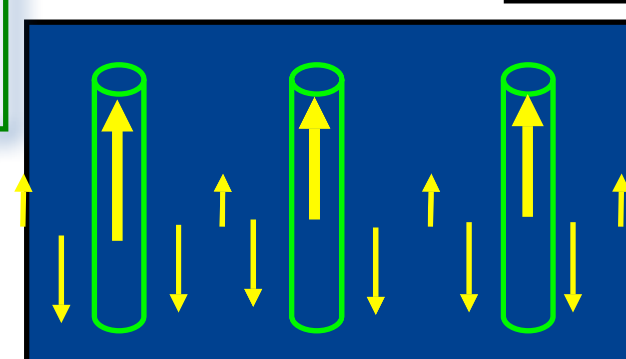

Katano et al.
Lake et al.

Spatial inhomogeneities (Distribution of T_1 values)

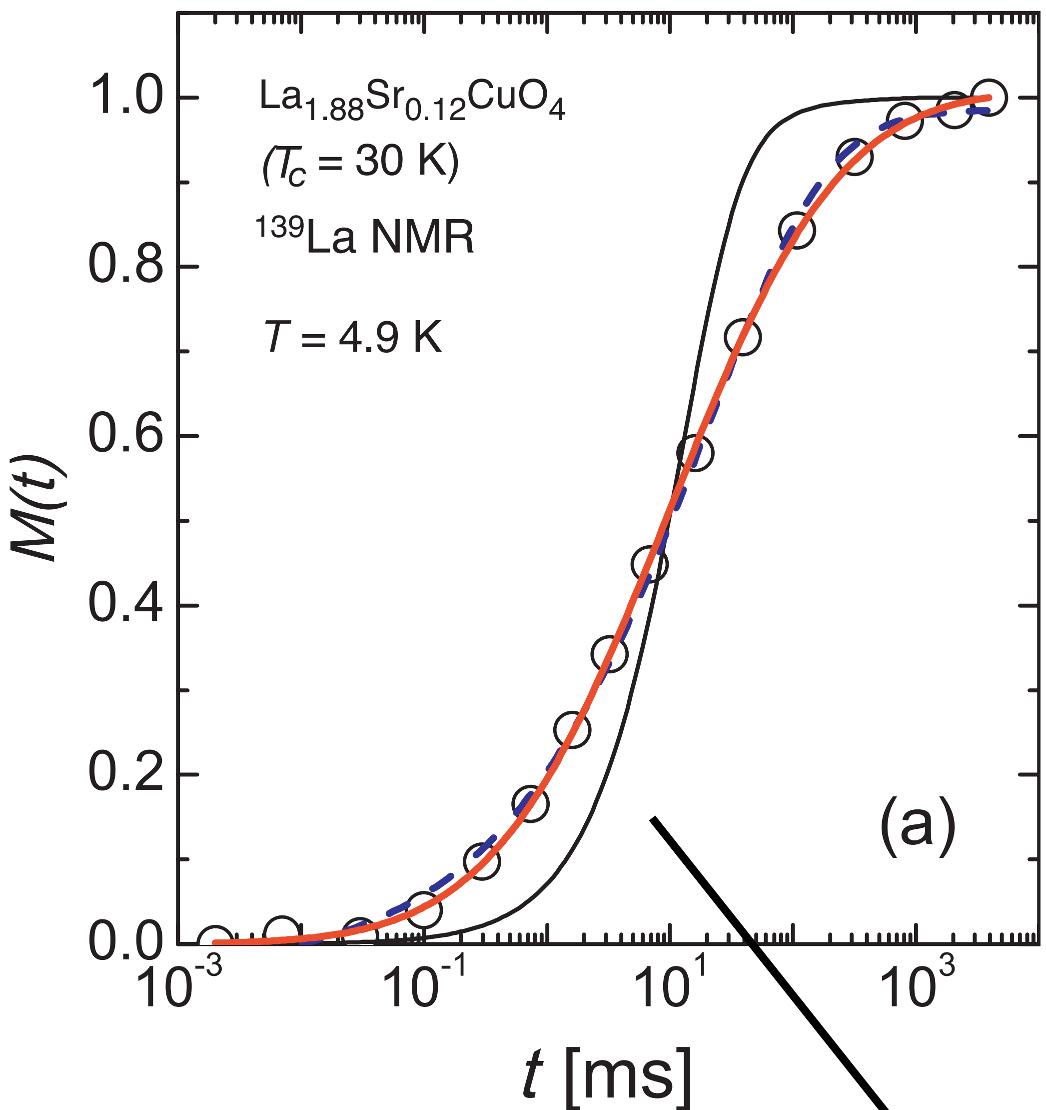

Case 1.
Spatially resolved measurement

Case 2. Not resolved
$\Longrightarrow$ phenomenological fit
exponent α quantifies disorder strength

Case 3. Not resolved
$\Longrightarrow$ convolute with distribution function
$\Longrightarrow$ deduce parameters

Single T_1 :

$$\frac{M_0 - M_\infty}{M_\infty} = \sum_k c_k \cdot e^{-b_k \frac{t}{T_1}}$$

Analysis of Spatial Inhomogeneities I

1. phenomenological fit:
exponent α quantifies disorder strength
good qualitative analysis

2. Convolute with distribution function of ***T_1***

Single *T_1*

$$\mathcal{M}_\alpha(t, T_1^{-1}) = 1 - 0.714\, e^{-\left(28\frac{t}{T_1}\right)^\alpha} - 0.206\, e^{-\left(15\frac{t}{T_1}\right)^\alpha} - 0.068\, e^{-\left(6\frac{t}{T_1}\right)^\alpha} - 0.012\, e^{-\left(\frac{t}{T_1}\right)^\alpha}.$$

$$\mathcal{M}_{\mathrm{G}}(t) = \left(\sqrt{\pi/2}\;\sigma_{\log}\right)^{-1} \times \int \mathrm{e}^{-2\left(\log R_1 - \log T_1^{-1}\right)^2/\sigma_{\log}^2}\; M_{\alpha=1}(t, R_1)\; d(\log R_1)$$

$$\downarrow$$

$$\mathcal{M}_{\mathrm{G}}(t) = \int P(\log R_1 - \log T_1^{-1})\; M_{\alpha=1}(t, R_1)\; d(\log R_1)$$

Analysis of Spatial Inhomogeneities I

1. phenomenological fit:
exponent α quantifies disorder strength
good qualitative analysis

2. Convolute with distribution function of T_1

Single T_1

$$\mathcal{M}_\alpha(t, T_1^{-1}) = 1 - 0.714\, e^{-\left(28\frac{t}{T_1}\right)^\alpha} - 0.206\, e^{-\left(15\frac{t}{T_1}\right)^\alpha} - 0.068\, e^{-\left(6\frac{t}{T_1}\right)^\alpha} - 0.012\, e^{-\left(\frac{t}{T_1}\right)^\alpha}.$$

$$\mathcal{M}_\mathrm{G}(t) = (\sqrt{\pi/2}\;\sigma_{\log})^{-1} \times \int \mathrm{e}^{-2\left(\log R_1 - \log T_1^{-1}\right)^2/\sigma_{\log}^2}\; M_{\alpha=1}(t, R_1)\; d(\log R_1)$$

$$\downarrow$$

$$\mathcal{M}_\mathrm{G}(t) = \int P(\log R_1 - \log T_1^{-1})\; M_{\alpha=1}(t, R_1)\; d(\log R_1)$$

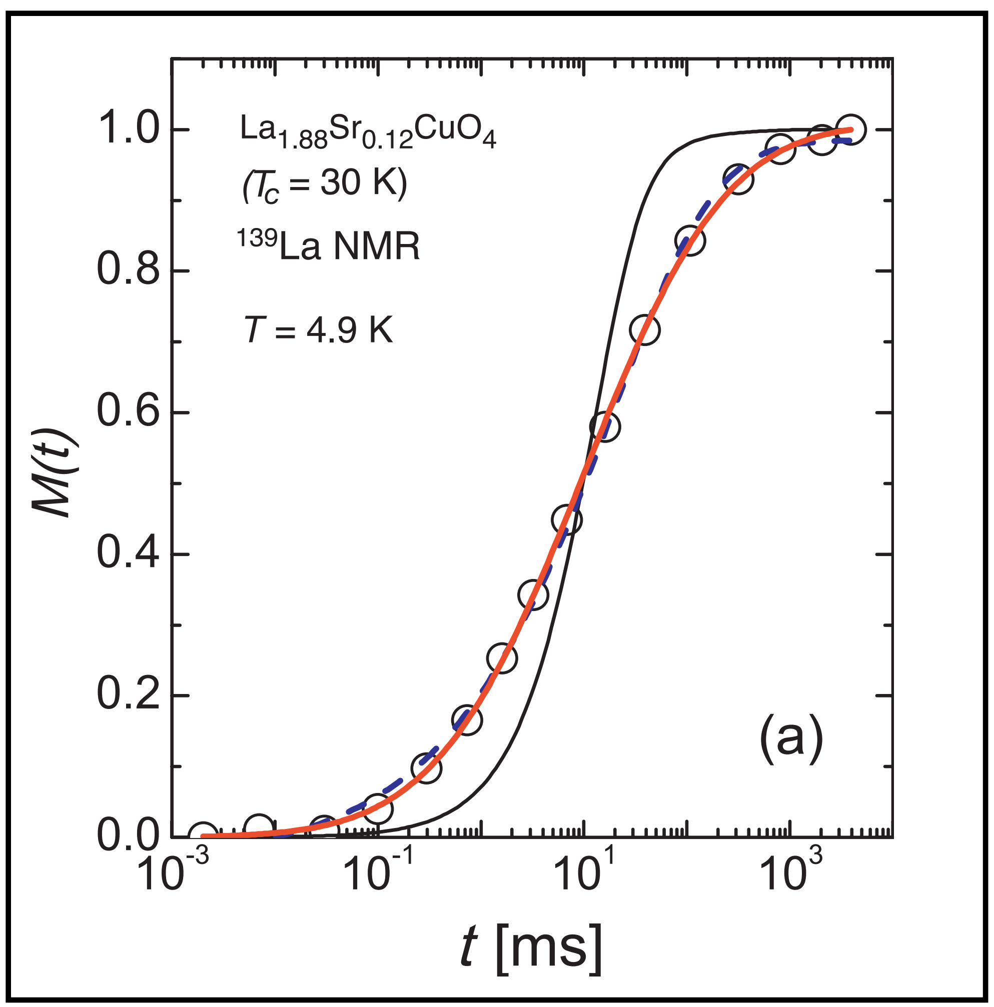

T_1 Distribution: x = 12 % (T_c= 30 K)

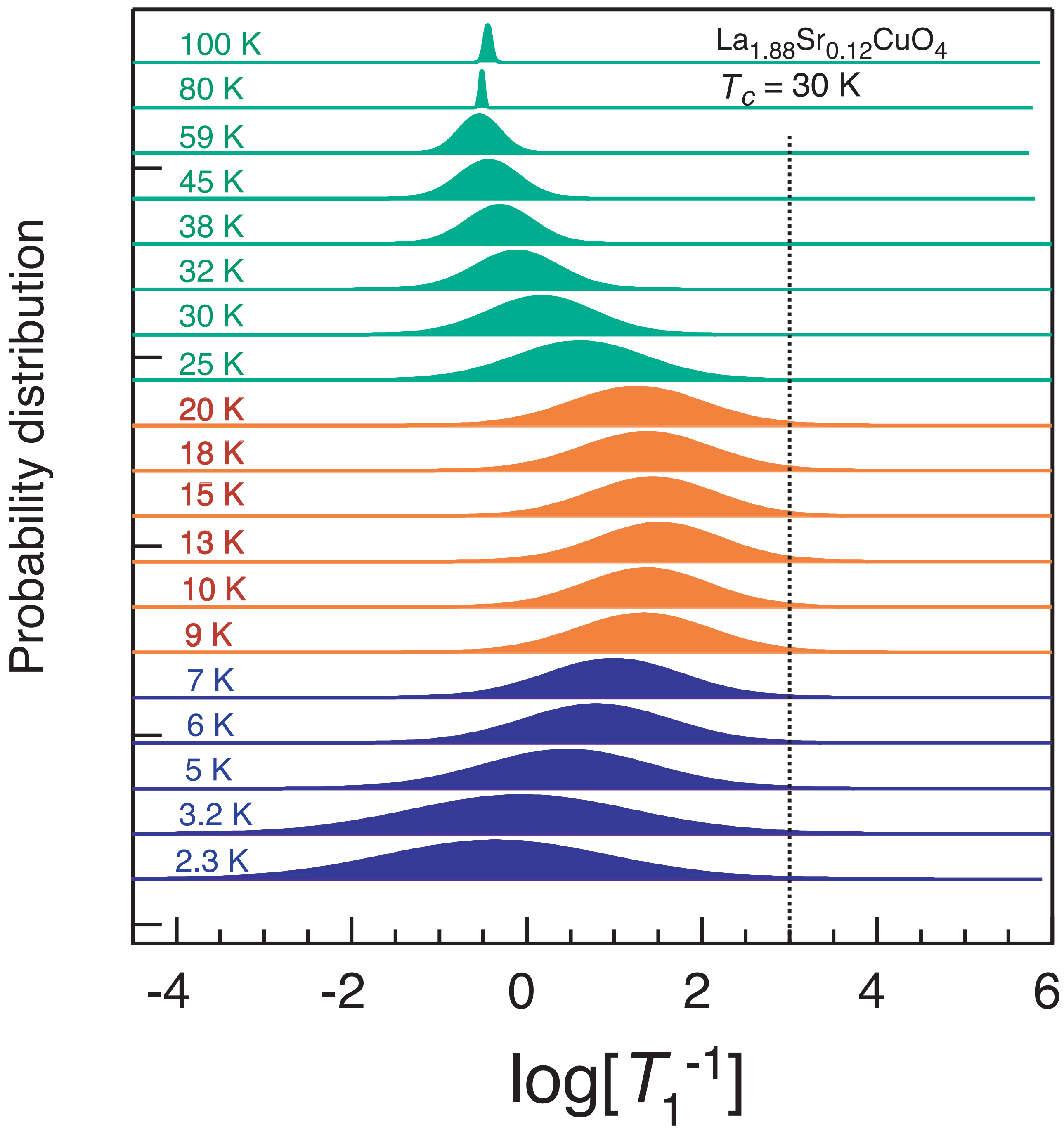

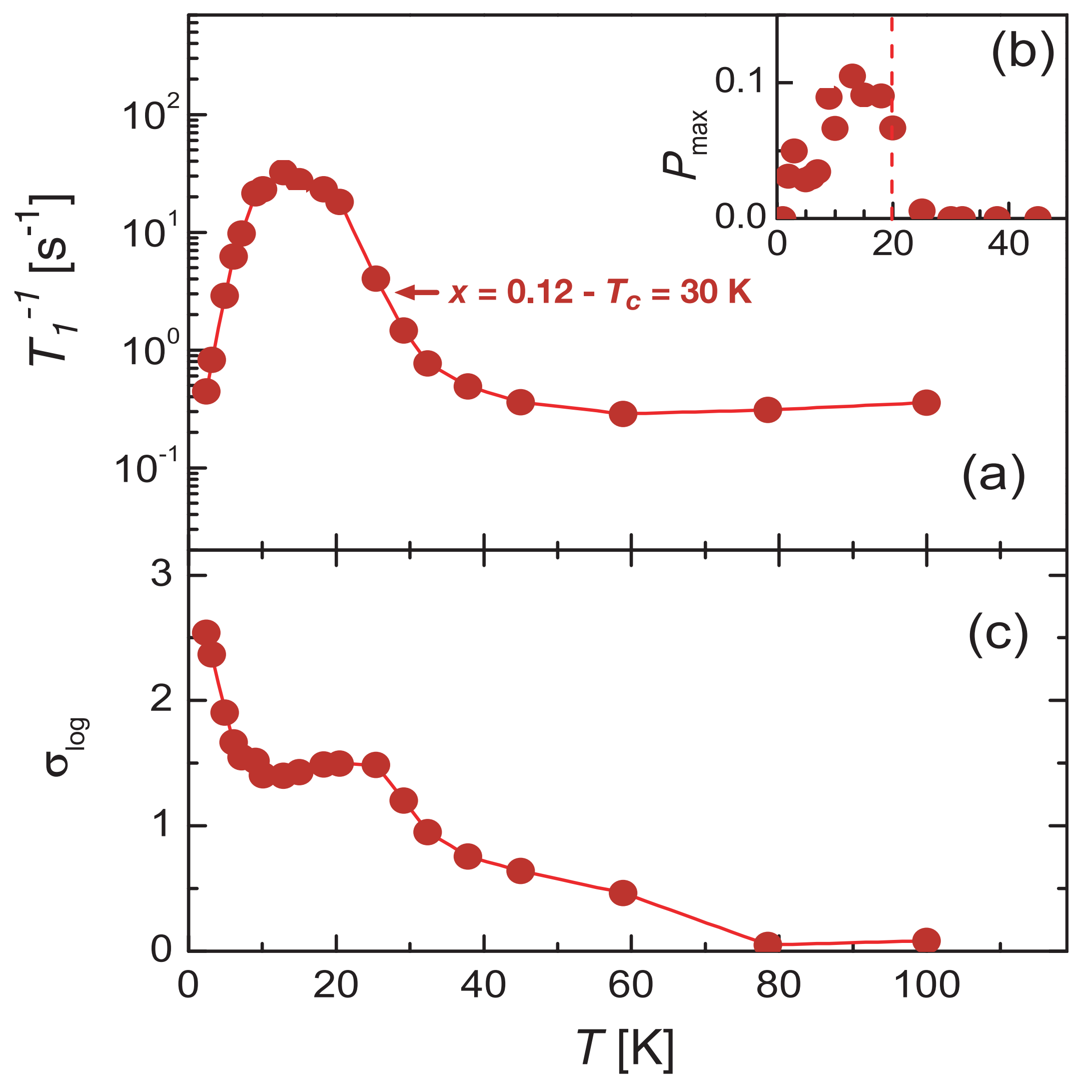

$$\left(T_1^{-1}\right)_{average} \approx \left(T_1^{-1}\right)_{\alpha}$$

$$\alpha \propto \sigma_{\log}$$

- T_g from μSR = 20 K
- Inhomogeneities develop below ~ 80 K

Probing spin dynamics with T_1

Time fluctuations of the hyperfine field

$$\frac{1}{T_1} = \frac{\gamma_n^2}{2}(A)^2 \int_{-\infty}^{+\infty} \langle S(0)S(t)\rangle e^{i\omega_n t} dt \propto J(\omega_n)$$

Simple Model:

$$\langle S(0)S(t)\rangle = S_\perp^2 e^{-t/\tau_c} \xrightarrow[\text{BPP}]{} \frac{1}{T_1} \propto \frac{\tau_c}{1+\omega_n^2\tau_c^2}$$

Slowing down of fluctuations

$\tau_c \rightarrow \infty$

***T_1^{-1}* enhancement**

until maximum when $\tau_c^{-1} = \omega_n$

T_1 Distribution: x = 12 % (T_c= 30 K)

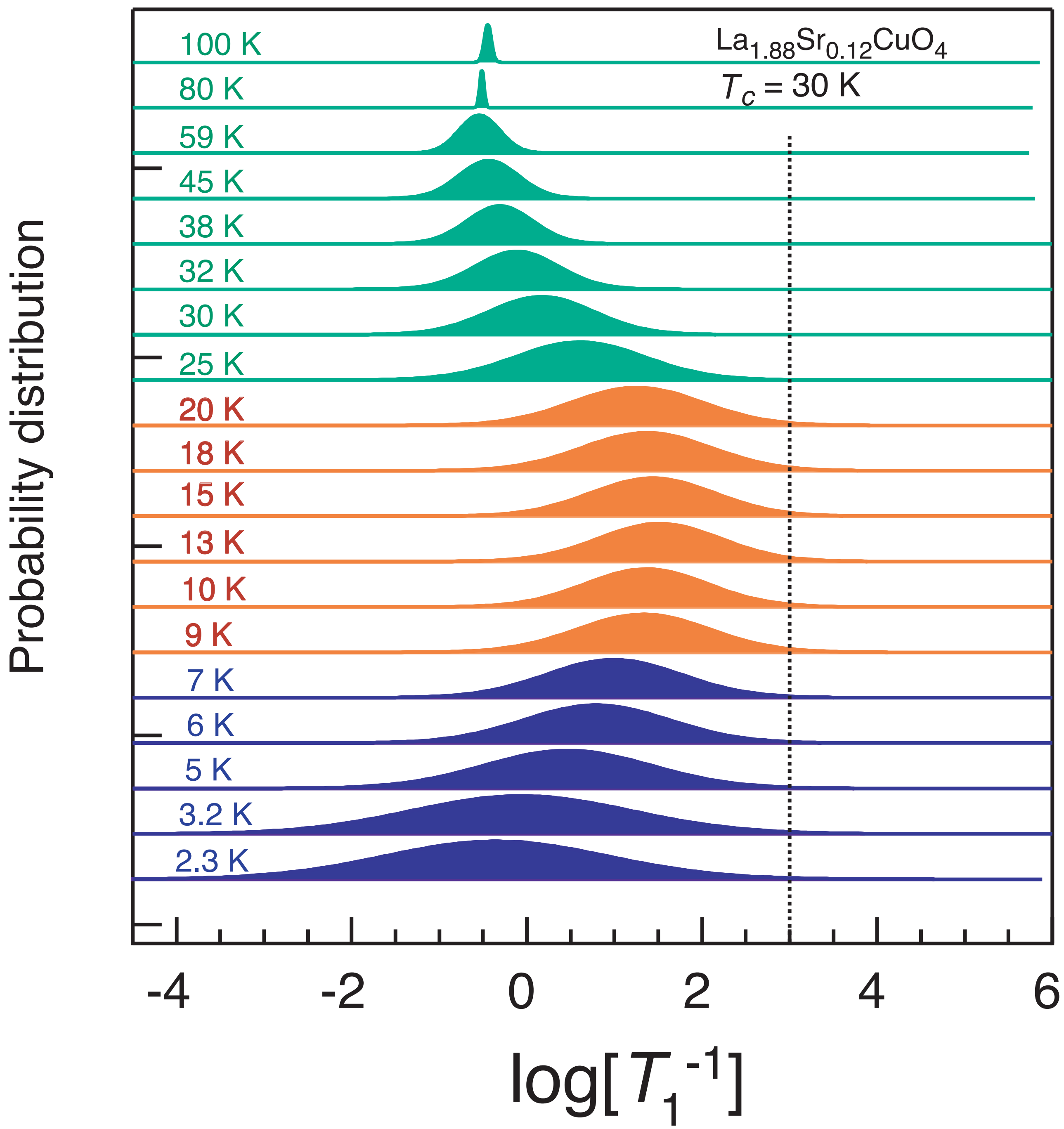

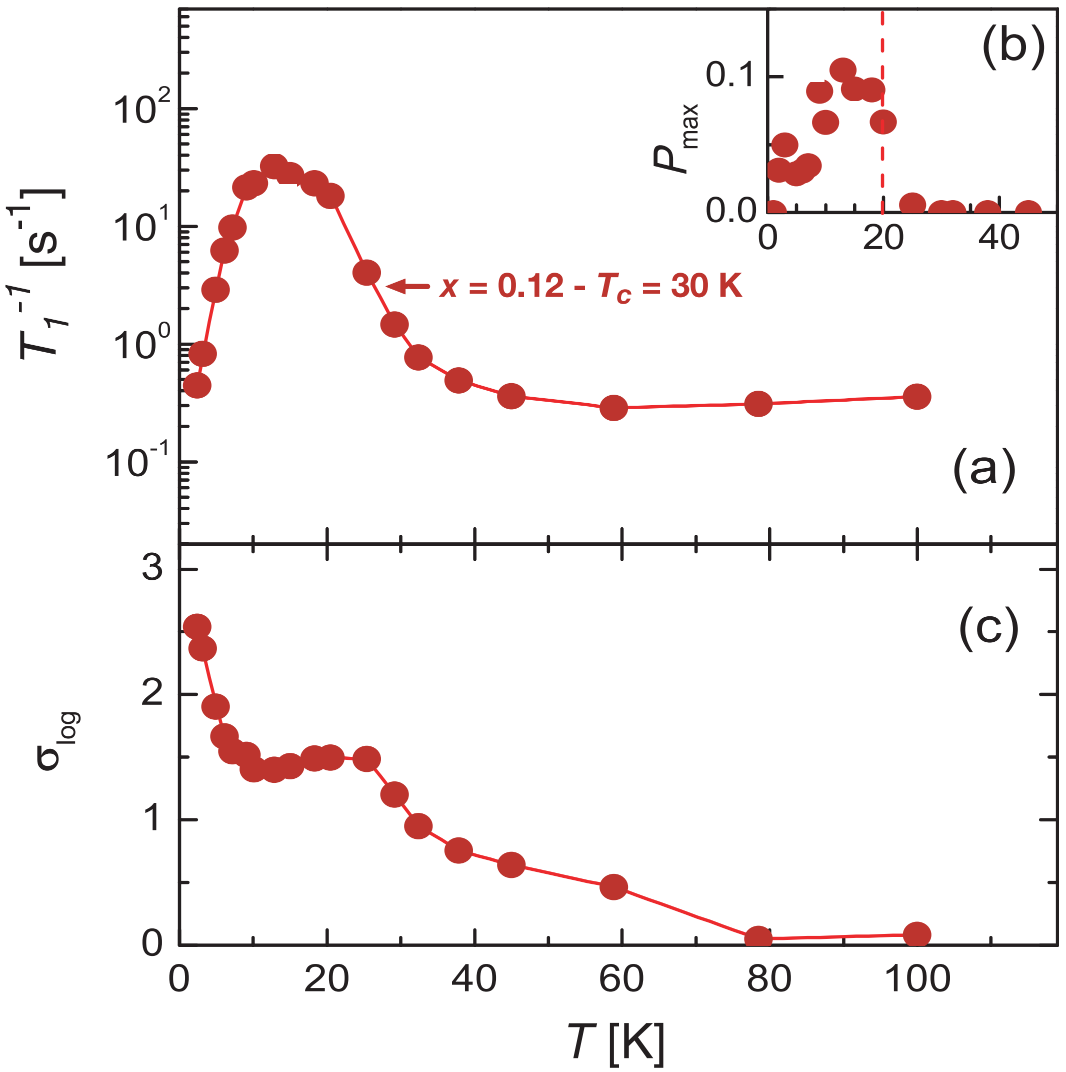

$$\left(T_1^{-1}\right)_{average} \approx \left(T_1^{-1}\right)_{\alpha}$$

$$\alpha \propto \sigma_{\log}$$

- T_g from μSR = 20 K
- Inhomogeneities develop below ~ 80 K

Spatial inhomogeneities (Vortex States)

Case 1.
Spatially resolved measurement

Case 2. Not resolved

$\Longrightarrow$ phenomenological fit

exponent α quantifies disorder strength

Case 3. Not resolved

$\Longrightarrow$ convolute with distribution function

$\Longrightarrow$ deduce parameters

Real Space Magnetic Field Distribution in the Vortex Lattice

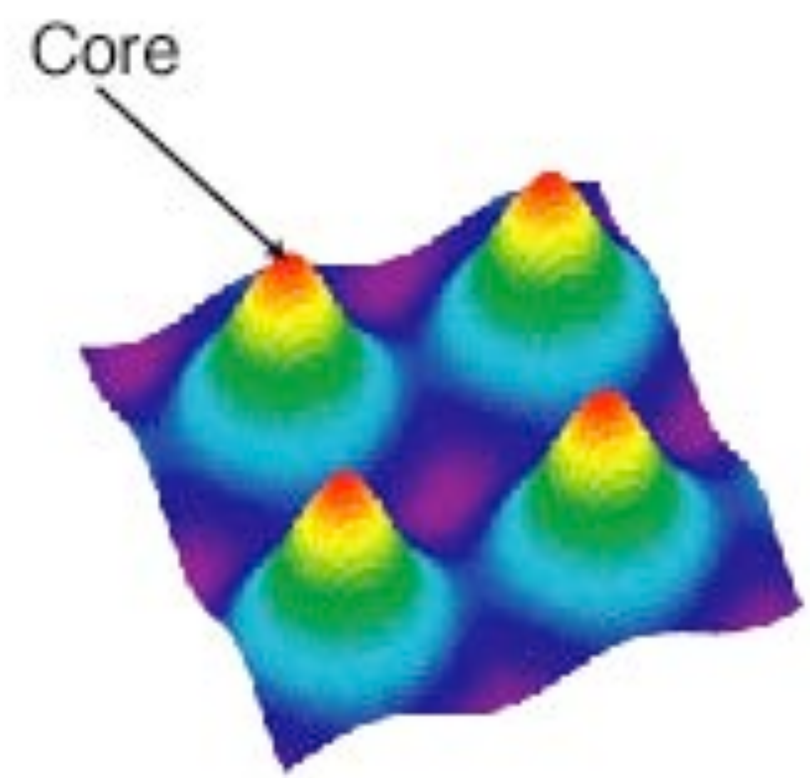

NMR Microscopy

Field Probability Distribution ~ NMR Spectrum

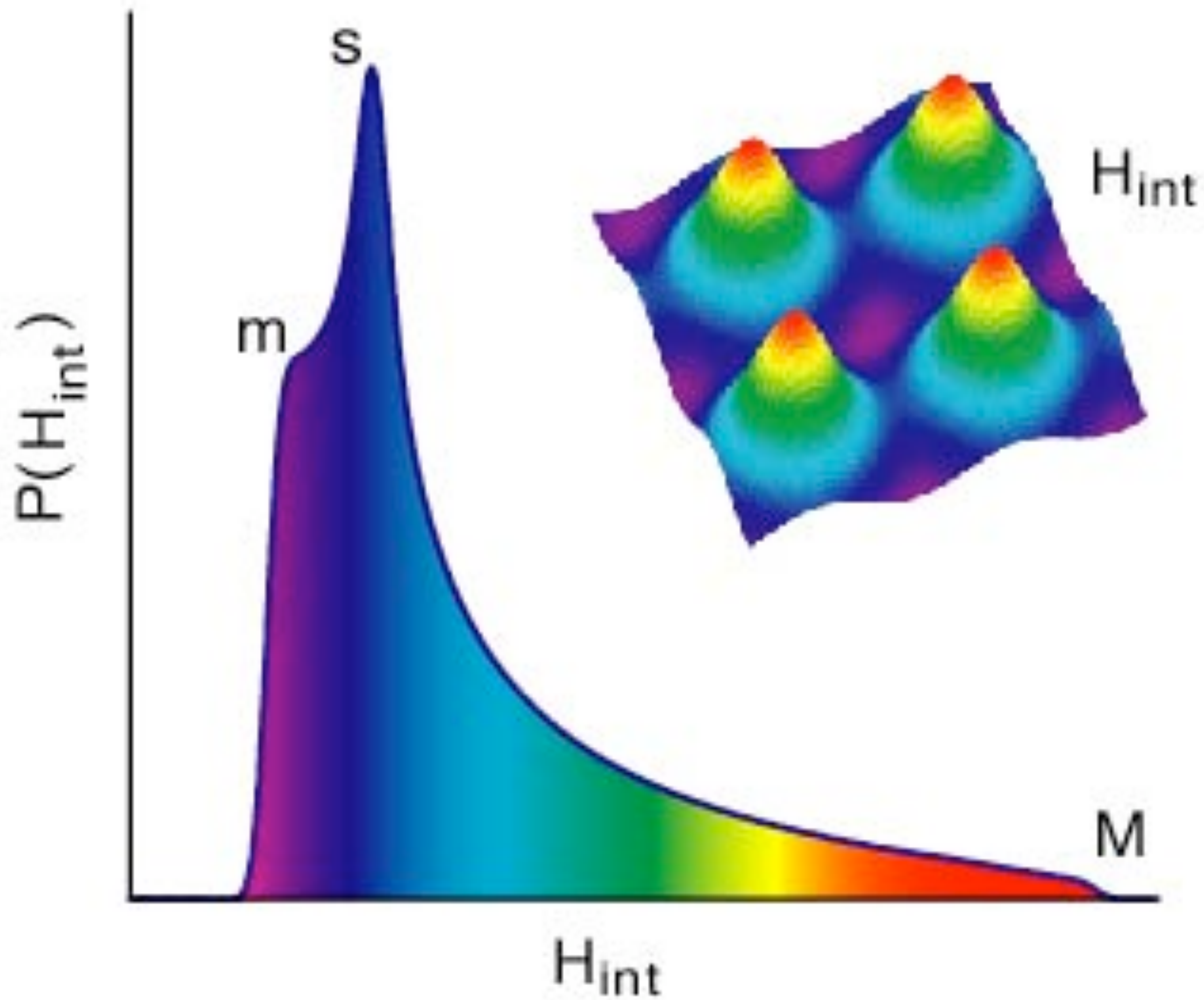

M. Takigawa *et al*.,
PRL **83**, 3057 (1999)
-R. Wortis *et al*.,
PRB **61**, 12342 (2000)
-D. Morr and R. Wortis,
PRB **61**, R882 (2000)
-N. J. Curro *et al*.,
PRB **62**, 3473 (2000)

Normal State vs. Low Temperature Spectra

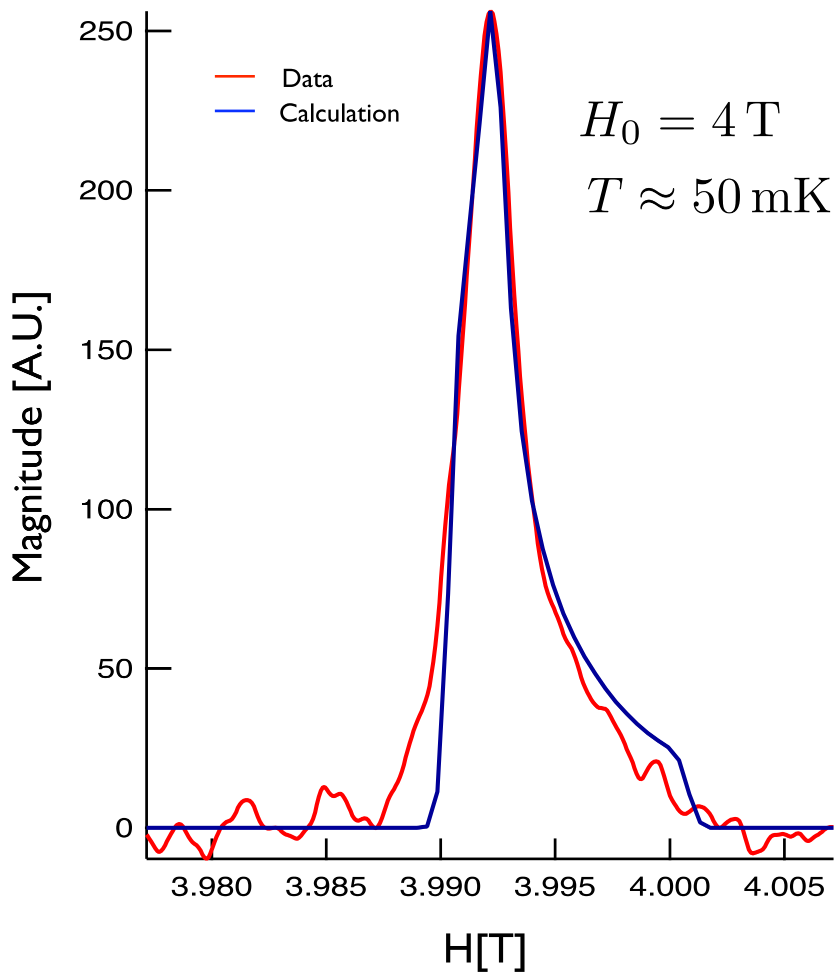

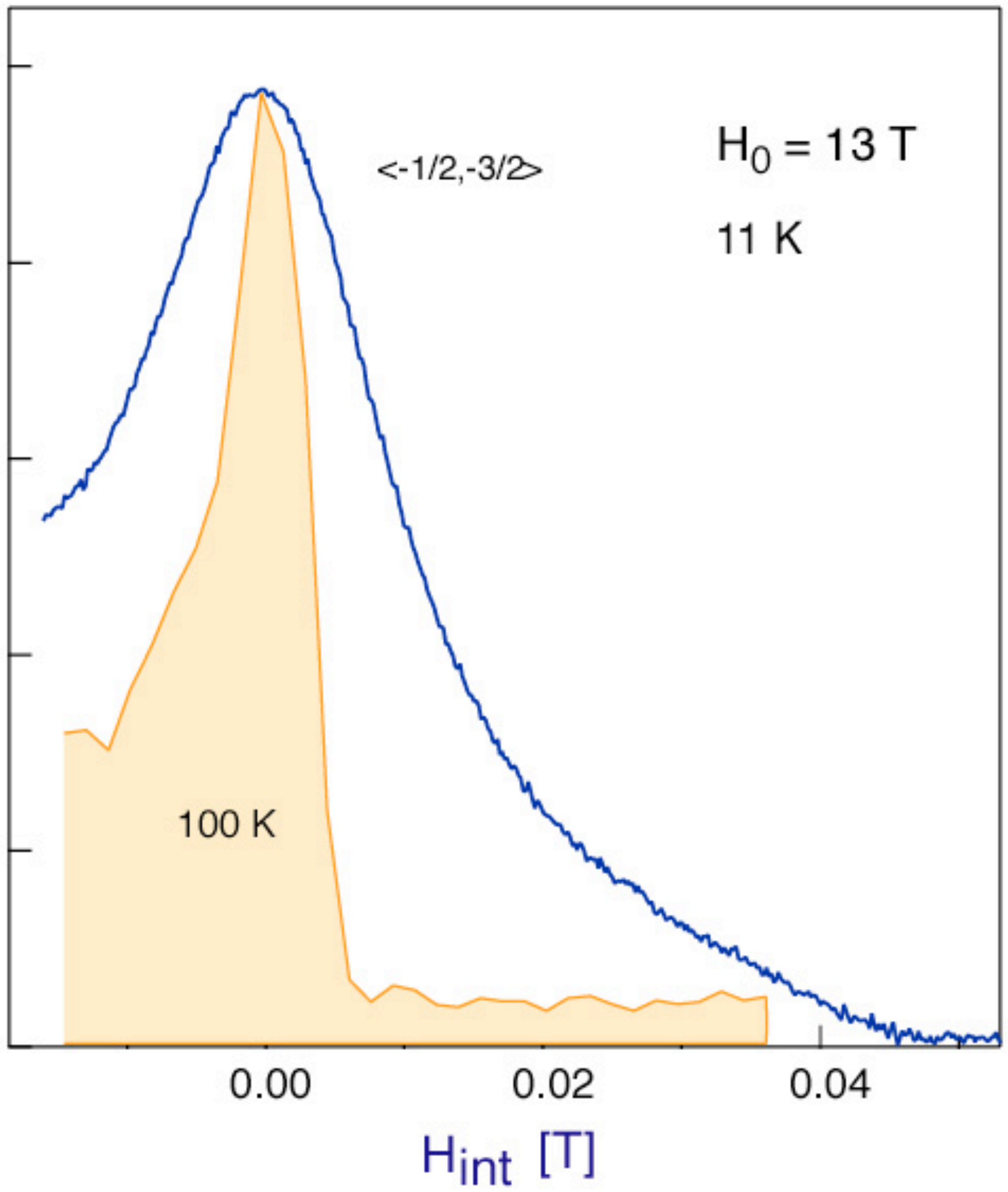

Normal State vs. Low Temperature Spectra

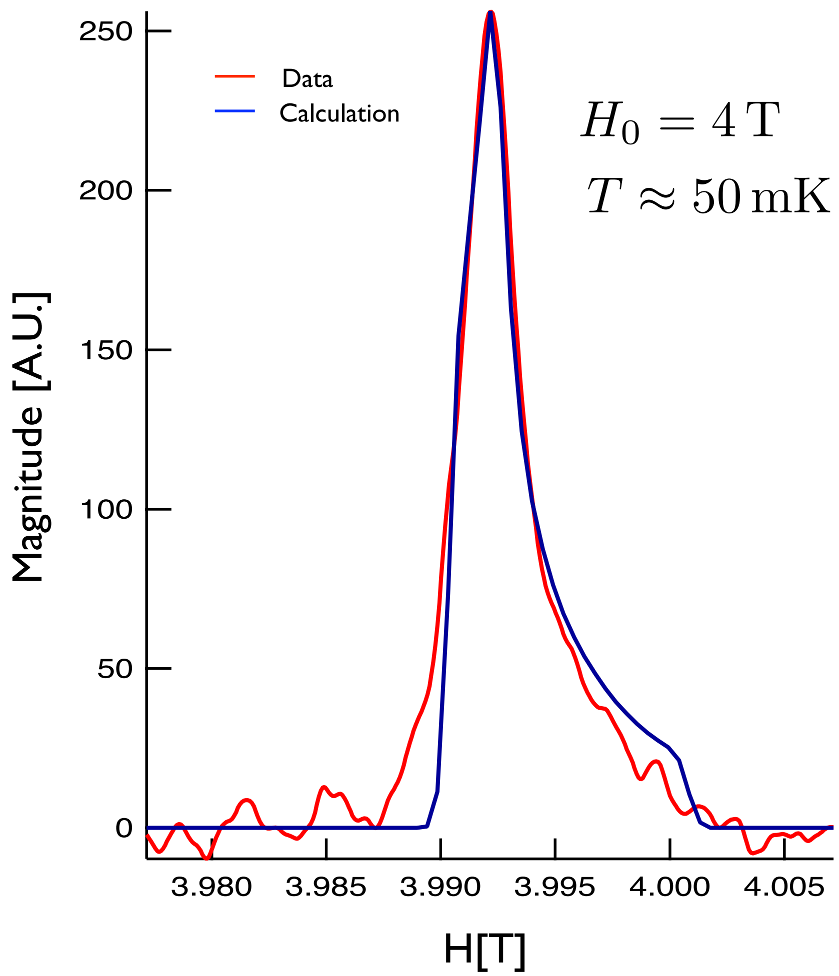

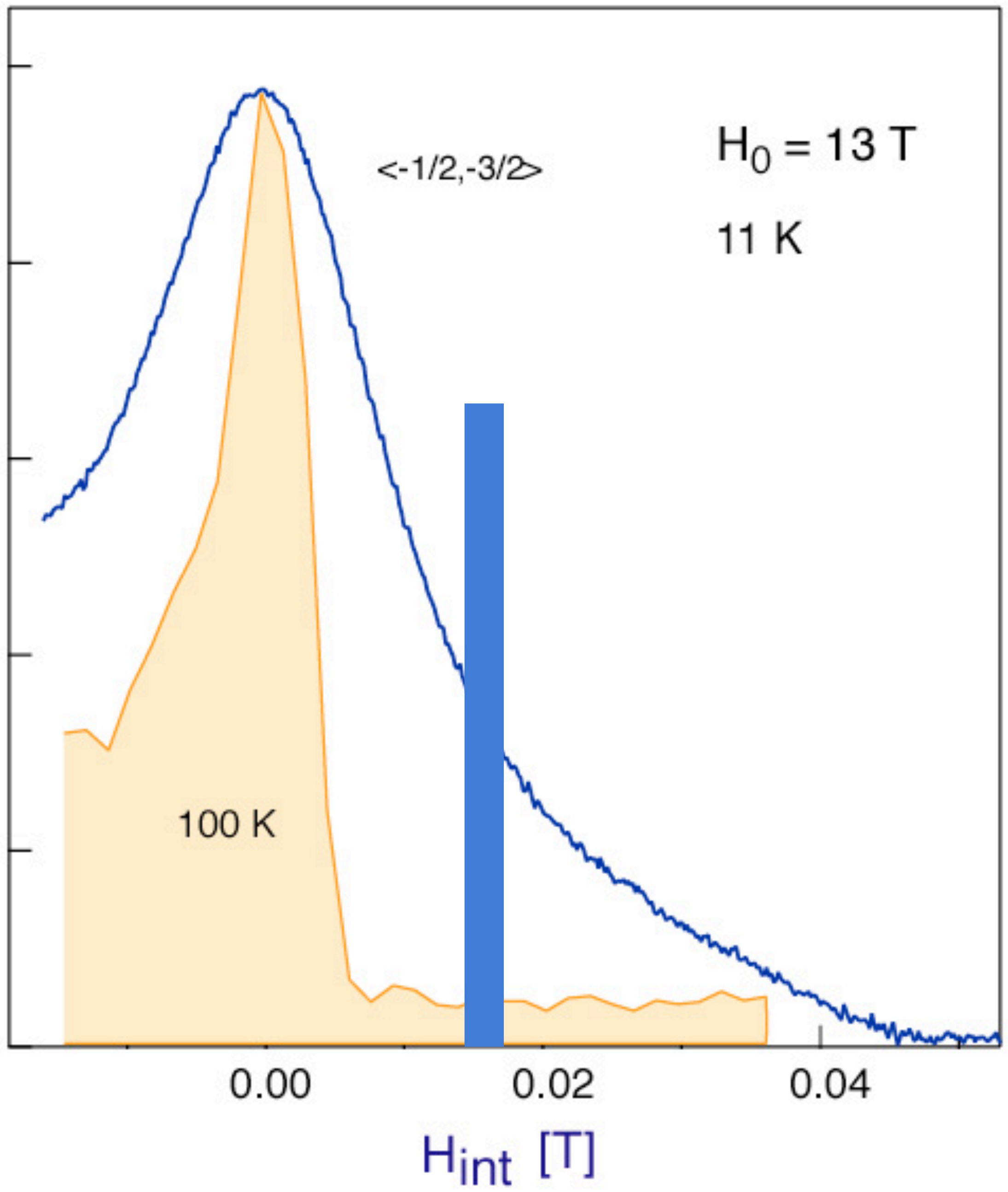

Spectra - $f(T_R)$

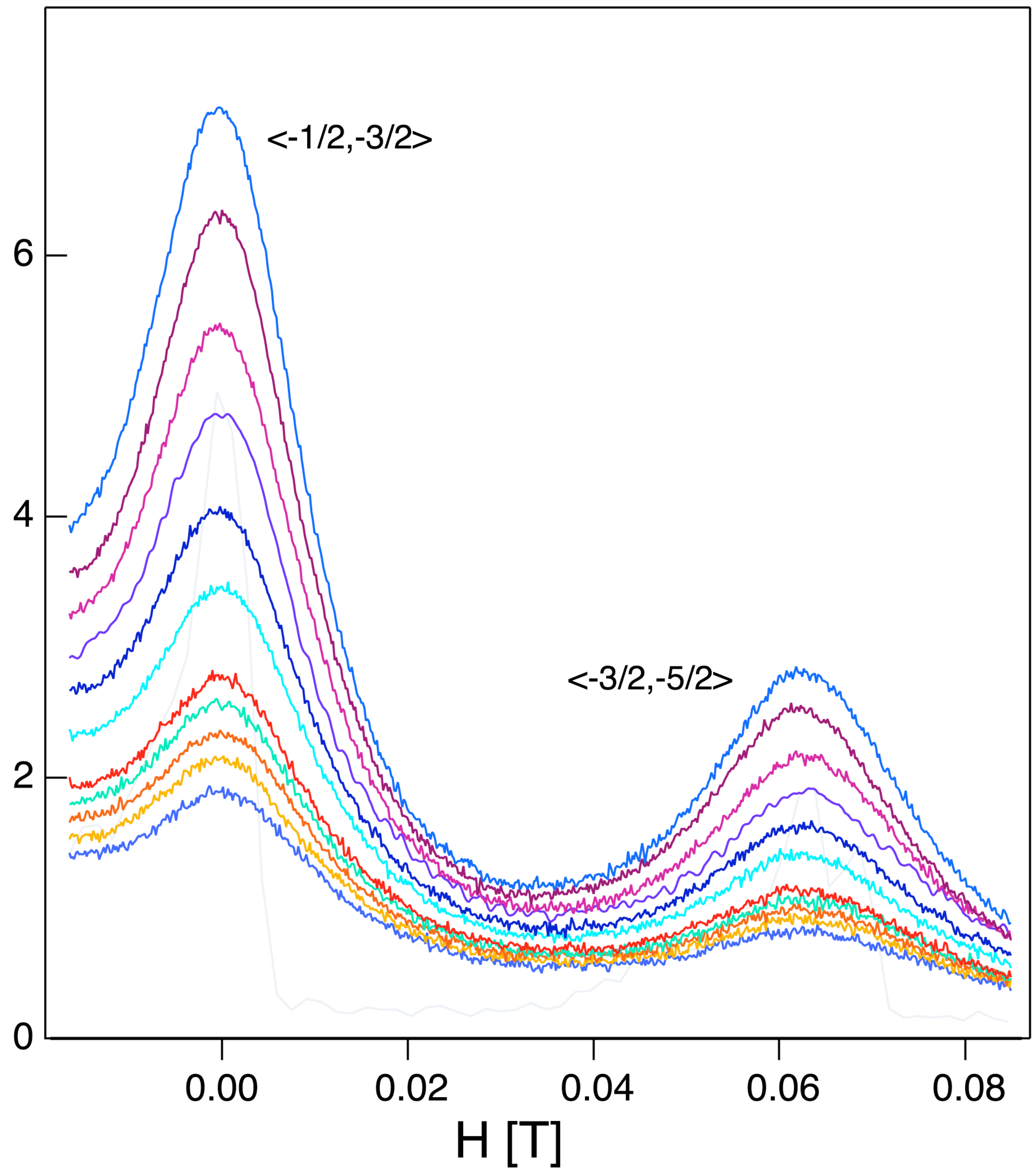

Spectra - $f(T_R)$

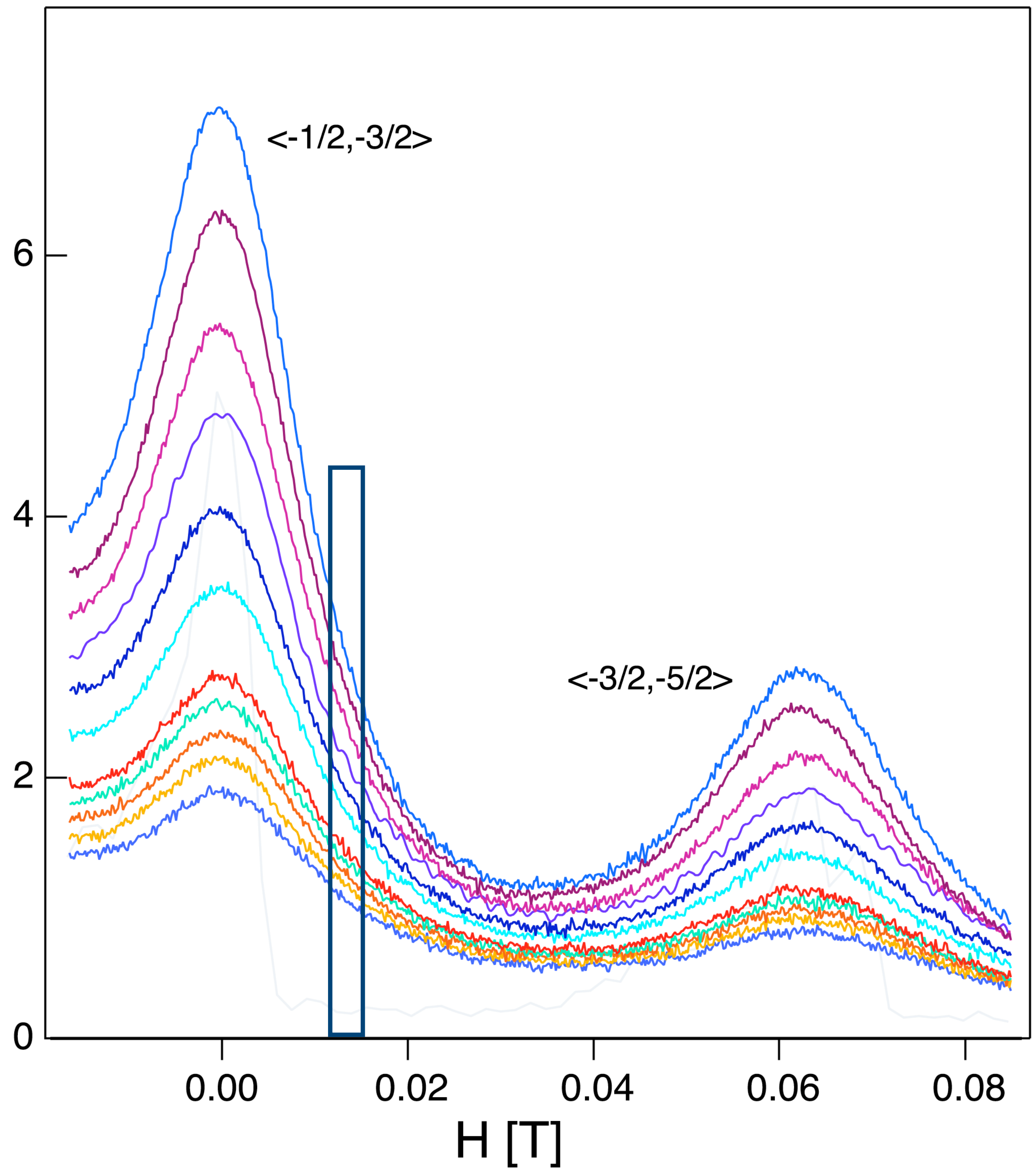

Low Temperature T_1 vs. H_0 & H_{int}

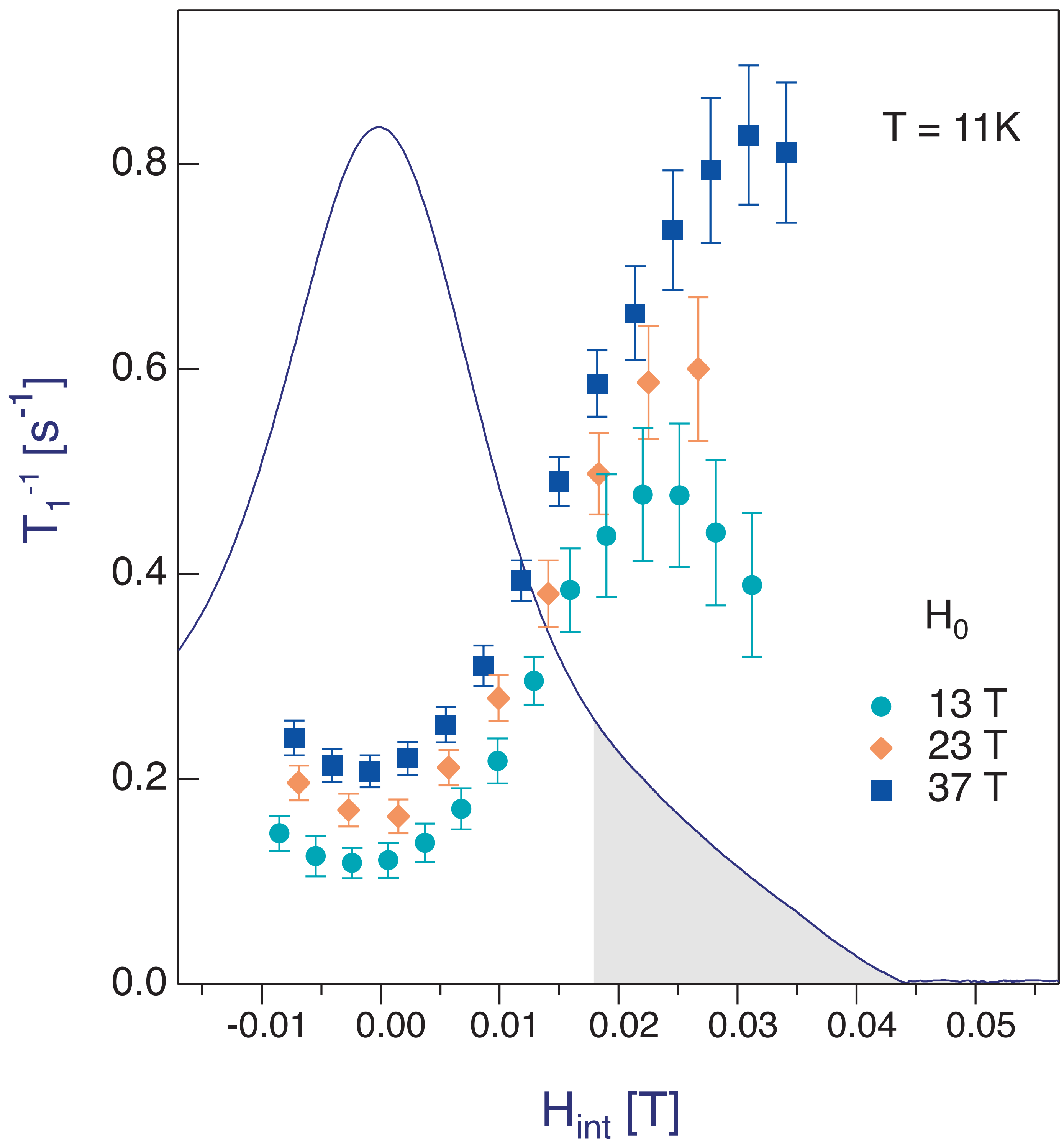

Low Temperature T_1 vs. H_0 & H_{int}

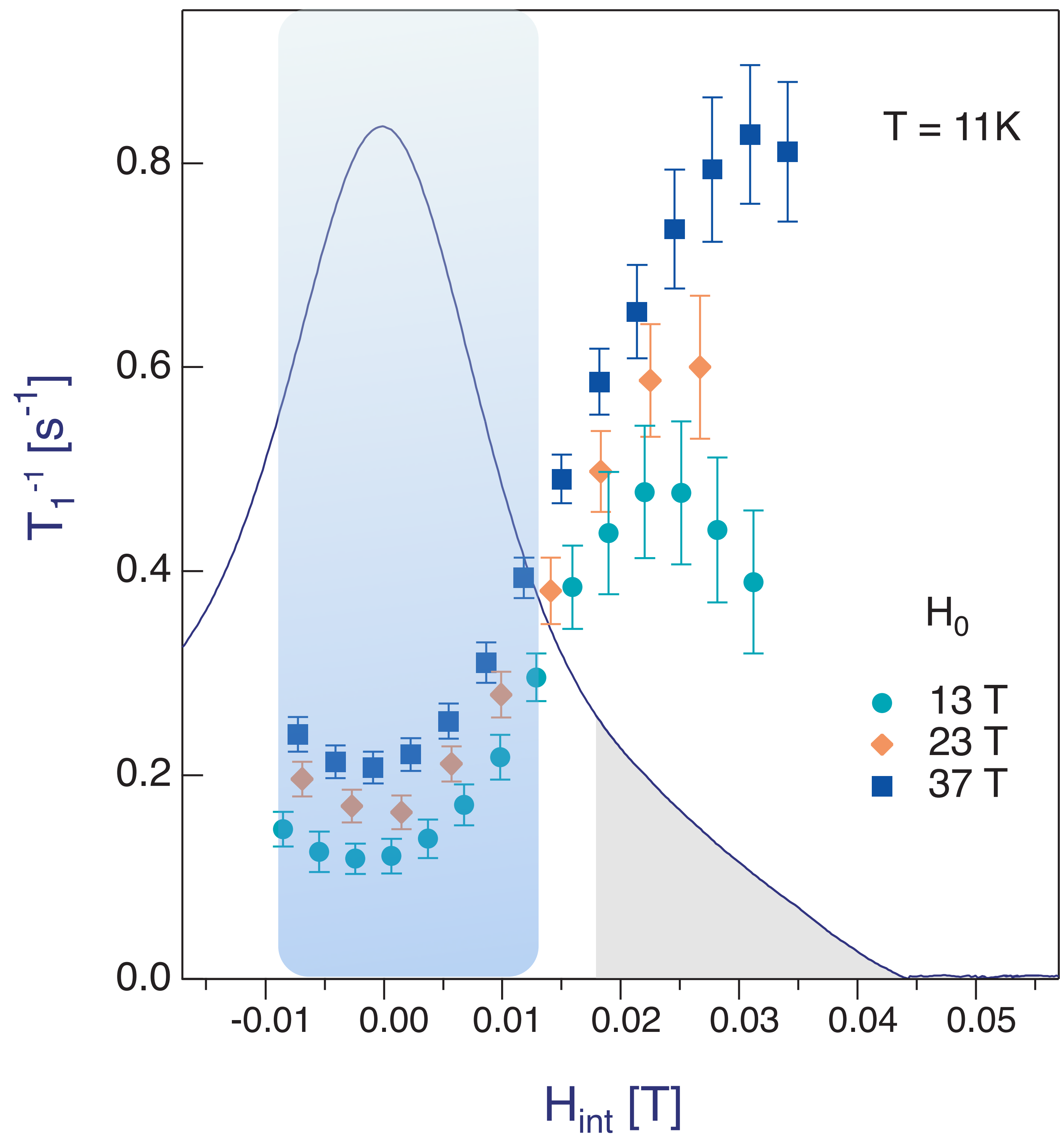

Low Temperature T_1 vs. H_0 & H_{int}

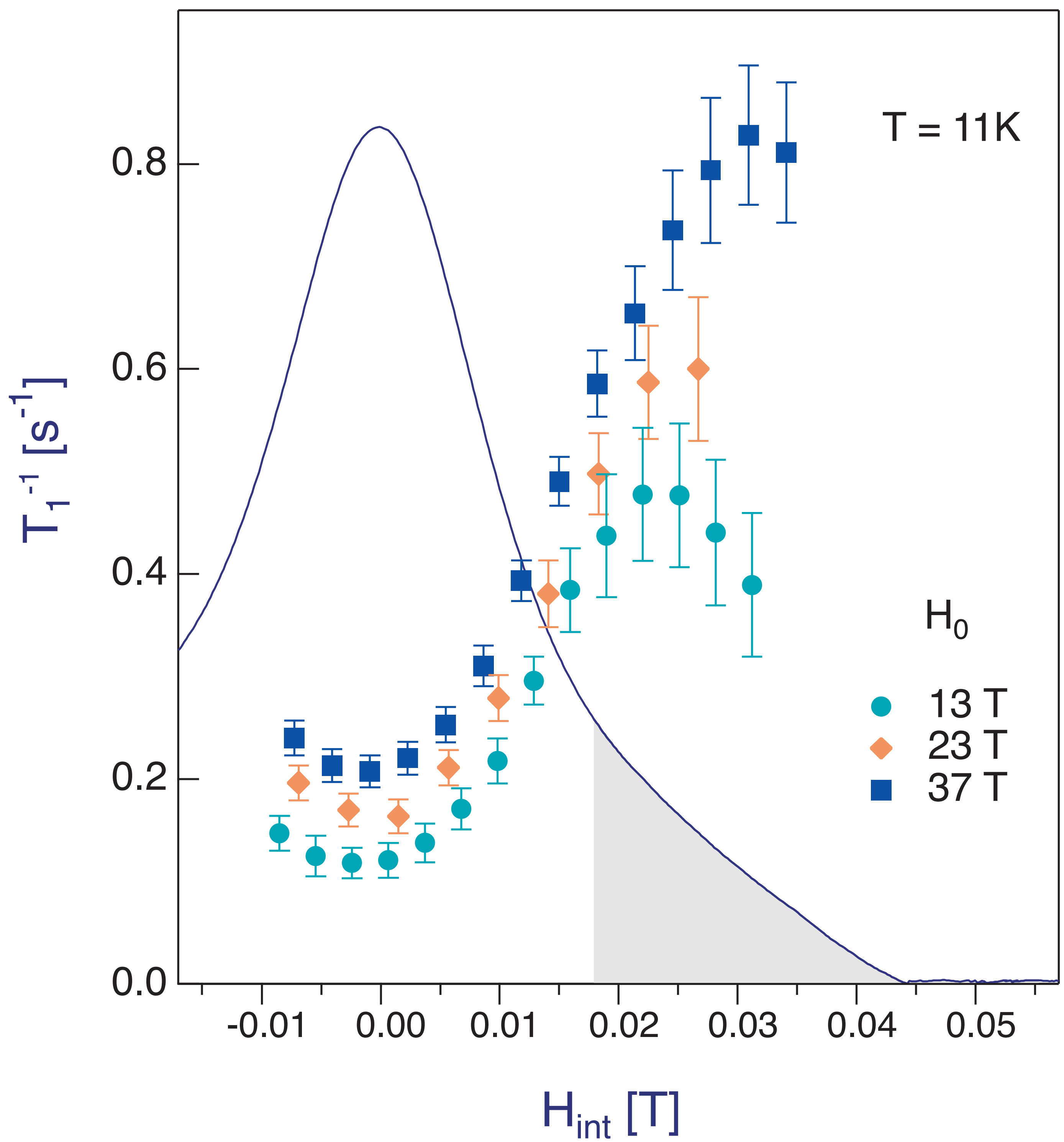

Low Temperature T_1 vs. H_0 & H_{int}

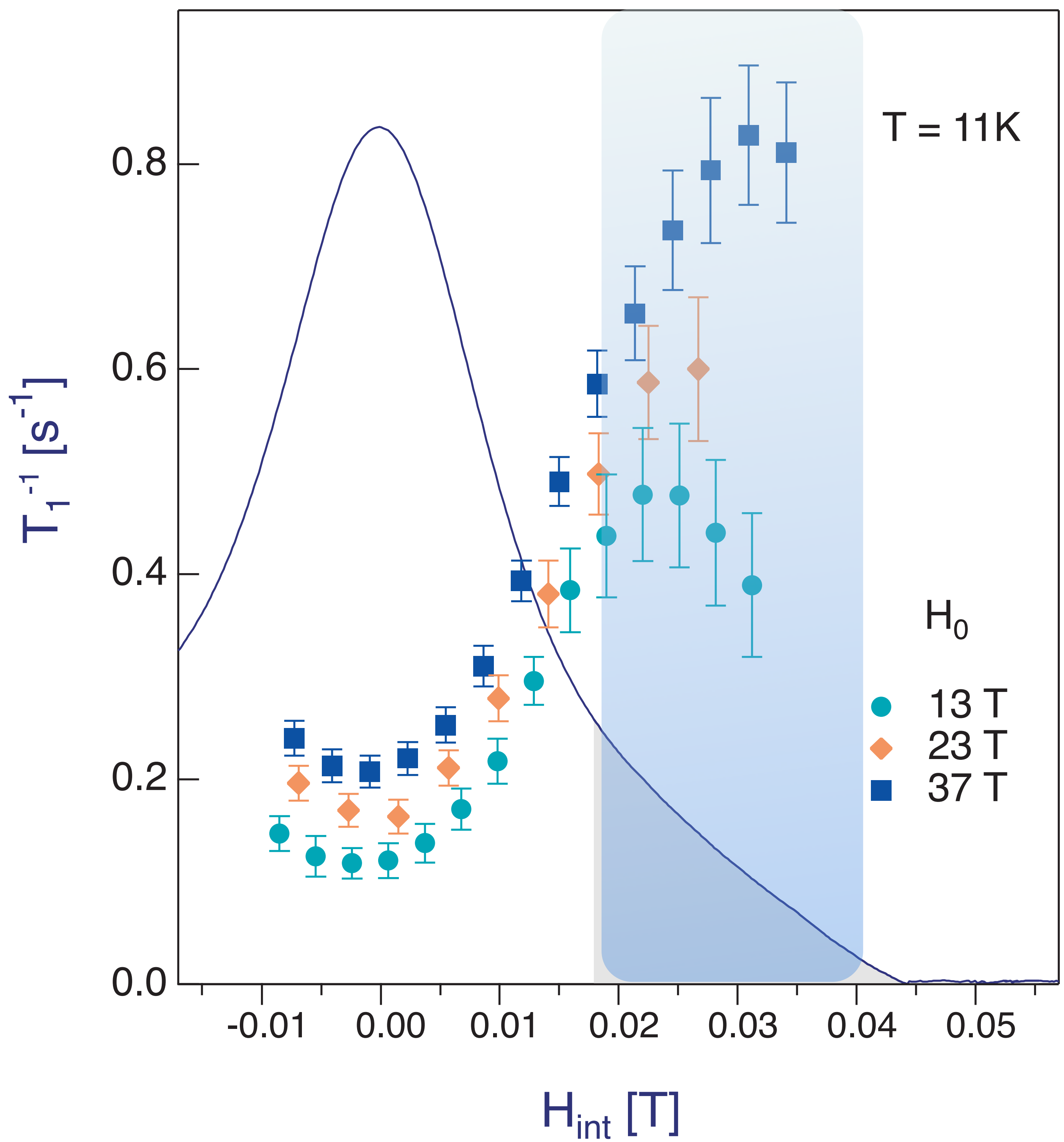

Outside the Cores

- T_1^{-1} increases with increasing H_0
- T_1^{-1} increases with increasing H_{int}, *i.e.* on approaching vortex core
- $(TT_1)^{-1} = Constant$
- T_1 lower then inside

Low Energy Excitations

s-wave

Low energy excitations ***bound*** to the core region and

and occupy a fraction ~ $B\backslash H_{c2}$

(Caroli-deGennes-Matricon States).

C. Caroli, P. G. deGennes, J. Matricon, J., Phys. Lett. **9**, 307, (1964)

H. F. Hess *et al*., PRL **62,** 214, (1989)

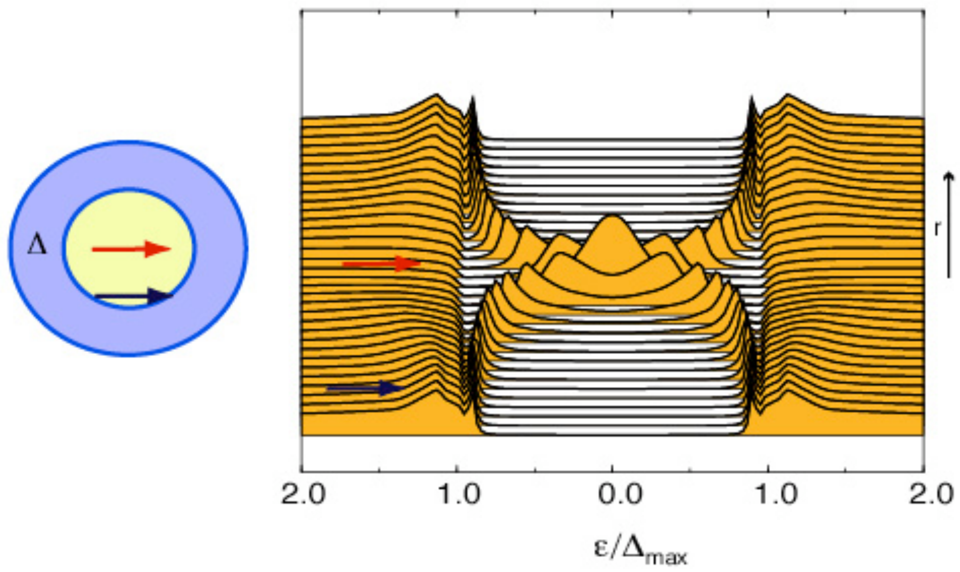

d-wave

Low energy excitations **extended** along

nodal directions.

G. E. Volovik, JETP Lett. **58**, 469 (1993)

Nature of the core states?

I. Maggio-Aprile *et al*., PRL **75**, 2754 (1995)

Ch. Renner Ch. *et al*., PRL **80**, 3603 (1998)

S. H. Pan *et al*., PRL **85**, 1536 (2000)

J. E. Hoffman *et al*., Science **295**, 452 (2002)

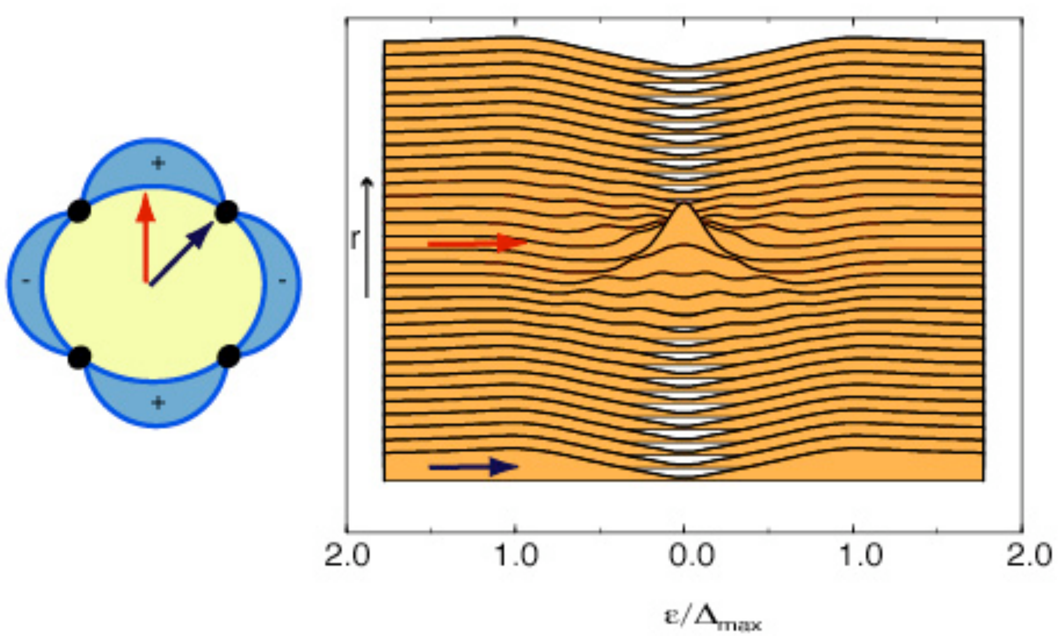

Outside the Cores - Energy Spectrum of Nodal QP

$$T_1^{-1} \propto \langle N_i(E) N_f(E) \rangle$$

In the nodal region quasiparticle DOS varies linearly on energy

T_1 depends on the product of initial and final QP energies

QP energy depends on temperature, applied field, and internal field

$$E_k = \sqrt{\epsilon_k^2 + \Delta_k^2} \pm \frac{1}{2}\gamma_e \hbar H_0 + \vec{v}_f(k) \cdot \vec{p}_s = E_T \pm Z + D$$

Low Temperature T_1 vs. H_0 & H_{int}

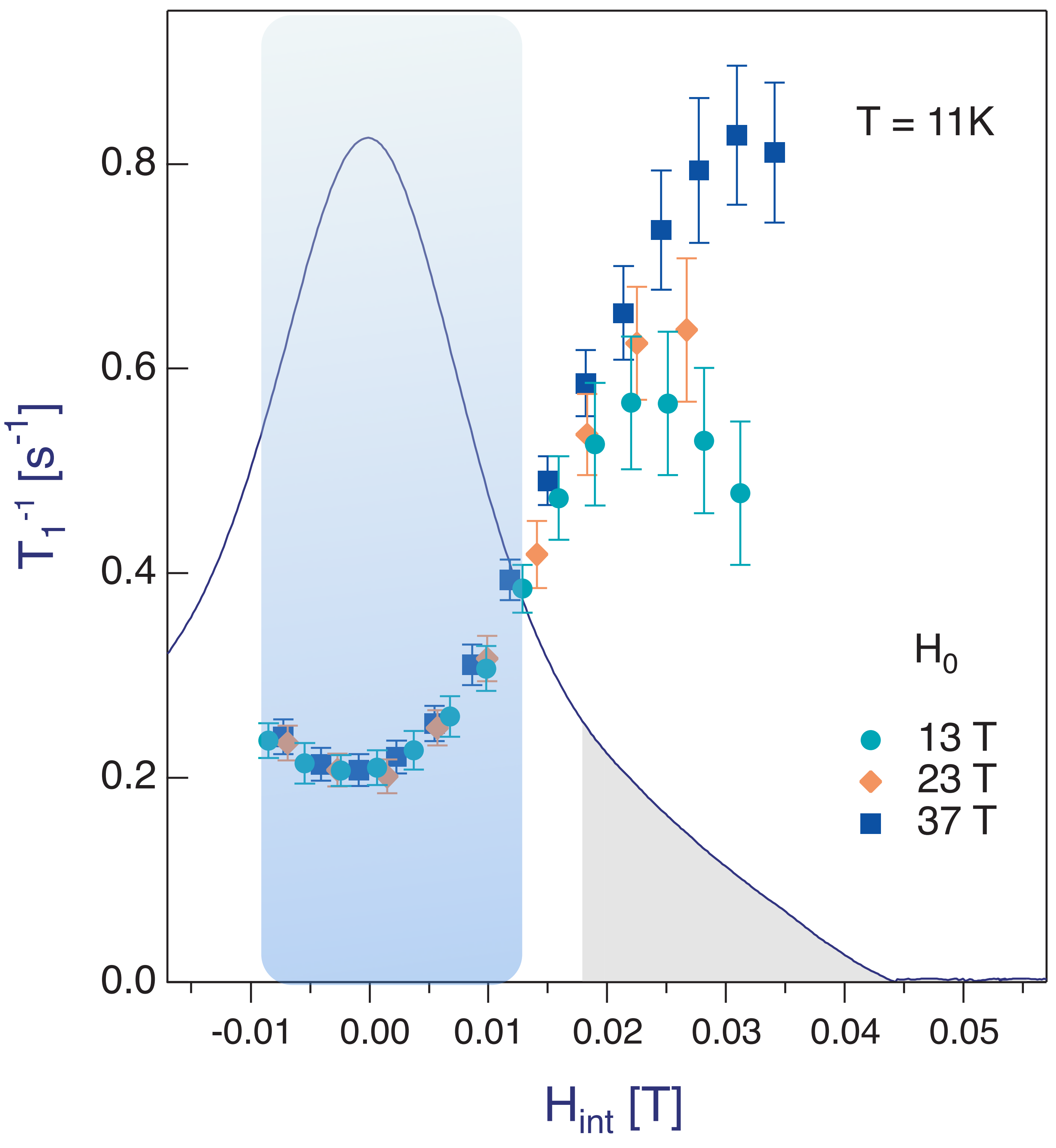

Outside the Cores - Energy Spectrum of Nodal QP

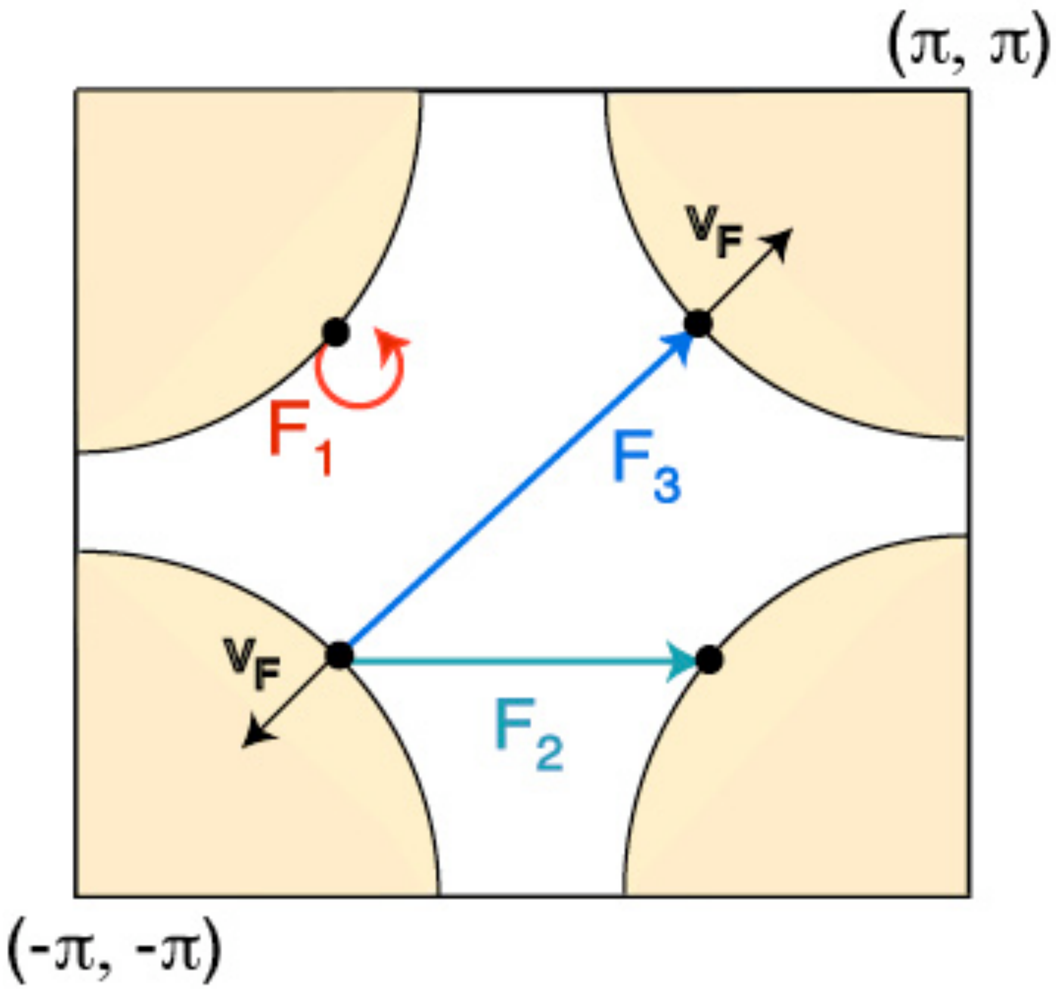

$$T_1^{-1} \propto \langle N_i(E) N_f(E) \rangle \propto \langle E_i E_f \rangle$$

$$E_k = E_T \pm Z + D$$

$$\boxed{T_1^{-1} \propto |E_T + D_i + Z| \; |E_T + D_f - Z|}$$

$$\boxed{T_1^{-1} \sim \left| D^2 - Z^2 \right|}$$ **F_1**

$$\boxed{T_1^{-1} \sim \left| D^2 + Z^2 \right|}$$ **F_3**

Outside the Cores - Energy Spectrum of Nodal QP

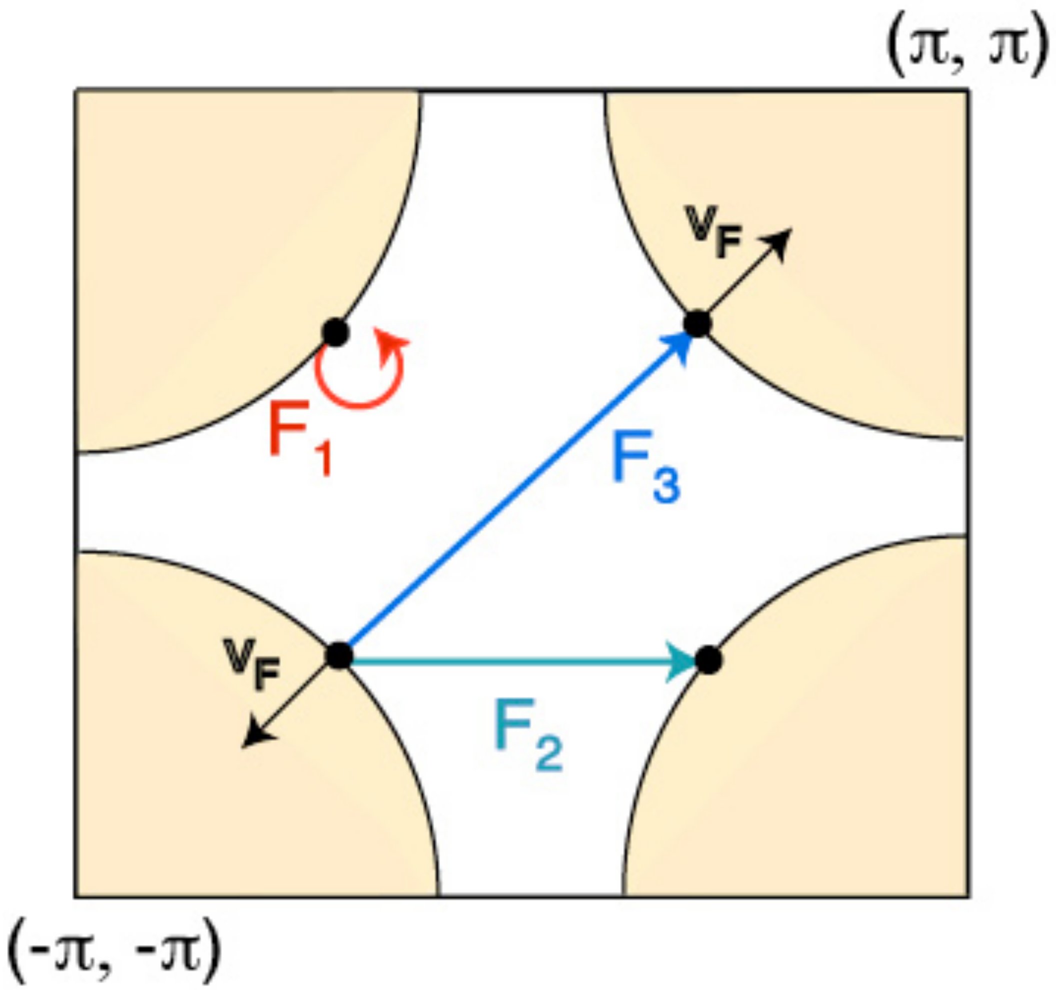

$$\boxed{T_1^{-1} \sim \left|D^2 + Z^2\right|}$$

$\mathbf{F_3}$

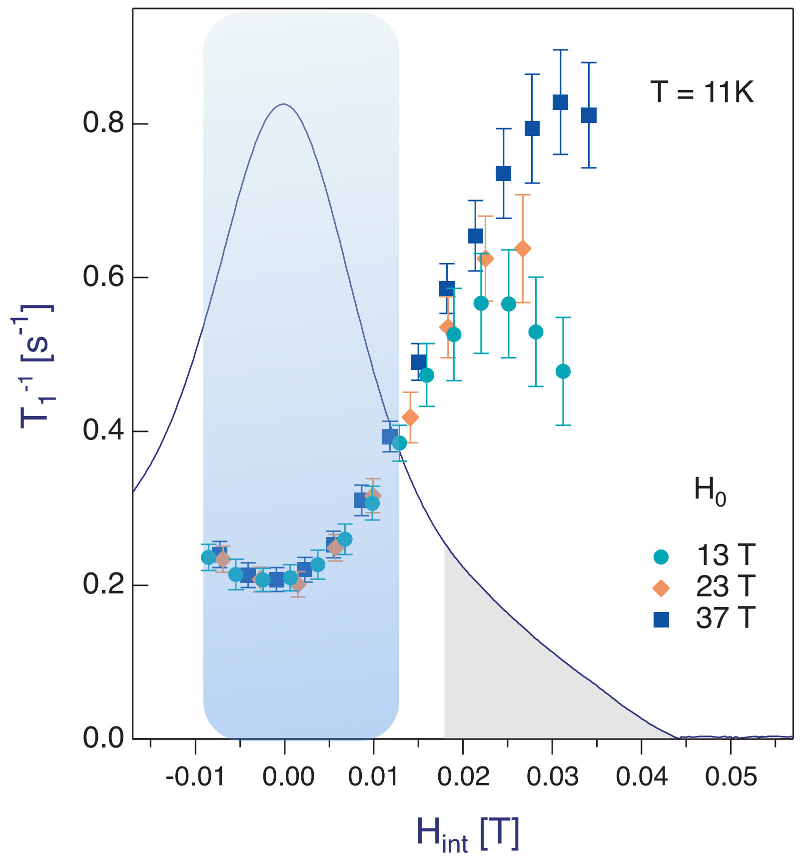

$\mathbf{F_3}$ dominant scattering process

BUT $q \sim (\pi, \pi)$ required => QP are **AF correlated**

Spatial inhomogeneities (FFLO)

The destruction of SC by a magnetic field.

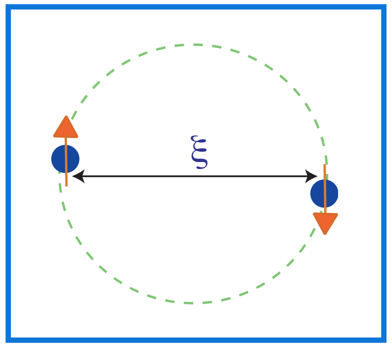

I. Orbital Effect

↓

Abrikosov Vortex Lattice

↓

G-L Equation: $H_{c_2}^{orb} = \dfrac{\Phi_0}{2\pi\xi^2}$

II. Pauli paramagnetism

↓

Cooper-pairs Breaking

↓

$$E_P = E_c \Rightarrow H_{c_2}^{P} = \frac{\sqrt{2}\Delta}{g\mu_B}$$

$$\frac{1}{2}\chi_n H_0^2 = \frac{1}{2}N(0)\Delta^2$$

$$\chi_n = \frac{1}{2}(g\mu_B)^2 N_0$$

➡ Relative importance of the two effects described by the Maki Parameter: $\alpha = \sqrt{2}\dfrac{H_{c_2}^{orb}}{H_{c_2}^{P}}$

The FFLO State

Basic Idea: Pauli pair breaking dominates over the orbital effects

$$\left(\alpha \equiv \sqrt{2}\frac{H_{C_2}^{orb}}{H_{C_2}^{P}} > 1.8\right)$$

Formation of a new pairing state with finite center-of-mass momentum can reduce the paramagnetic pair-breaking effect. → The critical field can be further enhanced!

P. Fulde and R. A. Ferrell, Phys. Rev. **135**, A550 (1964);
A. I. Larkin and Y. N. Ovchinnikov, Zh. Eksp. Teor. Fiz. **47**, 1136 (1964).

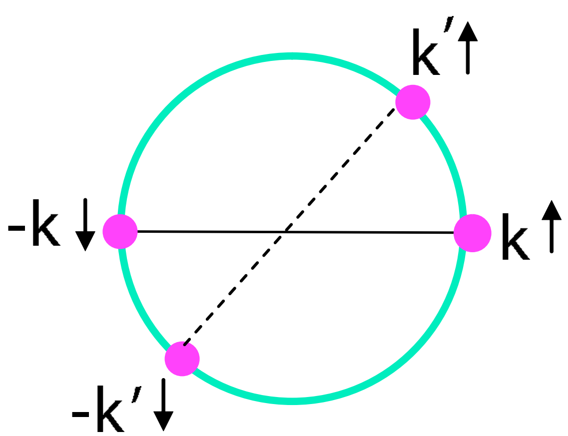

BCS $\left(\vec{k}\uparrow, -\vec{k}\downarrow\right)$

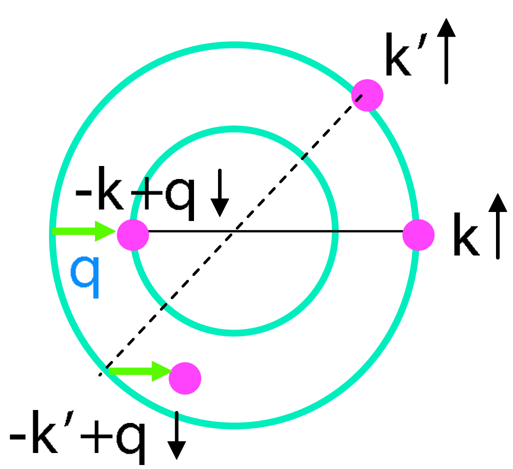

FFLO $\left(\vec{k}\uparrow, -\vec{k}+\vec{q}\downarrow\right)$

$$q \sim \frac{2\mu_B H}{\hbar u_F}$$

The FFLO State

Basic Idea: Pauli pair breaking dominates over the orbital effects $\left(\alpha \equiv \sqrt{2} \frac{H_{C_2}^{orb}}{H_{C_2}^{P}} > 1.8 \right)$

Formation of a new pairing state with finite center-of-mass momentum can reduce the paramagnetic pair-breaking effect. $\Rightarrow$ The critical field can be further enhanced!

P. Fulde and R. A. Ferrell, Phys. Rev. **135**, A550 (1964);
A. I. Larkin and Y. N. Ovchinnikov, Zh. Eksp. Teor. Fiz. **47**, 1136 (1964).

The FFLO State

Finite $\vec{q}$ breaks spatial symmetry. → SC order parameter oscillates in real space.

(FF) $\Delta\left(\vec{r}\right) = |\Delta_q|\, e^{i\vec{q}\cdot\vec{r}}$

(LO) $\Delta\left(\vec{r}\right) = |\Delta_q|\, cos\left(\vec{q}\cdot\vec{r}\right)$

More generally:

$$\Delta\left(\vec{r}\right) = \sum_m \Delta_m e^{i\vec{q_m}\cdot\vec{r}}$$

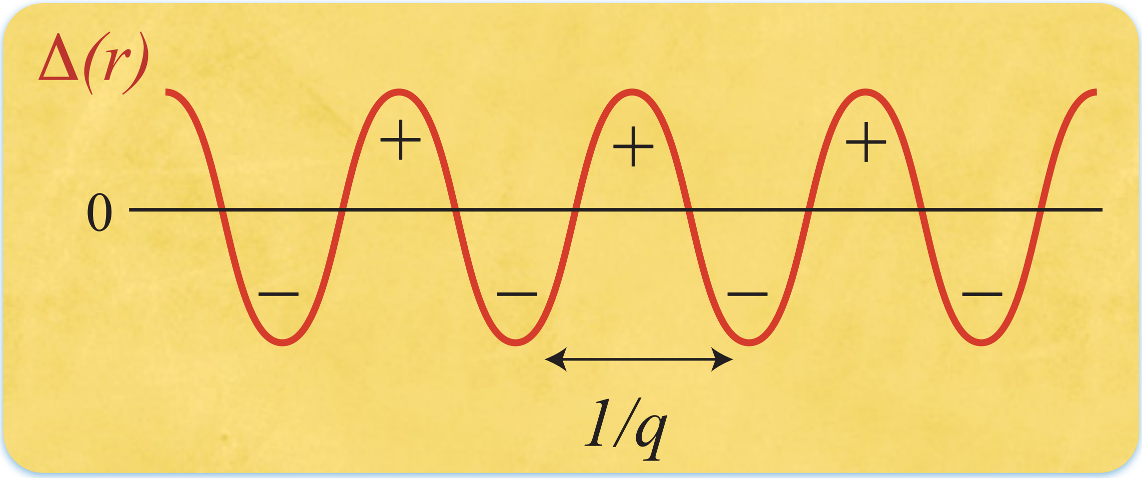

Y. Matsuda & H. Shimahara

The FFLO State

Finite $\vec{q}$ breaks spatial symmetry. ⟶ SC order parameter oscillates in real space.

(FF) $\Delta(\vec{r}) = |\Delta_q|\, e^{i\vec{q}\cdot\vec{r}}$

(LO) $\Delta(\vec{r}) = |\Delta_q|\, cos\left(\vec{q}\cdot\vec{r}\right)$

More generally:

$$\Delta(\vec{r}) = \sum_m \Delta_m e^{i\vec{q}_m\cdot\vec{r}}$$

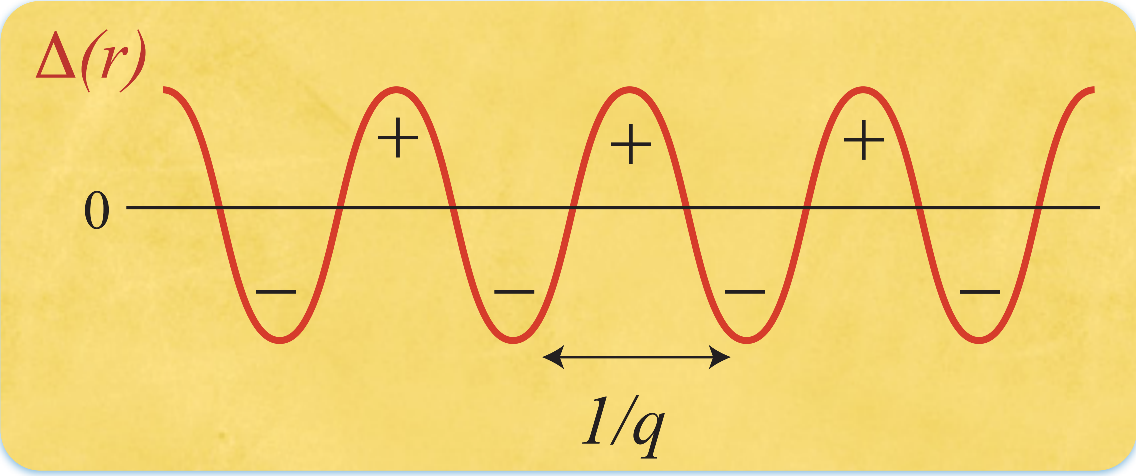

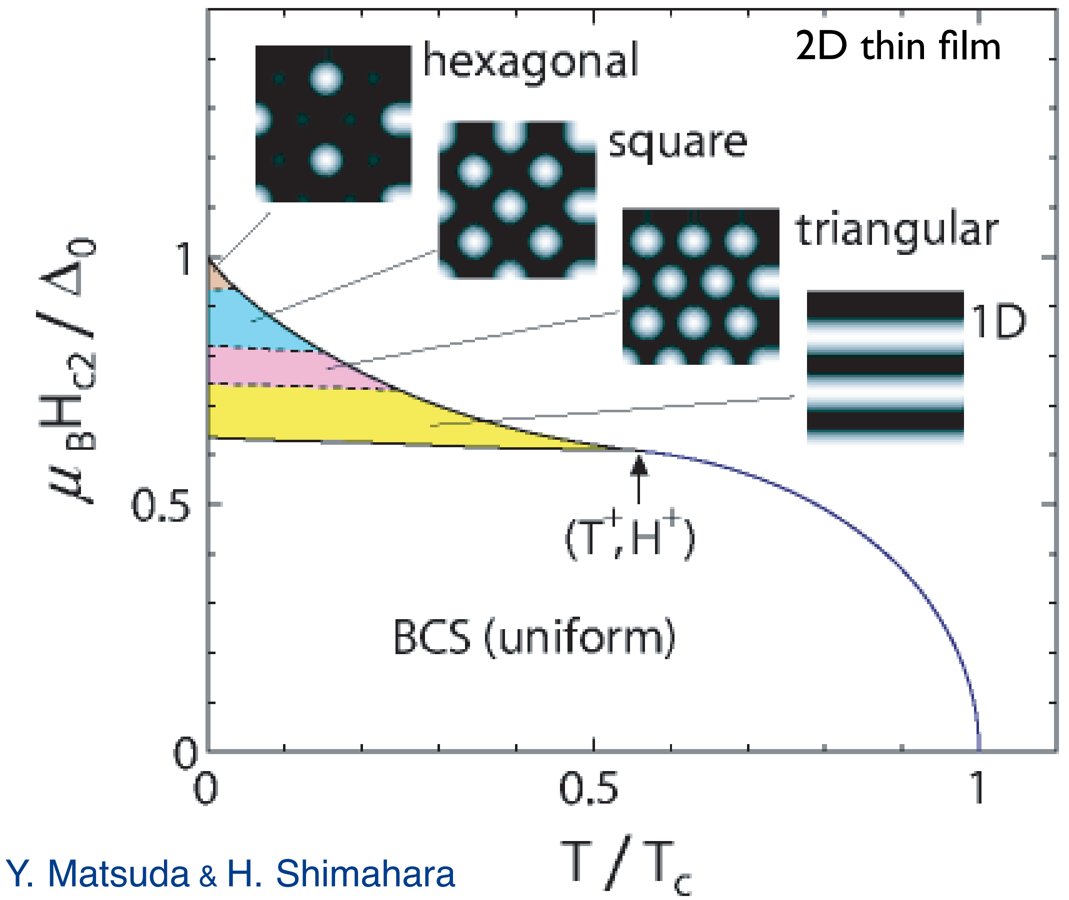

Y. Matsuda & H. Shimahara

FFLO ⇔ SC Imbalanced Spin Populations

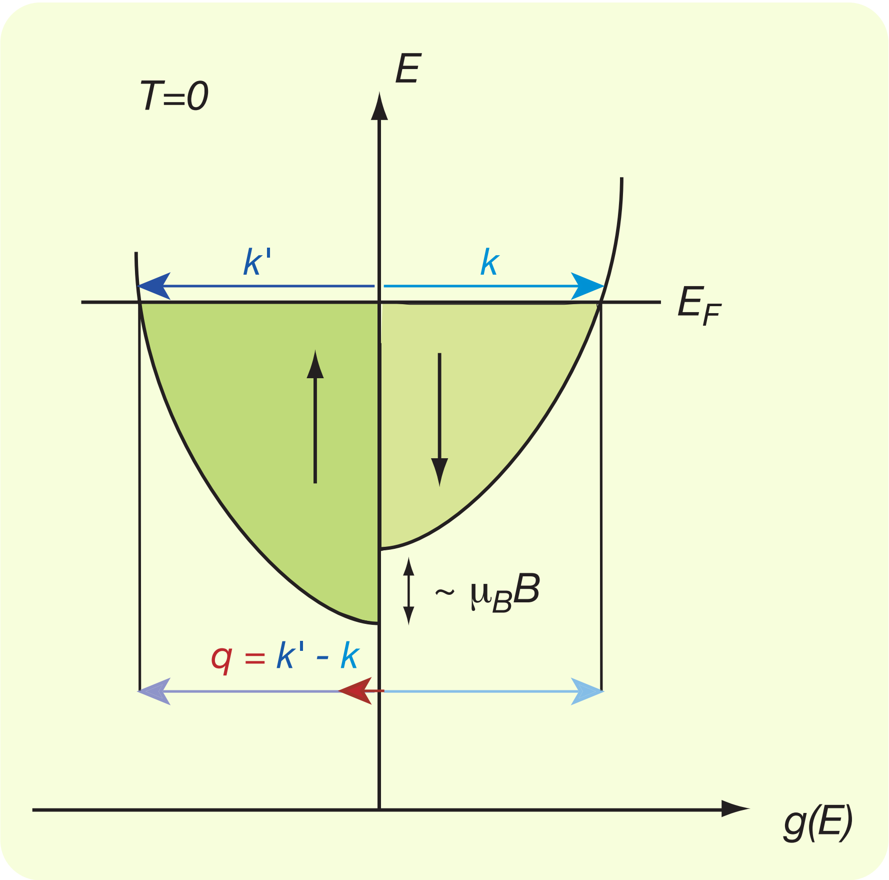

Nature and stability of SC phase with population imbalanced?

FFLO

P. Fulde and R. A. Ferrell, Phys. Rev. **135**, A550 (1964);
A. I. Larkin and Y. N. Ovchinnikov, Zh. Eksp. Teor. Fiz. **47**, 1136 (1964).

Phases with gapless excitations

G. Sarma, J. Phys. Chem. Solids **24**, 1029 (1963);
breached pair SC - W. V. Liu and F. Wilczek, PRL. **90**, 047002 (2003);
R. Casalbuoni and G. Nardulli, Rev. Mod. Phys. **76**, 263 (2004).

Mixed Phases of SC and Normal

P. F. Bedaque, H. Caldas, G. Rupak PRL **91**, 247002 (2003);
H. Caldas, PRA **69**, 063602 (2004);
J. Carlson, S. Reddy, PRL **95**, 060401 (2005);
M. W. Zwierlein *et al.*, Science **311**, 492 (2006).

Microscopic Probes?

Order Parameter

d-wave

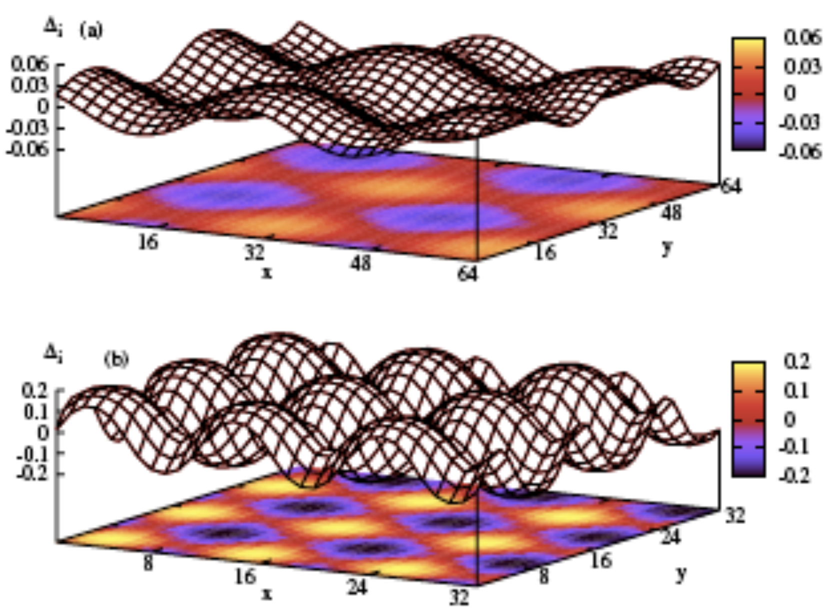

Magnetization

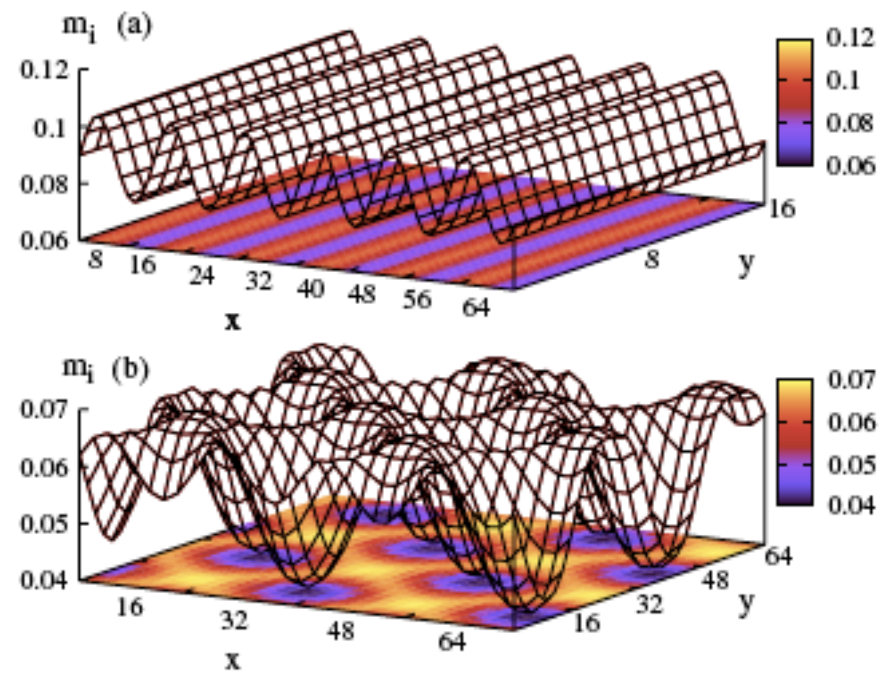

s-wave

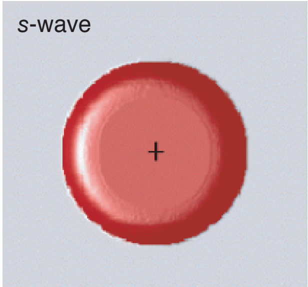

d-wave

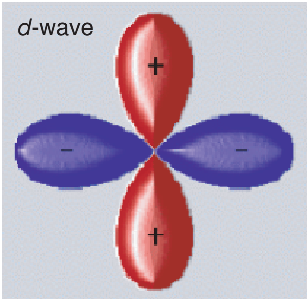

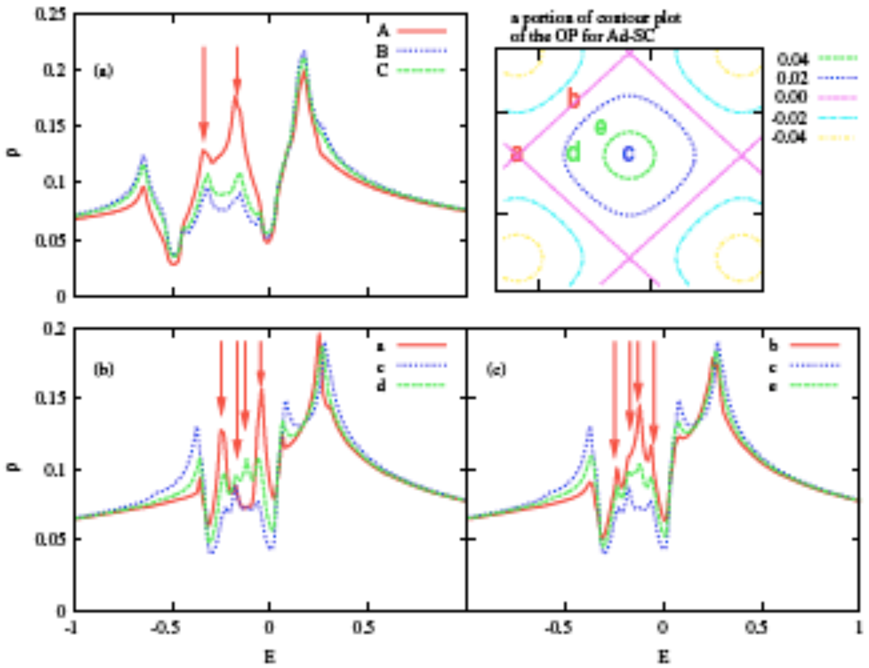

d-wave

LDOS (spin-up; low energy peak)

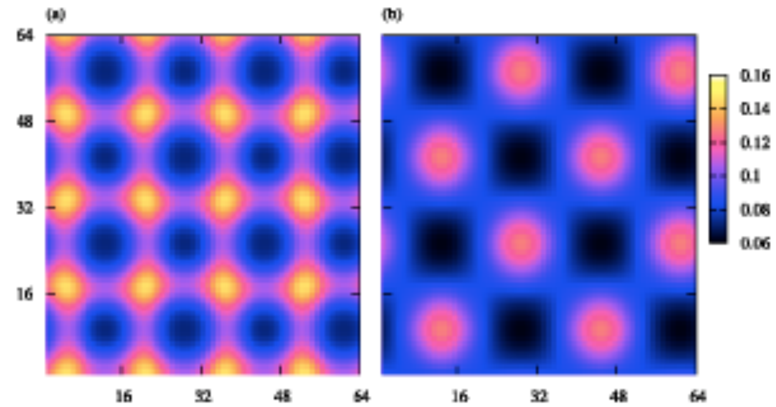

Q. Wang *et al.*,
PRL 96, 117006 (2006)

The NMR Probe

Image of Local Magnetic Field Probability Distribution

Local Magnetic susceptibility (LDOS)

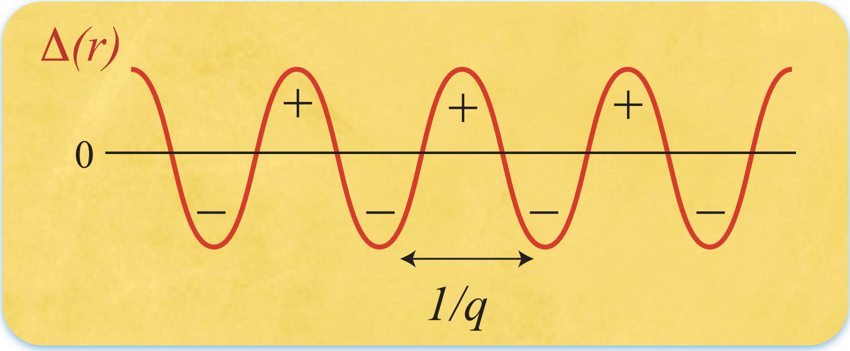

⇒

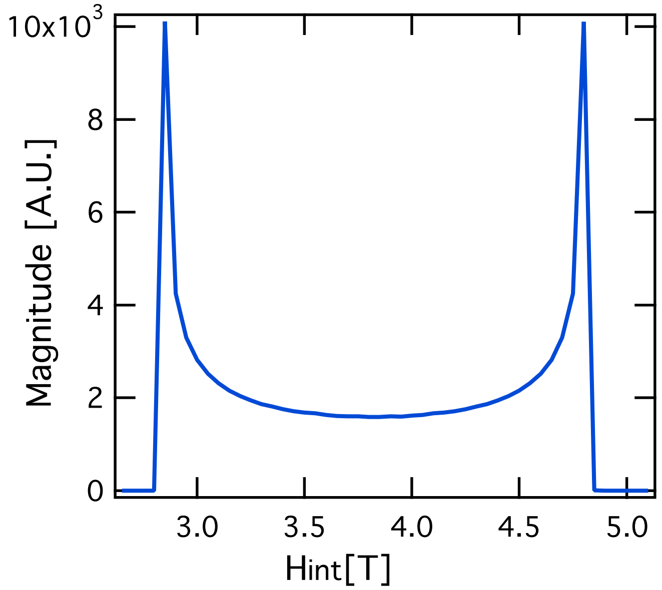

1D

d-wave

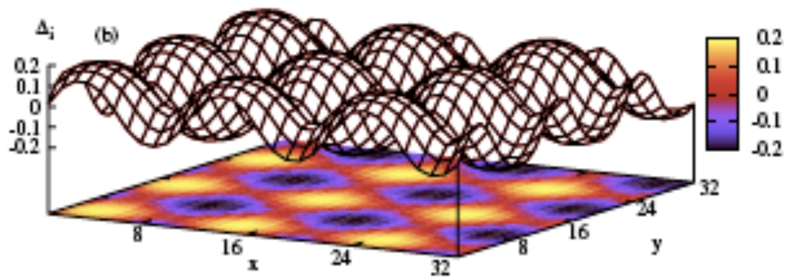

⇒

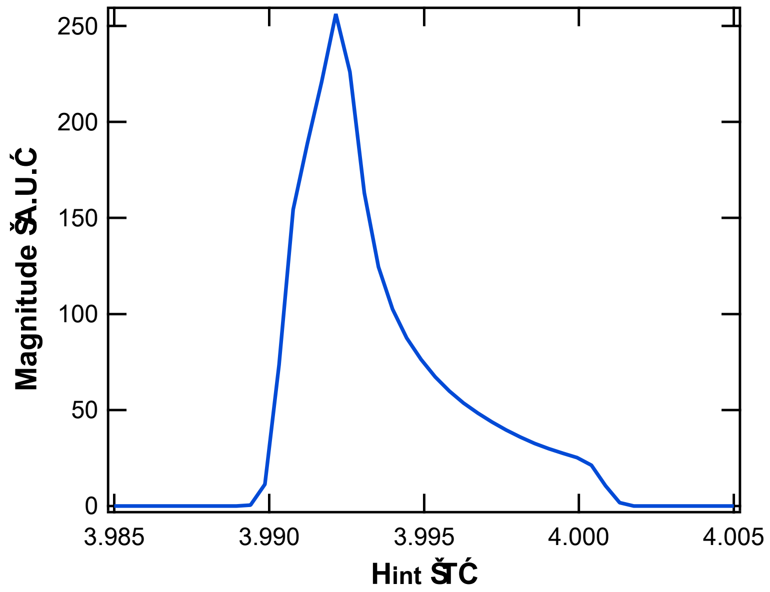

2D

The NMR Probe

Image of Local Magnetic Field Probability Distribution

Local Magnetic susceptibility (LDOS)

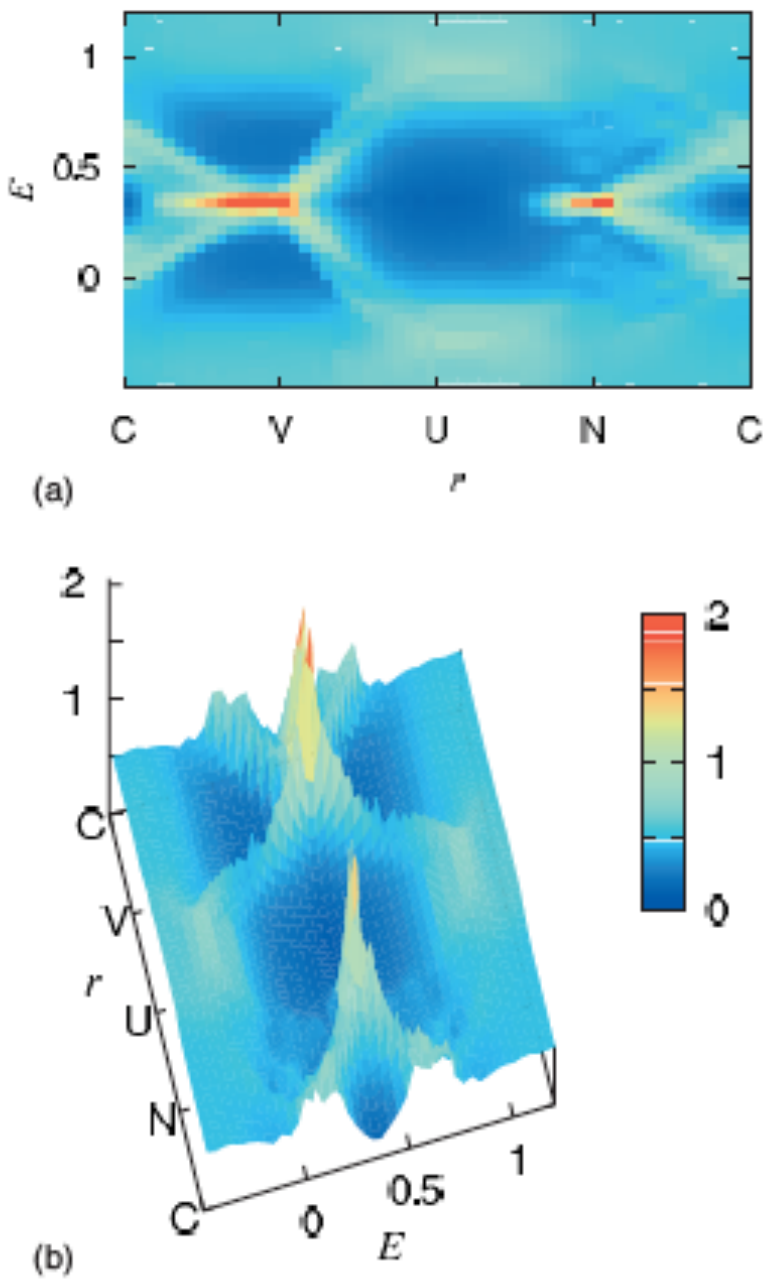

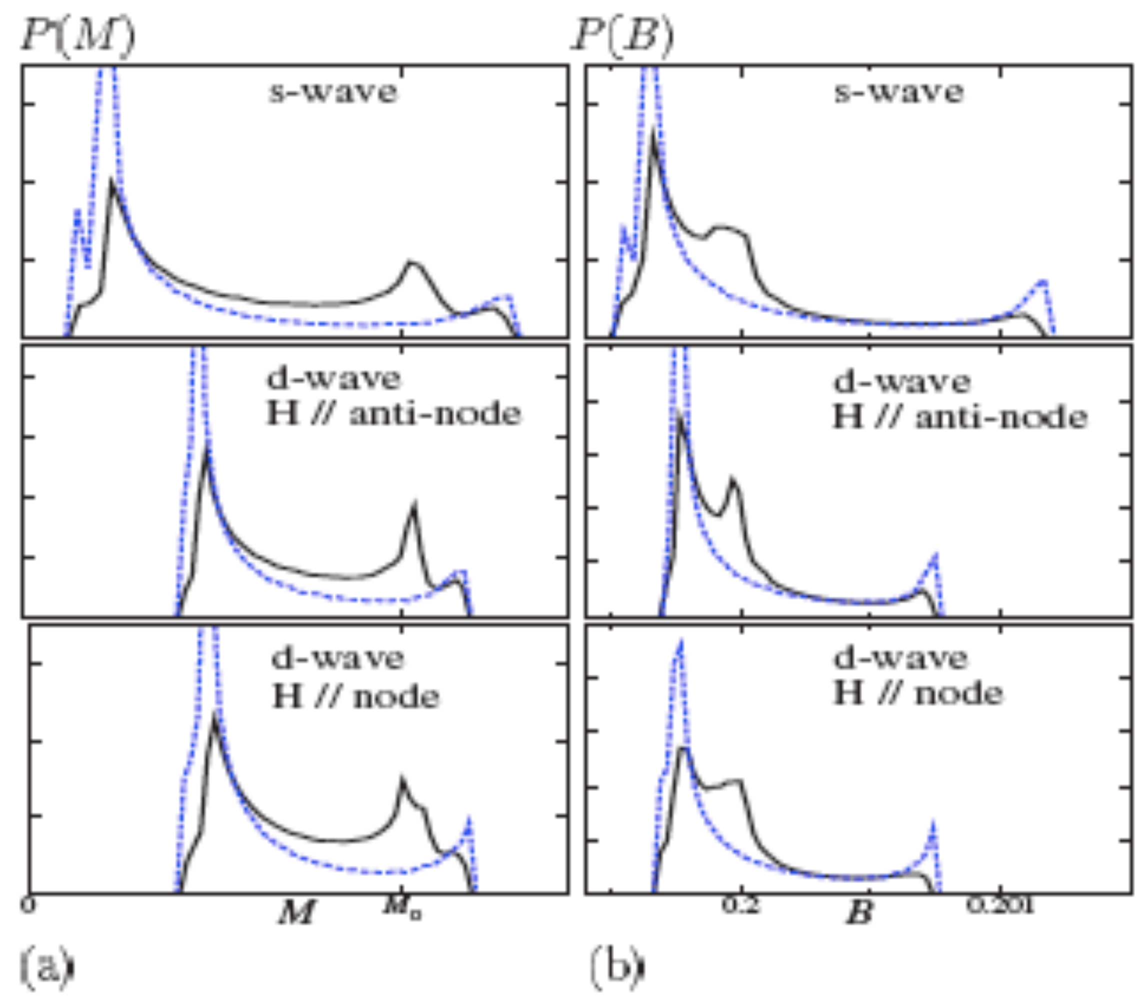

M. Ichioka and K. Machida, PRB **76**, 064502 (2007).

Pseudogap

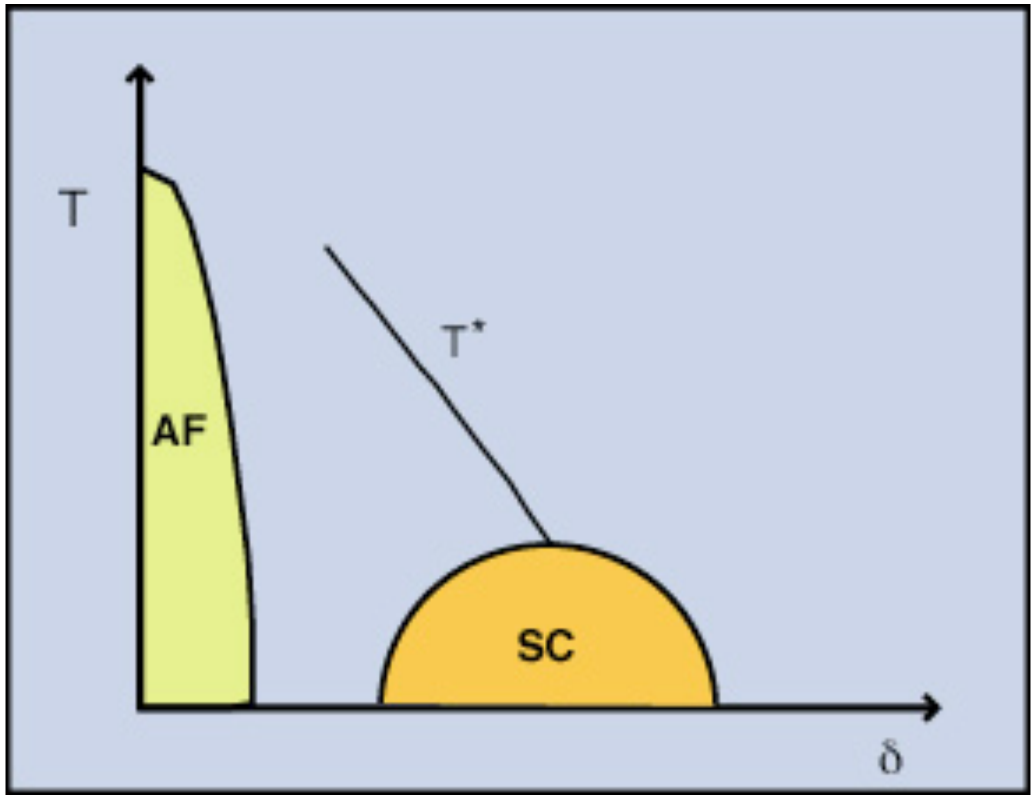

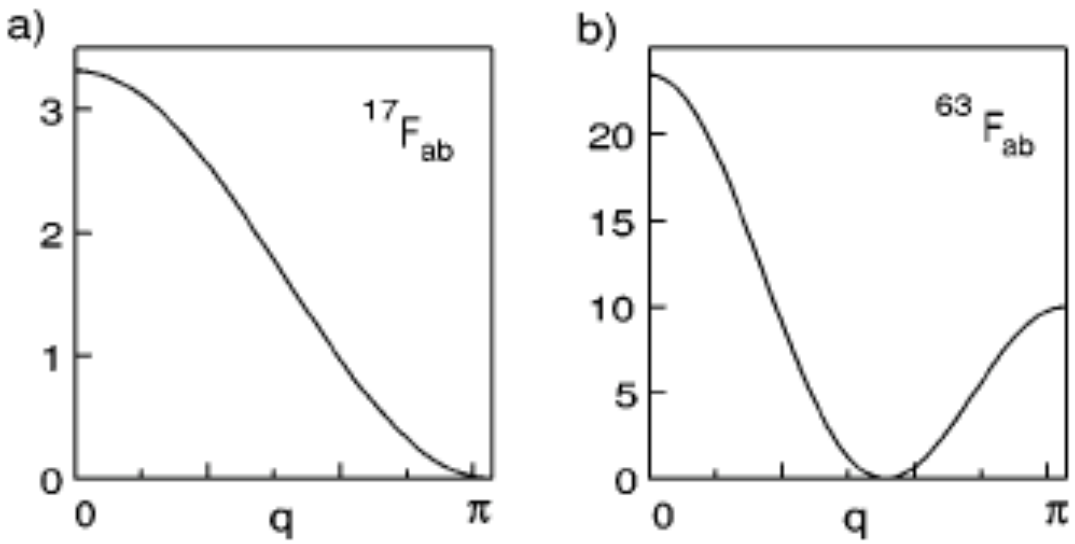

Shastry-Mila-Rice form factors for HTS, Physica C **157**, 561 (1989).

$$\boxed{\frac{1}{{}^{\nu}T_{1z}T} = C\sum_{q} F_{\beta}\frac{\Im m\,\chi_{\beta}(q,\omega_{nn'})}{\hbar\omega_{nn'}}}$$

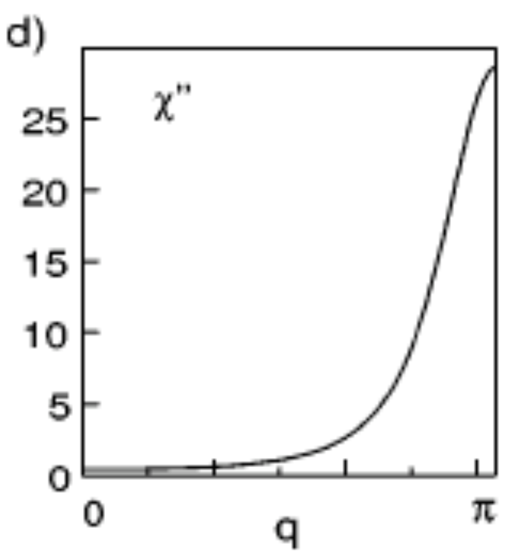

Examine magnetic field responce of the pseudogap in different regions of the Brillouin zone => **spin gap vs pairing gap**?

Pseudogap

Explore magnetic field dependece of T_1

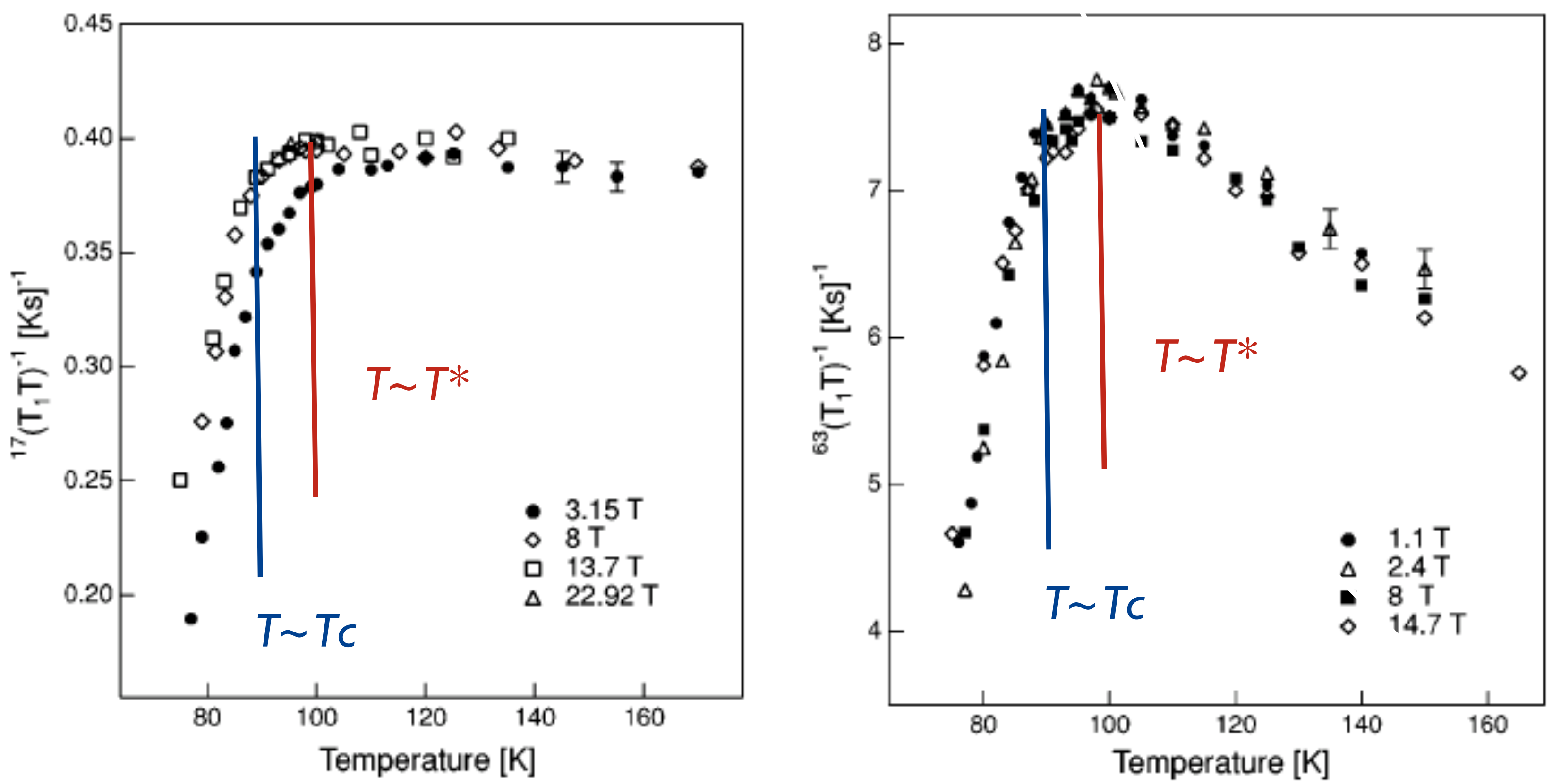

MMP - (Millis 1990)

$$\chi(\mathbf{q},\omega) = \chi_{AF} + \chi_{FL} = \frac{1}{4}\sum_j \frac{\alpha\xi^2\mu_B^2}{1+\xi^2(\mathbf{q}-\mathbf{Q}_j)^2 - i\omega/\omega_{SF}} + \frac{\chi_0}{1-i\pi\omega/\Gamma}$$

χ_{AF}: $q \approx (\pi,\pi)$ $\quad$ χ_{FL}: $q \approx (0,0)$

$$\mathbf{Q}_i = (\pi \pm \delta, \pi \pm \delta)$$

Pseudogap

SF-MMP: $$\chi(\mathbf{q},\omega) = \chi_{AF} + \chi_{FL} = \frac{1}{4}\sum_j \frac{\alpha\xi^2\mu_B^2}{1+\xi^2(\mathbf{q}-\mathbf{Q}_j)^2 - i\omega/\omega_{SF}} + \frac{\chi_0}{1-i\pi\omega/\Gamma}$$

$$\lim_{\omega\to 0}\frac{\chi''(q,\omega)}{\omega}$$

$$\frac{1}{T_1T} = \frac{k_B}{2\mu_B^2\hbar^2}\times\sum_q F_c(\mathbf{q})\cdot\left[\frac{1}{4}\sum_j \frac{\alpha\xi(T)^2\mu_B^2/\omega_{SF}}{[1+\xi(T)^2(\mathbf{q}-\mathbf{Q}_j)^2]^2} + \frac{\chi_0\pi}{\Gamma}\right]$$

$$\xi(T) = \xi_0\sqrt{\frac{T_x}{(T_x+T)}}$$

Spin-Gap:

$$\omega_{SF}^{-1} \propto \frac{\left[\tanh\left(\frac{(T-T_p)}{c_1}\right)\right]}{[\xi_0^{-2}\xi(T)^2]}$$

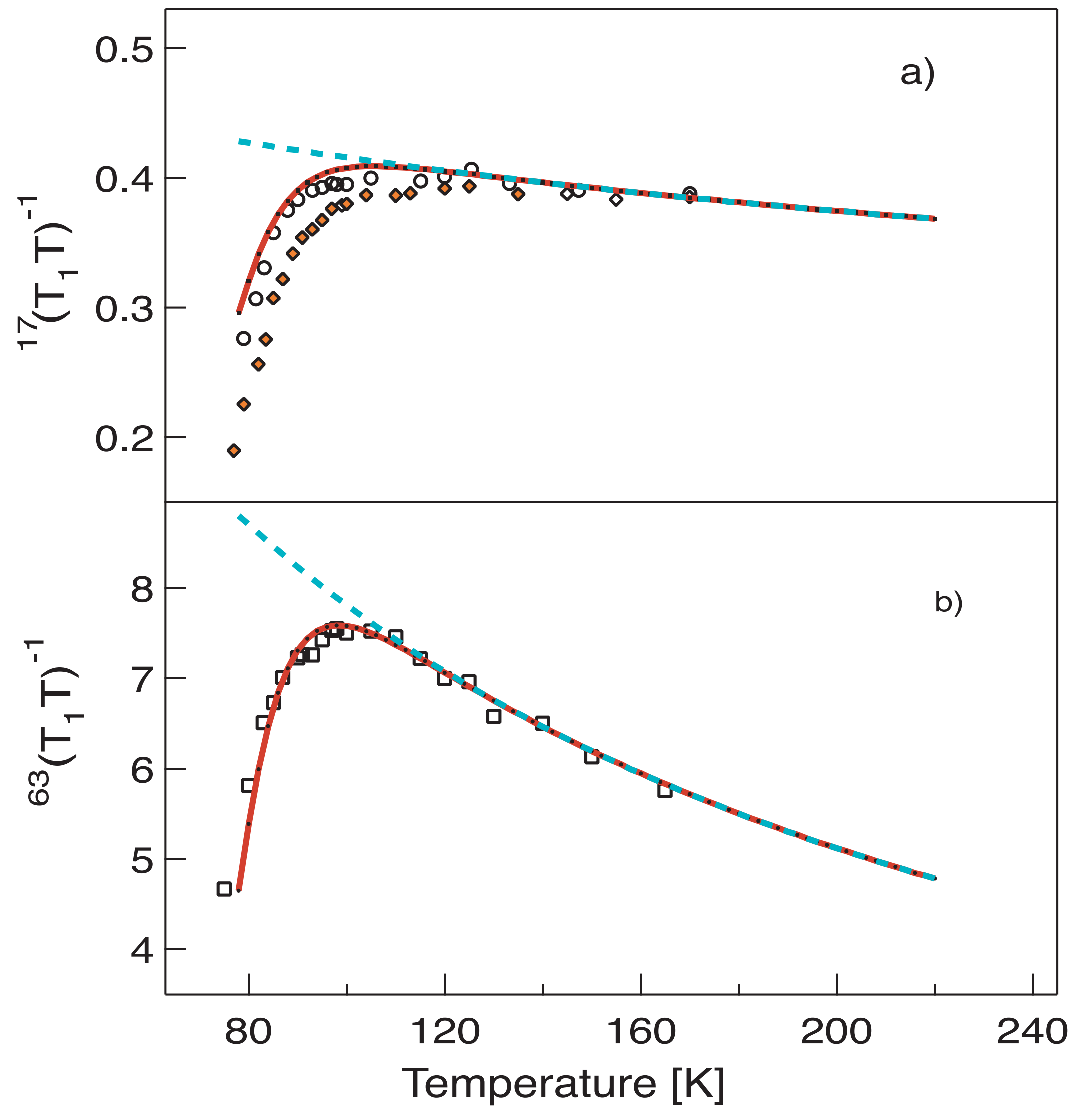

Pseudogap

AF correlations ($q \approx (\pi,\pi)$) supprressed below T^*

away from ($q \approx (\pi,\pi)$) pseudo gap shows magnetic field dependence ($H_0 < 10$ T) => pairing fluctuations - precursory effetc to SC

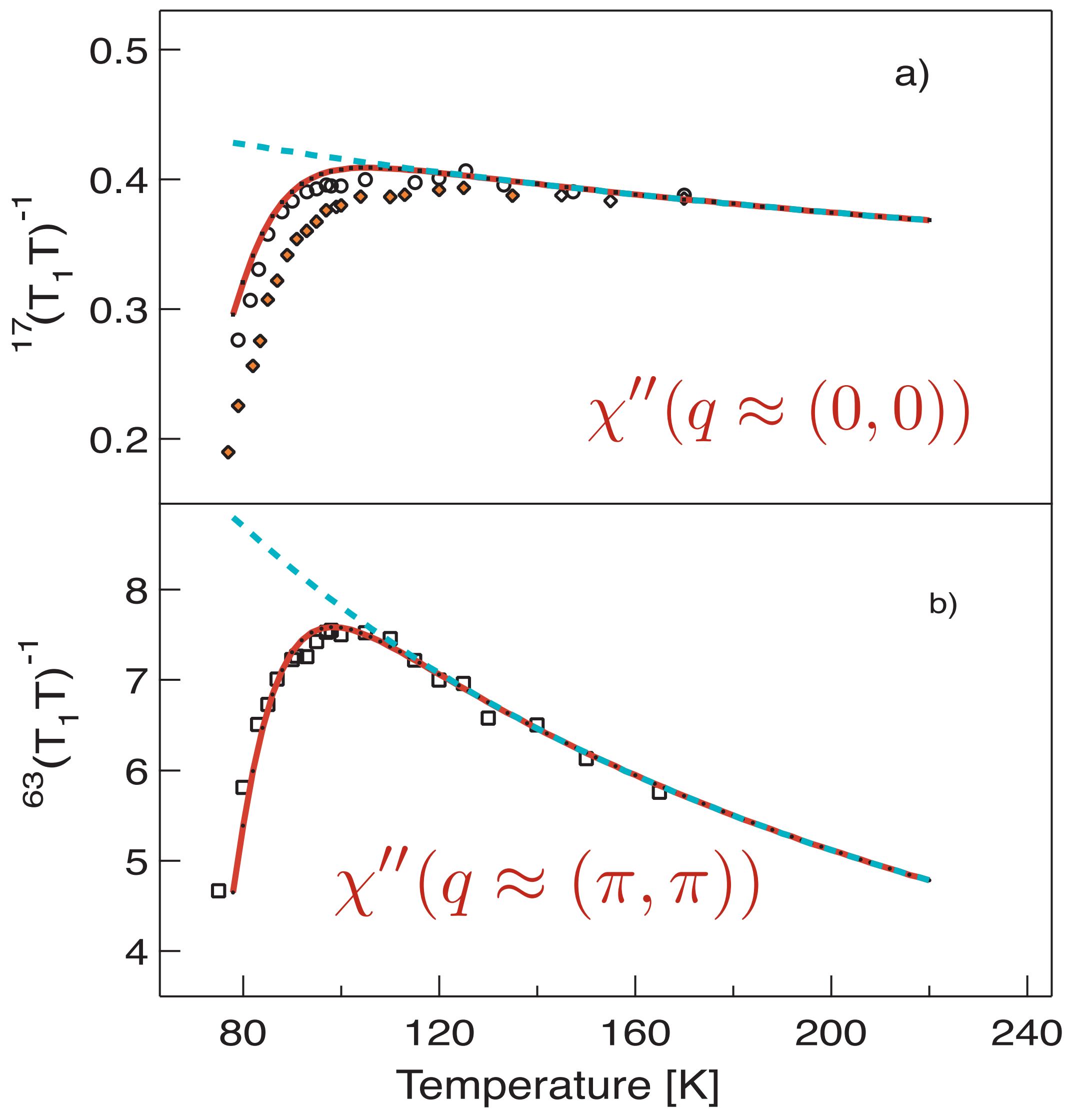

NMR in SC

$$K \propto \chi(q=0,\omega=0) \propto N(E_F)$$

For singlet SC:

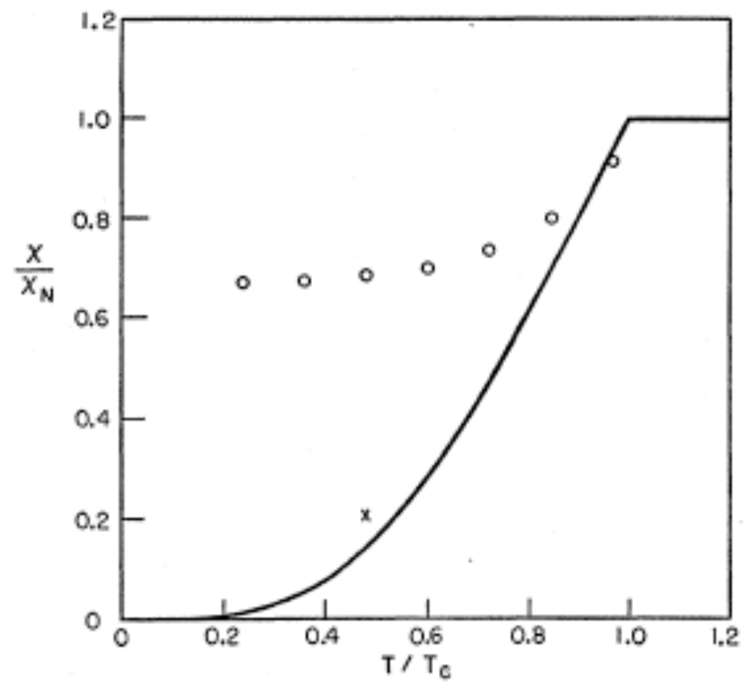

Yoshida (1958)

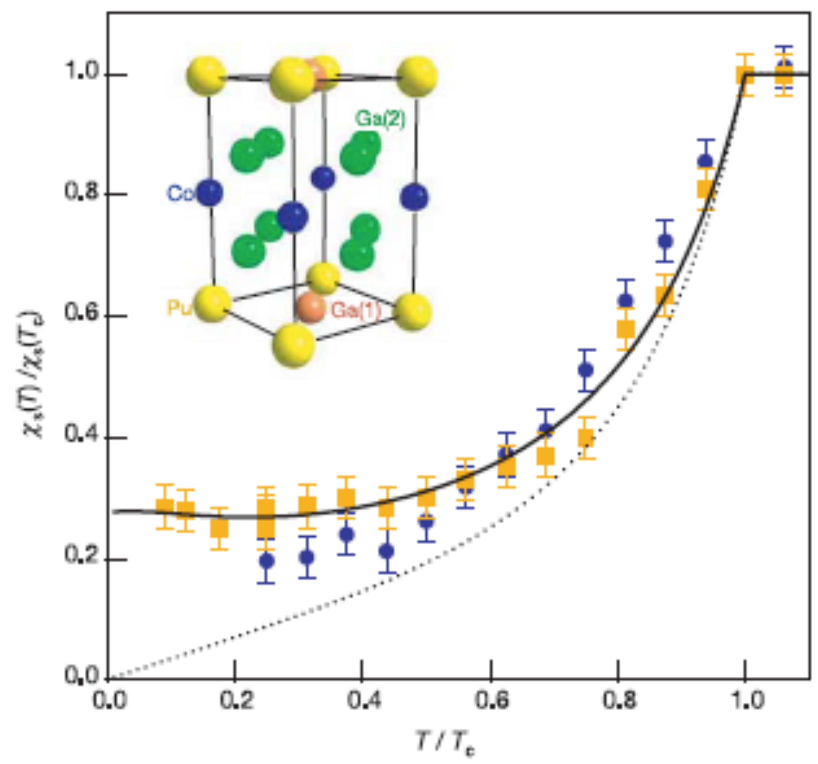

Curro(2005)

NMR in SC

$$\frac{1}{T_1} \propto \chi''(q,\omega=0) \propto N_i(E_F)N_f(E_F)$$

s-wave:

d-wave:

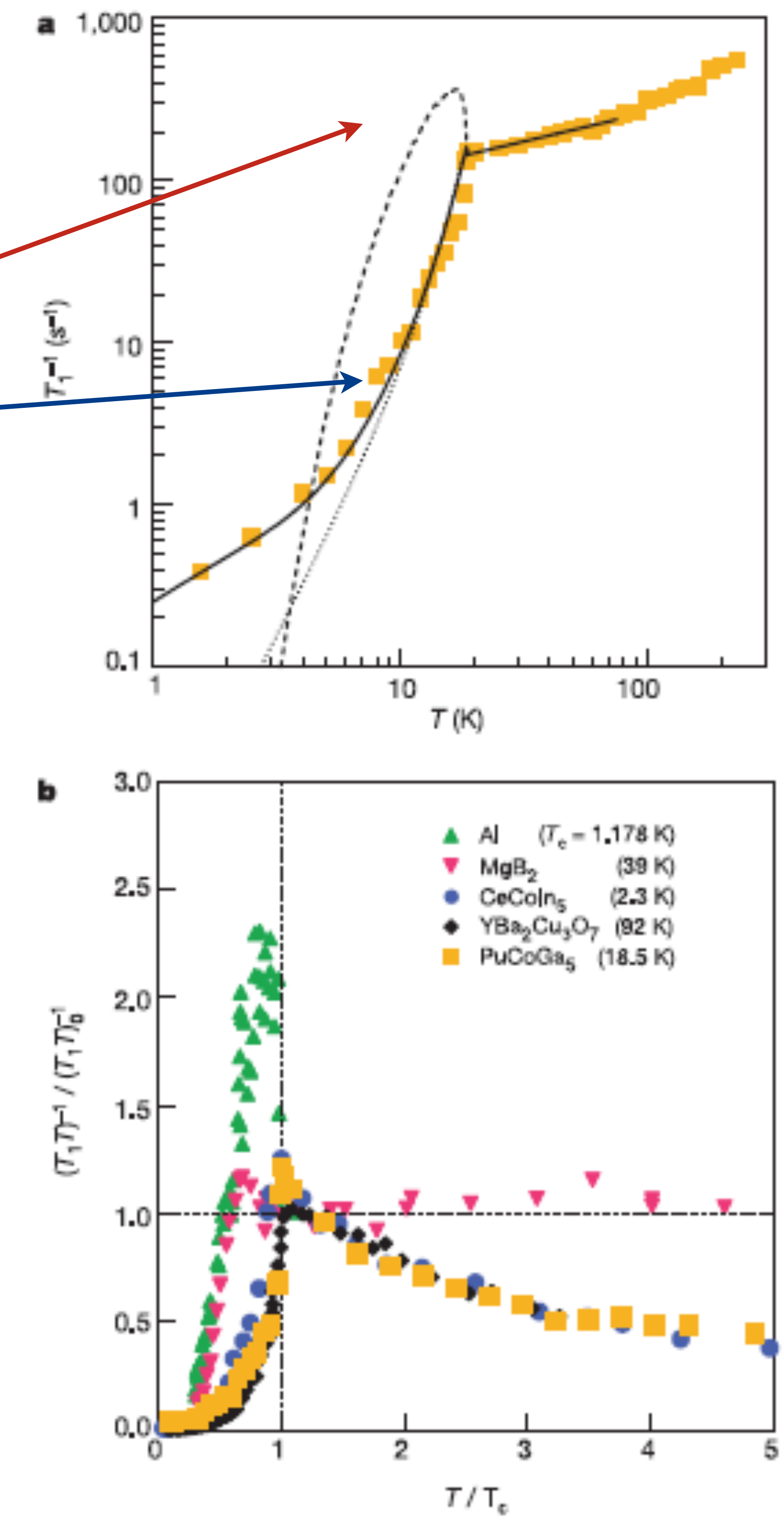

d-wave: $\frac{1}{T_1} \propto T^3$

s-wave: Habel-Slichter Peak
(u & v - coherence factors)